The role of surfactant protein A in immunity to HPV16 pseudovirus infection

Sylvia Dominique Ujma

Supervisor:

Dr Georgia Schäfer

Co-supervisors:

Professor Arieh Katz and

Associate Professor William Horsnell

Presented for the Degree

Master of Science in Medicine

Medical Biochemistry

Division of Medical Biochemistry and Structural Biology

Department of Integrative Biomedical Sciences

Faculty of Health Sciences

University of Cape Town

December 2017

Declaration

I, Sylvia Dominique Ujma, hereby declare that the work on which this dissertation/thesis is based is my original work (except where acknowledgements indicate otherwise) and that neither the whole work nor any part of it has been, is being, or is to be submitted for another degree in this or any other university.

I empower the university to reproduce for the purpose of research either the whole or any portion of the contents in any manner whatsoever.

Signature: Signed by candidate

Date: 18 December 2017

Acknowledgements

I would like to express my sincerest gratitude to my supervisor, Dr. Georgia Schäfer, for guiding me throughout this project. Georgia, thank you for all your support, for teaching me so many new techniques, for all your expertise in mouse work, for the opportunity to travel and present at an International conference, as well as for the countless hours of editing my writing! I got extremely lucky to have had such a wonderful, kind and motivating supervisor for the past few years.

I would like to thank my co-supervisor Professor Arieh Katz for all the input received on my writing, for all his guidance and wisdom, and for hosting me in his laboratory.

I would like to thank my co-supervisor Associate Professor William Horsnell for all his help with my writing (especially with writing my Review article), as well as for assisting with all surfactant protein related issues.

I would like to thank Professor Howard Clark and Associate Professor Jens Madsen for their assistance with SP-A issues, as well as for providing purified SP-A, and SP-A and SP-D antibodies.

I would like to thank Ms. Alisha Chetty and Ms. Sinead Carse for their assistance with mouse work. I would also like to thank Associate Professor Dirk Lang and Mrs. Susan Cooper for their assistance with the confocal microscope and image analysis; their assistance was always accompanied by great kindness and I really appreciate it.

In terms of the smooth running of the laboratory, I would like to thank Xolani Nonzinyana, Graham Christians and Roshan Ebrahim. Their constant hard work behind the scenes is greatly appreciated!

I would like to thank my family and friends for all their support throughout this project. Thanks to my parents, Roman and Dominique Ujma, for all their love as well as their financial and emotional support. I would not have had such a pleasant postgraduate experience without Melissa Blumenthal and George Cooper, and I am so grateful to have made such wonderful friends. I would also like to give special thanks to Christopher de Klerk for his constant love and support, I would have really struggled without it.

Lastly, I would like to thank the National Research Foundation as well as the University of Cape Town for funding my studies as well as my conference attendance. This support has been vital for the completion of this project, and I am deeply grateful for it.

Table of contents

List of Figures and Tables

List of abbreviations

°C	Degrees Celsius
AF488	Alexa Fluor 488
APC	Antigen presenting cell
APES	3-Aminopropyltriethoxysilane
BSA	Bovine serum albumin
BALF	Bronchoalveolar lavage fluid
CMC	Carboxymethylcellulose
Co-IP	Co-immunoprecipitation
CRD	Carbohydrate recognition domain
DMEM	Dulbecco's Modified Eagle Medium
dH_2O	deionised water
dNTP	deoxynucleotide triphosphates
DTT	Dithiothreitol
EDTA	Ethylenediaminetetraacetic acid
FACS	Fluorescence Activated Cell Sorter
FSC	Forward scatter
FLuc	Firefly luciferase
FT	Flow through
g	gram
GIT	Gastrointestinal tract
GLuc	Gaussia luciferase

HEK293TT	Embryonal human kidney cells transformed with sheared adenovirus type 5 and simian virus-40
HeLa	Human epithelial cervical adenocarcinoma cells
HIV	Human immunodeficiency virus
HSPG	Heparan Sulphate Proteoglycan
HRP	Horseradish peroxidase
HPV	Human papillomavirus
HPV16-PsVs	Human papillomavirus type 16 pseudovirus
IAV	Influenza A virus
IFN	Interferon
IHC	Immunohistochemistry
IL	Interleukin
IP	Intraperitoneal
i.vag.	Intravaginal
kDa	Kilo Daltons
L	Litre
LPS	Lipopolysaccharide
m-	milli-
-m	-metre
M	Molar
M.tb	*Mycobacterium tuberculosis*
n	nano
N-9	Nonoxynol-9
OCT	Optimal Cutting Temperature

ORF	Open reading frame
PAMP	Pathogen associated molecular pattern
PBS	Phosphate buffered saline
PCR	Polymerase chain reaction
p.i.	Post infection
PsVs	Pseudovirions
RAF	Research Animal Facility
RNA	Ribonucleic acid
rpm	rotations per minute
RSV	Respiratory syncytial virus
RT	Room temperature
s.c.	Subcutaneous
SDS-PAGE	Sodium Dodecyl Sulphate Polyacrylamide Gel Electrophoresis
SEM	Standard error of the mean
SIRP-α	Signal inhibitory regulatory protein alpha
SSC	Side scatter
SP	Surfactant protein
SP-A	Surfactant protein A
SP-D	Surfactant protein D
S phase	Synthesis phase
TEMED	Tetramethylethylenediamine
TLR	Toll-like receptor
UCT	University of Cape Town

UTI	Urinary tract infection
VLP	Virus-like particle
v/v	volume per volume
WT	Wildtype
w/w	weight per weight
µ	micro

Abstract

Infection by oncogenic human papillomavirus (HPV) is known to be the causative agent for the development of various anogenital cancers, including cervical cancer. Worldwide, the majority of cervical cancer cases occur in less developed regions, and while prophylactic vaccines exist to combat HPV infection, they are largely unattainable in these areas. Therefore, alternative preventative measures against HPV infection are needed to help eradicate cervical cancer over time. Since HPV employs multiple mechanisms to evade the host immune response, a proposed method for preventing infection may be by enhancing HPV recognition by the immune system. Surfactant proteins A and D (SP-A and SP-D) are innate immune proteins with a variety of functions including recognition and opsonisation of pathogens. They are primarily found in the lung, but have also been shown to be expressed at other sites of the body, including the female reproductive tract. It was hypothesised that SP-A and/or SP-D may enhance immune recognition of HPV, thereby preventing infection. To assess this hypothesis, co-immunoprecipitation and flow cytometry experiments were performed to determine whether SP-A and/or SP-D bind to HPV16 pseudovirions (HPV16-PsVs). SP-A was shown to bind to HPV16-PsVs as well as enhance viral uptake by RAW264.7 murine macrophages, while SP-D bound HPV16-PsVs weakly and had no effect on viral uptake. To confirm these observations and to assess whether SP-A had an effect on HPV16-PsVs infection *in vivo*, a well-established, but not yet available murine HPV16-PsVs cervicovaginal challenge model system was set up at UCT. It was determined that neither naïve nor C57BL/6 mice challenged with HPV16-PsVs expressed SP-A in the female genital tract. However, under the experimental conditions established herein, pre-incubation of HPV16-PsVs with purified SP-A at a 1:10 weight per weight ratio resulted in a reduction in infection. This study is the first to describe a biochemical and functional association of HPV16 virions with the innate immune molecule SP-A. In the long term, these observations may contribute to the development of topical microbicides incorporating recombinant fragments of SP-A to reduce the burden of new HPV infections.

1. Introduction

1.1. Human papillomavirus and cervical cancer

Human papillomavirus (HPV) is known to be the most common viral infection of the reproductive tract [1,2]. There are over 180 different HPV types, which can be classified as either low-risk or high-risk depending on their ability to cause malignant cell transformation [3]. Low-risk HPV types are known to cause low-grade benign lesions or warts, whereas high-risk (oncogenic) types are associated with multiple carcinomas including head and neck cancers and anogenital cancers [4]. It is estimated that approximately 5% of all human cancers are caused by HPV [5]. Most notably, virtually all cervical cancer cases can be attributed to high-risk HPV infection, and the predominant HPV types associated with cervical cancer are HPV16 and HPV18 [6]. Together, HPV16 and 18 account for over 70% of cervical cancer cases [1,6]. However, infection with high-risk HPV is necessary, but not sufficient for the development of cervical cancer [7]. Other co-factors, such as chronic inflammation and immunosuppression, facilitate cancer development [7], as outlined in more detail below.

Worldwide, cervical cancer is the fourth most common cancer in women [8]. The disease is substantially more prevalent in developing countries as compared to developed countries, with 84.3% of cases occurring in less developed regions (Figure 1.1.A.) [8]. In South Africa, cervical cancer is the second most common cancer in women and is the leading cause of female cancer-associated deaths (Figure 1.1.B.) [8,9]. Since cervical cancer is nearly always caused by oncogenic HPV infection, it is a cancer which is potentially totally preventable. Highly efficient prophylactic vaccines against the most common oncogenic HPV types are available (described in section 1.1.4.). Additionally, early detection of pre-malignant or abnormal cells is possible with cervical cytology screening, allowing for early treatment and prevention of development of cervical cancer. Unfortunately, vaccination and screening programs have been difficult to establish in developing countries, which quite likely explains why these countries have the highest burden of cervical cancer [10]. Developing countries are also highly burdened by the human immunodeficiency virus (HIV)/AIDS epidemic, a disease known to cause immunosuppression. HIV and HPV co-infection is common due to shared routes of transmission, and HIV infection increases HPV persistence and the relative risk of cancer

development as compared to HPV infection alone [11,12]. This is likely due to the low CD4+ cell count observed in HIV-positive individuals, making HPV clearance less efficient which may result in HPV persistence and cancer development [13].

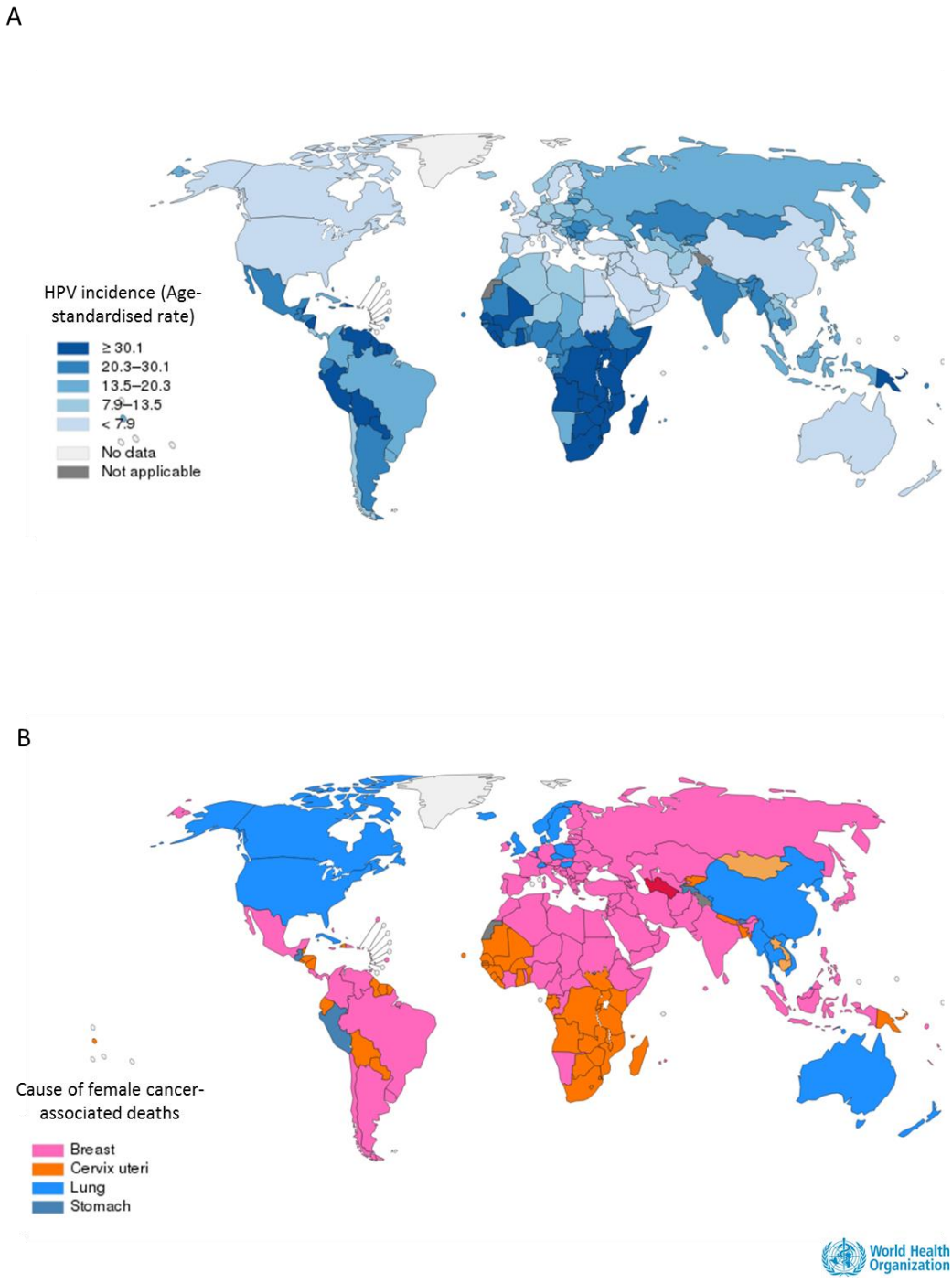

Figure 1.1: Cervical cancer is a disease of the developing world. A) Incidence of cervical cancer worldwide in 2012, displayed as estimated age-standardized rates. **B)** Leading causes of female cancer-associated deaths worldwide in 2012. Data retrieved from GLOBOCAN and displayed using CANCER TODAY [8].

1.1.1. HPV genome and structure

HPV is a non-enveloped, double stranded DNA virus [14]. The HPV genome is approximately 8000 base pairs and encodes for "early" and "late" genes (Figure 1.2.A.) [14]. The early genes code for E1, E2, E4, E5, E6 and E7 proteins. E1 and E2 are involved in replication and transcriptional regulation and E4 has a role in viral particle release [5]. Although the role of E5 is not well-characterised, it has been implicated in immune evasion (see section 1.1.3.) [5]. E6 and E7 have important roles in the viral life cycle of both high- and low-risk HPVs, such as episomal maintenance [15,16]. In high-risk HPV types, E6 and E7 also function as oncoproteins ensuring viral replication and persistence and thereby potentially influencing many cancer hallmarks [7]. E6 binds the central tumour suppressor protein p53 and marks it for degradation, therefore preventing p53 from arresting the cell cycle during cellular stress [17]. E7 binds retinoblastoma proteins, thereby preventing them from modulating the function of the transcription factor E2F, which augments entry of cells into synthesis phase (S phase) of the cell cycle and results in increased cellular proliferation [17]. The combinatory result of these events overrides cell cycle checkpoints and allows for viral DNA replication to continue as the cell is maintained in S phase [5]. In addition to these functions, E6 and E7 have a role in immune evasion (section 1.1.3).

The late genes code for the major (L1) and minor (L2) capsid proteins. The L1 protein can self-assemble into icosahedral virus-like particles, and the L2 protein seems to have a vital role in the establishment of infection [18]. The capsid is formed by 360 L1 proteins which organise into 72 pentamers, as well as approximately 30 L2 proteins which are mostly hidden from the capsid surface [19,20].

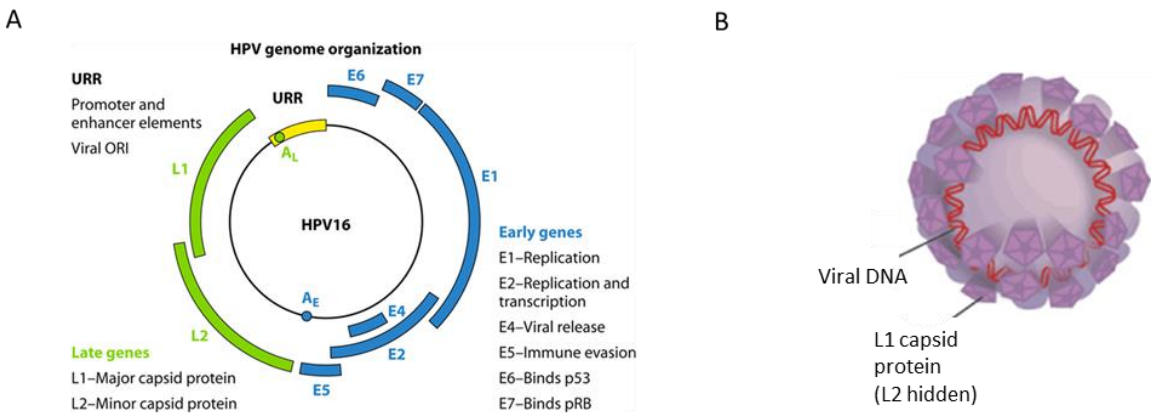

Figure 1.2: HPV genome organisation and viral structure. A) The HPV genome is organised into two distinct sets of genes, the early (blue) and late (green) genes. **B)** The viral DNA is harboured by an icosahedral capsid formed by the major L1 and minor L2 proteins. Figure adapted from [5].

1.1.2. HPV infectious cycle and malignant transformation

HPV is transmitted via direct skin-to-skin contact rather than through body fluids. As the virus' life cycle is exclusively intraepithelial and closely linked to keratinocyte differentiation, HPV needs to infect mitotically active basal cells of the host's cutaneous and mucosal epithelia that have been exposed due to microabrasions. During the early attachment steps, the virus binds to heparan sulphate proteoglycans (HSPGs) on the epithelial basement membrane or cell surface, via the L1 capsid protein [21,22]. Laminin-332 that is secreted onto the extracellular matrix by keratinocytes can also be bound by HPV transiently [23]. This initial binding is thought to result in a conformational change of the capsid which facilitates L1 cleavage by the serine protease kallikrein-8 [24]. Following this, viral interaction with the host chaperone protein cyclophilin B results in exposure of the N-terminus of the L2 protein [25]. This N-terminus of L2 contains a conserved cleavage site for the proprotein convertase furin, and cleavage by furin is believed to be essential for endosomal escape at a later stage of infection rather than at the early stages of binding and entry [26]. After conformational changes of the capsid, the virus loses affinity to HSPGs and binds to a still unknown entry receptor [27]. Following entry, HPV is trafficked through the endosomal system [28]. This occurs by HPV interacting with sorting nexin 17 in the endosome, as well as with gamma secretase in the Golgi apparatus and endoplasmic reticulum [29,30]. This occurs 2-3 hours post entry [28]. After 12 hours, viral uncoating

occurs in the late endosome, and the viral genome, complexed with L2, is released into the cytoplasm [22]. The L2-complexed genome then travels to the nucleus along microtubules via dynein-mediated transport [31].

The infectious cycle of HPV lasts for at least 3 weeks and is closely linked to the differentiation program of keratinocytes. Following infection, viral gene expression is mostly suppressed, but low levels of the early genes E1 and E2 are expressed which results in an increase in viral genome copy number (approximately 50-100 copies per cell) [5,32]. Once the keratinocyte leaves the mitotic phase and begins differentiation in the spinous layer, the expression of E6 and E7 increases [17]. The viral genome copy number then increases to over 1000 per cell followed by the expression of the late genes, resulting in the formation of the L1 and L2 capsid proteins [5]. Self-assembly of icosahedral, infectious HPV virions occurs which are then released from the upper, cornified epithelium (Figure 1.3) [17].

For neoplastic transformation to occur, the HPV genome needs to integrate into the host cell genome of the keratinocyte [33]. Integration results in disruption of the E1 and/or E2 genes as well as the open reading frames (ORFs) adjacent to E2 (affecting E4 and E5 expression) [33], leading to non-productive infection (i.e. infectious viral progeny is no longer produced). The ORFs of E6 and E7 remain undisrupted and therefore these two oncoproteins are expressed [3]. The lack of E2 expression also results in higher E6 and E7 expression since E2 normally regulates their expression [33]. The high levels of E6 and E7, in turn, result in uncontrolled cell proliferation and increased DNA damage [33].

In reality, the time period between HPV infection and the appearance of abnormal cells or lesions is highly variable and can range from weeks to months, suggesting that the virus efficiently evades host defence mechanisms.

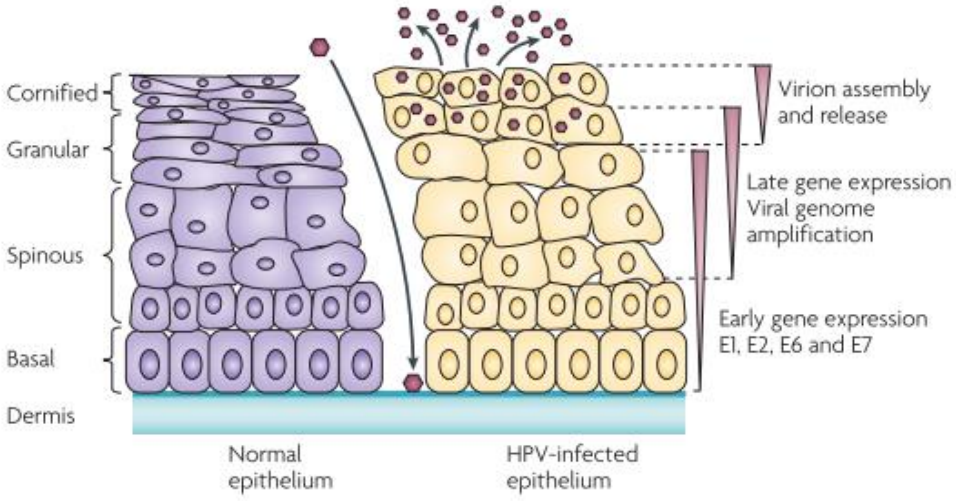

Figure 1.3: The HPV infectious cycle is closely linked to keratinocyte differentiation. Viral gene expression remains low and tightly controlled in basal keratinocytes. Once the cell has begun differentiation (enters the spinous epithelial layer), viral gene expression is upregulated. Late genes are then expressed and the virions are assembled and released from the cornified layer. Figure from [17].

1.1.3. Immune evasion strategies of HPV

As a pathogen, HPV can be seen as rather successful, since it manages to evade the host immune response. As mentioned above, HPVs have a replication cycle closely linked to keratinocyte differentiation, which has important consequences in terms of immunity. The viral life cycle is non-lytic, as virus particles are shed from fully differentiated cornified keratinocytes in the upper epithelium, i.e. cells fated for desquamation [17]. This provides little opportunity for antigen retrieval by antigen presenting cells (APCs) as particles are shed from areas that are far away from active immune surveillance. Langerhans cells and macrophages (as the most likely APCs) are mostly located in the lower epithelial layers and they are relatively ineffective in non-inflammatory environments. The lack of virus-induced cell lysis results in insufficient release of proinflammatory cytokines, therefore APCs are neither activated nor induced to migrate to sites of infection [5]. The infected keratinocytes are also unlikely to release any cytokines to stimulate an inflammatory response, due to the very low levels of viral protein expression in these cells [5]. Furthermore, since HPV is exclusively intraepithelial there is no blood-borne phase of infection, meaning that the virus is not exposed to immune defences outside of the skin [34].

During viral infection, one of the first lines of host defence is the interferon (IFN) response. Type I IFNs (IFN-α and IFN-β) have antiviral and anti-proliferative effects, but HPV has mechanisms by which it can minimize the type I IFN response via its E6 and E7 proteins [5]. E7 inhibits induction of IFN-α inducible genes as well as activation of the IFN-β promoter, and both E6 and E7 directly interact with components of IFN signalling cascades, thereby downregulating the interferon response [5,34,35]. In addition to affecting the IFN response, HPV E6 also reduces expression of the proinflammatory cytokine interleukin (IL)-18 which negatively impacts on IFN-γ production as well as priming of T-cells to launch $CD8^+$-mediated responses [36]. High-risk HPV E6 and E7 further reduce the innate immune response by interfering with the transcription of toll-like receptor 9 (TLR9) [37] which normally recognises CpG motifs in viral or bacterial double-stranded DNA, thereby triggering the release of proinflammatory cytokines [37,38]. The E5 protein is also suggested to have a role in immune evasion by inhibiting the acidification of endosomes, affecting antigen processing and presentation by APCs [34]. By evading the innate immune response, HPV is practically invisible to host defences and manages to delay adaptive immune responses for long periods of time which may eventually contribute to persistence of the virus.

Despite these immune evasion strategies, most HPV infections are cleared within 1-2 years by host cell-mediated immune responses [39]. Unfortunately, approximately 10% of infections remain persistent, and women with persistent high-risk HPV infection are at risk for developing cervical cancer [5]. The precise reason for persistence is still unknown, but it is believed that immunosuppression may play a role here [3,40].

1.1.4. HPV prophylaxis and challenges

Currently, there are no treatments for HPV infection, but highly efficient prophylactic vaccines have been developed to prevent infection in unexposed individuals. These are non-infectious subunit vaccines which form virus-like particles (VLPs) from the L1 capsid protein [10]. To date, three different prophylactic vaccines against HPV have been made commercially available. Cervarix, produced by GlaxoSmithKline in insect cells, protects against high-risk HPV16 and 18 [41] and Gardasil, produced by Merck in yeast cells,

protects against HPV16 and 18 as well as low-risk HPV6 and 11 [42]. The most recently developed HPV vaccine is Gardasil 9 (also produced by Merck in yeast) which protects against low-risk HPV6 and 11, and against high-risk HPV16, 18, 31, 33, 45, 52 and 58 [43]. All three vaccines contain an aluminium salt adjuvant which precipitates the VLPs, leading to the slow release of antigen and increased B cell responses, resulting in the production of neutralizing IgG antibodies to L1 [44].

The invention of these prophylactic vaccines has been a huge step towards combating HPV infection and ultimately cervical cancer, but some challenges remain. In South Africa, the Department of Health has introduced HPV vaccination schemes in public schools, where 9-year-old girls receive 2 doses of Cervarix [45]; while this is an important step in the right direction, it only targets a small percentage of the population. Any individuals who do not fit into this group would need to get the vaccine privately. This can be a major issue in developing countries as the vaccines are expensive, and therefore unattainable for a large percentage of women in South Africa [46,47]. Another drawback of the vaccines is that they are only effective as prophylaxis and there is very little evidence displaying that they may offer any benefit to individuals already infected with HPV [48,49]. Furthermore, the vaccines only elicit antibody production against specific HPV types, and cross-protection against other HPV types is limited [50,51]. HPV45 and 35 are highly prevalent in sub-Saharan Africa, where Gardsasil-9 is still unavailable. Taking these challenges into account, it is important to develop alternative means of treatment as well as therapies. Alternative means that have been investigated thus far include small molecule inhibitors of the early stages of HPV infection which can be incorporated into inexpensive topical microbicides [52]. Additionally, the naturally-derived sulphated polysaccharide carrageenan has been shown to inhibit HPV infection by blocking HPV attachment to cells [53]. Carrageenan has been developed into the microbicide Carraguard which in addition to inhibiting HPV infection also effectively reduces herpes simplex virus 2 (HSV-2) prevalence; however, it was not found to be effective against HIV infection [54].

Enhancing recognition of HPV by the innate immune system represents another alternative approach to prevent HPV infection. Identifying innate immune molecules which recognise HPV could be beneficial, as these molecules could be incorporated into

topical microbicides to prevent infection, especially in immunocompromised individuals. Innate immune molecules, such as opsonins which enhance pathogen recognition and phagocytosis, generally have a broader range of recognition and therefore could potentially be protective against several different HPV types as well as other sexually transmitted pathogens.

1.2. Surfactant proteins

Surfactant proteins (SPs) were first identified in pulmonary surfactant, a complex of phospholipids and proteins which is responsible for reducing surface tension at the air-liquid interface of the lung [55]. There are four different surfactant proteins, namely SP-A, SP-B, SP-C and SP-D. Together, these SPs make up approximately 7% of lung surfactant, with SP-A being the most predominant (5.3%), followed by SP-B (0.7%), SP-D (0.6%) and SP-C (0.4%) [56]. SP-B and SP-C are small, hydrophobic proteins which have important roles in phospholipid packaging and reducing lung surface tension [56]. SP-A and SP-D however, are larger hydrophilic proteins which are strongly involved in the innate immune response, and their expression is not restricted to the lung (see section 1.2.3.) [57,58].

1.2.1. Structure of SP-A and SP-D

SP-A and SP-D belong to a family of proteins known as collectins, which are soluble, collagenous pattern recognition receptors that tend to be calcium dependent [59]. In humans, the genes encoding SP-A and SP-D have been mapped to a cluster on the long arm of chromosome 10 (10q 21-24), and SP-A is transcribed by two different genes, namely SP-A1 and SP-A2 [60,61]. SP-A and SP-D are mainly produced by type II alveolar cells in the alveolus or the non-ciliated bronchial epithelial cells (Clara cells) in the airways [57]. The primary structure of the monomeric forms of SP-A and SP-D consists of the following: a cysteine-containing amino terminal domain (forms disulphide bonds for structural stability), a collagenous domain (important for maintaining the shape and structure of the proteins), an alpha-helical neck domain and a carboxy-terminal carbohydrate recognition domain (CRD) (Figure 1.4.) [62]. The monomers of SP-A and SP-

D form trimers (Figure 1.4.), which mostly occurs by the alpha-helical neck domain forming a coiled coil with two other monomers, and it is considered that each SP-A trimer is formed by one SP-A1 and two SP-A2 monomers [63]. SP-A (30-36kDa monomer) is formed by the multimerization of 6 trimers, which forms a bunch-like octadecamer (Figure 1.4) [57]. SP-D (43kDa monomer) is formed by the multimerization of 4 trimers, which forms a cruciform-shaped dodecamer (Figure 1.4) [64].

The CRD is a common feature of the lectins and it is classified as a region with 14 invariant and 18 conserved amino acid residues, which includes 4 cysteine residues which form disulphide bonds [65]. The collectin CRDs are trimeric clusters which have a higher affinity for clustered oligosaccharides than single monosaccharides: this is thought to be valuable in identifying pathogens as the outer surface of pathogens most often comprises of clustered oligosaccharides [57]. The binding of CRDs to carbohydrates is often calcium dependent, and although structurally similar, SP-A and SP-D have different ligand-binding preferences. SP-A preferentially binds to mannose, fucose and lipid ligands, while SP-D mostly binds maltose, inositol, glucose and more complex carbohydrates [57,66]. These differences in ligand binding might be explained by subtle structural differences in the trimeric CRDs: in SP-A, these are flatter and more hydrophobic as compared to the hydrophilic CRDs of SP-D which bind to polar ligands [67]. In addition, the Gly-X-Y repeats in the collagen domain of SP-A are interrupted, which results in SP-A monomers being kinked, whereas in SP-D, the collagenous domain is slightly larger and not kinked which is suggested to offer more binding freedom to the distal CRDs [63]. Both SP-A and SP-D have very low affinities to galactose and sialic acid (sugars that often form the terminals of carbohydrates on animal cells) which is important for distinguishing self from non-self [57].

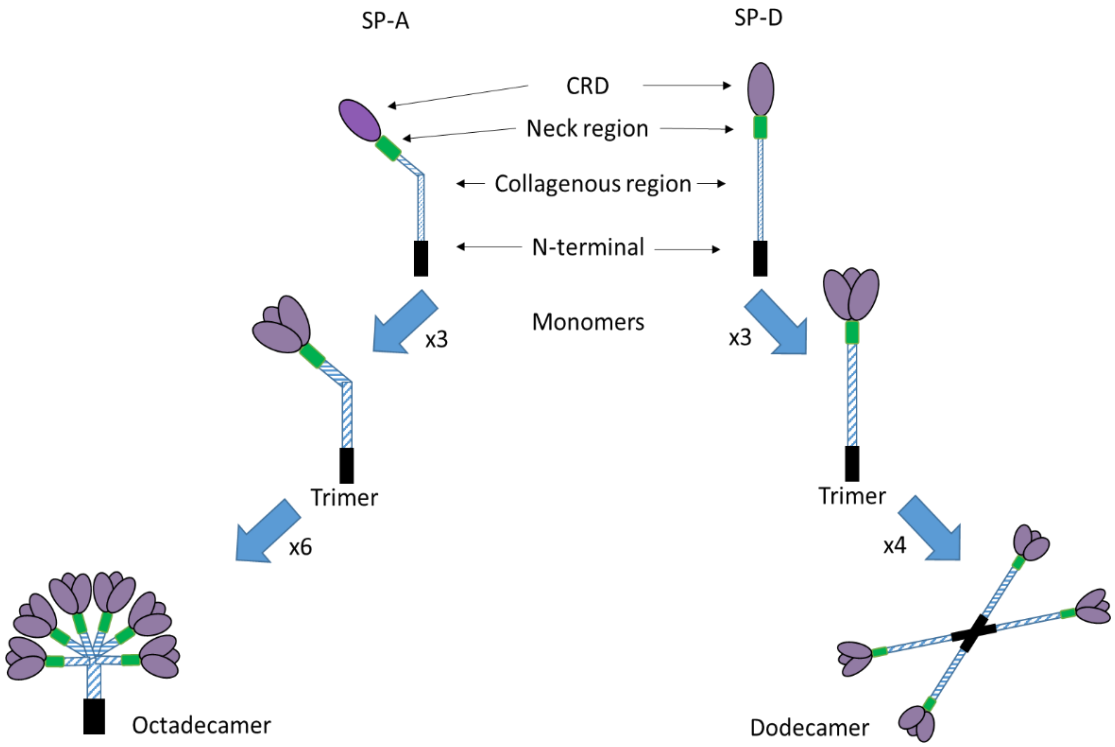

Figure 1.4: Structure and assembly of SP-A and SP-D. Monomers of SP-A and SP-D are composed of a carbohydrate recognition domain (CRD), neck region, collagenous region and N-terminal region. These form trimers which then multimerize to form an octadecamer (SP-A) or dodecamer (SP-D).

1.2.2. Immune functions of SP-A and SP-D

SP-A and SP-D have been described to have numerous innate immune functions, most of which have been described in the lung. These innate immune functions include pathogen recognition (section 1.2.2.1.) and maintaining lung homeostasis (section 1.2.2.2.). Recognition of pathogens by SP-A and SP-D often occurs via their CRDs, and this triggers various immune responses (Figure 1.5). These innate responses include opsonising the pathogen, which leads to enhanced phagocytosis by immune cells such as alveolar macrophages as well as enhanced pathogen killing by neutrophil oxidative responses [57]. Additionally, SP-A and SP-D can agglutinate pathogens, thereby causing them to aggregate and prevent them from entering host cells. SP-A and SP-D also assist with the clearance of apoptotic cells, and they are involved in regulating macrophage function and the production of mediators such as cytokines and reactive species [57,68].

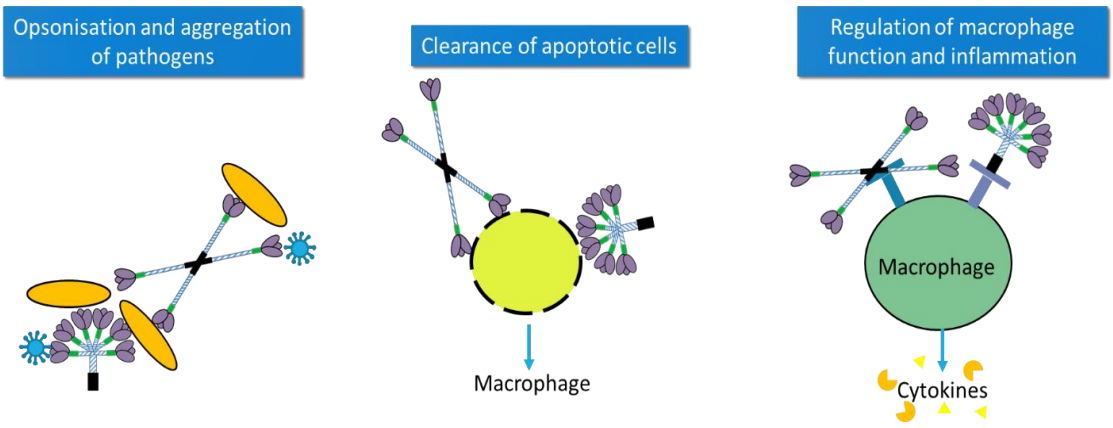

Figure 1.5: Innate immune functions of SP-A and SP-D. SP-A and SP-D have numerous innate immune functions which include interacting with pathogens to either opsonise or aggregate them, clearance of apoptotic cells, and regulating macrophage function and inflammation.

1.2.2.1. Interaction of SP-A and SP-D with pathogens in the lung

Research on the interaction of SP-A and SP-D with certain pathogens has been most extensively done in the context of the lung, but more recent studies have revealed non-pulmonary functions of SP-A and SP-D (section 1.2.3.).

In terms of bacterial recognition, SP-A and SP-D are able to recognise pathogen associated molecular patterns (PAMPs, usually comprising of clustered oligosaccharides) on bacterial surfaces. SP-A and SP-D interact with various bacteria including *Pseudomonas aeruginosa*, *Haemophilus influenza* and *Mycobacterium tuberculosis* (*M.tb*), and this often results in bacterial clearance [69–72]. Often, SP-A and SP-D perform similar functions, but this is not always the case. For example, SP-A and SP-D recognise *M.tb* with contrasting effects: SP-A enhances the uptake of *M.tb* by monocyte-derived macrophages, whereas SP-D agglutinates *M.tb* and inhibits bacterial uptake by these macrophages [71,72]. Additionally, SP-D increases the fusion of macrophage lysosomes with *M.tb* containing phagosomes, thereby facilitating *M.tb* clearance [73]. These results demonstrate that SP-A may be assisting *M.tb* access into its intracellular niche while SP-D is protecting the host from infection, suggesting that SP-D is a more effective innate immune protein in this context.

Early innate immune responses against viral infections are important to protect the host from any significant damage. Influenza A virus (IAV) predominantly infects the

respiratory tract, and it has been demonstrated that both SP-A and SP-D are involved in controlling IAV infection. SP-A interacts with the IAV glycoproteins haemagglutinin and neuraminidase through an N-linked oligosaccharide on the CRD, while SP-D interacts with these viral glycoproteins via the CRD in a calcium-dependent manner [74,75]. These interactions result in aggregation of IAV, which enhances neutrophil binding to the virus and respiratory burst by neutrophils, and this results in clearance of the virus from the lung [74]. SP-D levels in the bronchoalveolar lavage fluid (BALF) increase following IAV infection, further supporting that SP-D has an important role in controlling initial infection [76].

Respiratory syncytial virus (RSV) is an infectious agent of the respiratory system which can give rise to bronchiolitis or pneumonia, especially in infants [77]. The envelope of RSV contains two glycoproteins which are vital for the early stages of infection; the F protein, involved in viral fusion to host cell membranes, and the G protein, responsible for cell attachment [78]. SP-A binds to RSV via the F glycoprotein, and SP-D binds to both the F and G glycoproteins in a calcium-dependent manner [77,78]. These interactions result in RSV opsonisation and therefore, enhanced phagocytosis of RSV by alveolar macrophages. SP-A and SP-D may also act to neutralise the virus, causing a reduction in infection [77,78]. Individuals with polymorphisms in the SP-D gene, especially those located in the N-terminal of SP-D (Met11Thr), have a higher susceptibility to RSV [79]. Additionally, certain alleles of the SP-A2 gene have been linked to more severe RSV in infants [80]. These genetic studies emphasize the importance of SP-A and SP-D in immunity to RSV.

Herpes simplex virus type 1 (HSV-1) usually infects the mucosal layer of the mouth, but it can also cause respiratory infections, especially in immunocompromised individuals [81]. SP-A interacts with HSV-1 via its CRD, and it is suggested that the CRD recognises N- and O-linked carbohydrates on the surface of HSV-1 [82]. This results in HSV-1 being opsonised by SP-A, and this enhances HSV-1 uptake by alveolar macrophages. To date, no studies have been done on SP-D and HSV-1 interactions.

In addition to recognising a variety of bacteria and viruses, SPs also play a role in immune recognition and clearance of various fungi and allergens [63]. Additionally, SP-D has been shown to significantly contribute to host defences against the parasitic helminth

Nippostrongylus brasiliensis [83]. Overall, SP-A and SP-D have a vital role in protecting the lung from infection by pathogens.

1.2.2.2. Role of SP-A and SP-D in maintaining lung homeostasis

By binding to certain receptors on macrophages/immune cells, SP-A and SP-D mediate enhanced phagocytosis of various pathogens as described above. Moreover, SP-A and SP-D enhance apoptotic cell clearance by alveolar macrophages, although SP-A is more effective at this [84]. Clearance of apoptotic cells is vital in maintaining homeostasis, as ineffective clearance may result in post-apoptotic cytolysis or necrosis followed by tissue damage and extended inflammation [85]. SP-A and SP-D can also modulate the inflammatory response by binding to macrophage receptors which either enhances or suppresses the production of proinflammatory molecules; this depends on the binding orientation of the SP to the macrophage receptor. When SP-A or SP-D is bound to a pathogen or allergen by the CRD, the collagenous domain binds to CD91-calreticulin receptors on the macrophage to induce production of proinflammatory cytokines [86]. When there are no foreign particles to interact with, the CRD remains free to interact with signal inhibitory regulatory protein alpha (SIRP-α), suppressing proinflammatory mediator production [86].

The significance of SPs in maintaining lung homeostasis has been well demonstrated in SP-A or SP-D deficient mice. Not only do these mice have increased susceptibility to certain pathogens including *H. influenzae*, group B streptococcus and IAV, but the inflammatory response following infection is also exaggerated [69,87]. Increased inflammation and reactive oxygen species production has been linked to emphysema and pulmonary fibrosis, and mice lacking either SP-D or both SP-A and SP-D do indeed have an emphysemic phenotype [88,89].

In humans, decreased levels of SP-D have been linked to severe asthma and chronic obstructive pulmonary disease; illnesses characterised by increased inflammation [90]. Furthermore, SP-A and SP-D levels are reduced in smokers, which could further contribute to the development of emphysema and other chronic obstructive pulmonary disorders in

these individuals [91]. These findings emphasise the importance of SP-A and SP-D in maintaining lung homeostasis in order to prevent aberrant inflammation and the development of certain inflammatory disorders.

1.2.3. SP-A and SP-D in non-pulmonary sites

As mentioned, SP-A and SP-D were first discovered in the lung, but more recently these proteins were found to be expressed at other sites throughout the body. These non-pulmonary sites include the gastrointestinal tract (GIT), urinary tract, female reproductive tract, eye, coronary artery and central nervous system as reviewed recently by Ujma *et al.* [58]. Their expression at these diverse sites suggests that they have a more general role in innate immunity, rather than just protecting the lung.

In the GIT, SP-A and SP-D are expressed in the epithelial cells of the small and large intestine, and SP-D is also expressed at low levels in the stomach [92,93]. Their functions in the GIT appear to be related to controlling infection and inflammation. Experiments on porcine GIT have showed that SP-D aggregates and enhances the uptake of various gram-negative bacteria [94]. SP-A and SP-D also have protective roles in necrotising enterocolitis, a disease associated with overexpression of TLR4 in the intestine of pre-term infants. Pre-treatment of intestinal cell cultures with SP-D show reduced LPS-induced inflammation [95], while in a rat model of necrotising enterocolitis, oral administration of SP-A reduced intestinal pathology, inflammation and mortality [96]. SP-D in the GIT may also play a role in resolving helminth infections, based on the observation that non-pulmonary SP-D is involved in clearing *N.brasiliensis* infections; however, this is currently not well understood [83].

Urinary tract infections (UTIs) can be caused by external pathogens, and SP-A and SP-D may have a protective role in the urinary tract. Both SP-A and SP-D have been detected in the kidney and in the epithelium of the ureter and bladder [93,97]. SP-A and SP-D inhibit uropathogenic *E. coli* growth *in vitro* [97] and SP-D reduces the adherence of bacteria to human bladder cells [98]. SP-A and SP-D double knockout mice also display an increased susceptibility to UTIs by uropathogenic *E. coli* [97]. In addition to this, polymorphisms in

the SP-A1 or SP-A2 genes have been linked to an increased susceptibility to recurring UTIs, further emphasising that SPs are likely to play a protective role in the urinary tract [99].

In the human female reproductive tract SP-A is located in the myometrium, vaginal epithelium and vaginal lavage fluid, and SP-D has been found in the cervix, vagina and endometrium [100–102]. In pregnancy, SP-A and SP-D can be detected in the placenta, amnion, chorion and the amniotic fluid [102,103]. Numerous studies have shown that SP-A and SP-D may have a protective role in pregnancy. Both SP-A and SP-D levels are elevated in the first trimester decidua (maternal part of the placenta), and the potential function of this is to prevent bacterial infection [104]. This is supported by the observation that SP-A and SP-D reduce lipopolysaccharide (LPS)-induced inflammation by decidual macrophages [105]. Moreover, SP-A-treated amnion explants have decreased cytokine expression, suggesting that SP-A reduces amnion inflammation, therefore protecting the foetus [106].

In addition to having protective roles in pregnancy, the expression of SP-A and SP-D in the female reproductive tract has been suggested to contribute to innate immune defences against sexually transmitted pathogens. An example of this is the observation that SP-D inhibits infection of human cervical epithelial cells (HeLa) by *Chlamydia trachomatis*, and murine infections with *Chlamydia muridarum* enhance SP-D expression in the cervix [107,108]. SP-A and SP-D also interact with HIV via oligosaccharides on the HIV envelope protein gp120 [109,110]. HIV normally infects CD4 T-cells, and SP-A and SP-D binding to HIV inhibits its infectivity of CD4 T-cells, possibly by occluding the CD4 binding site of gp120 [109,110]. In contrast, SP-A and SP-D also enhance HIV uptake by dendritic cells, which can be seen as unfavourable in terms of host immunity to HIV as the dendritic cells transfer the virus to CD4 cells [109,110]. This inhibition of direct infection but enhancement of indirect infection indicate that SP-A and SP-D have contrasting effects in terms of modulating HIV infection.

SP-A and SP-D therefore seem to play a role in the innate immune response of the female genital tract; however, no research has been conducted on their interaction with HPV and on their potential to enhance immune recognition of HPV, thereby reducing or preventing infection.

1.3. Challenges of studying HPV infection in the laboratory

The ability to produce or isolate infectious HPV is important for the study of HPV binding and entry into host cells, as well as studying potential inhibitors of HPV infection. Unfortunately, generating native HPV in the laboratory has proven to be a difficult task. Since the HPV life cycle is linked to keratinocyte differentiation (section 1.1.2.), generating HPV in monolayer cell culture is not viable [14]. The use of organotypic raft cultures and mouse xenografts has allowed for native HPV production, but these methods are laborious and produce low yields of the virus [111–113]. The production of infectious HPV pseudovirions (HPV-PsVs) has been a major breakthrough in the field, as high titres can be produced in a relatively simplistic manner. To produce HPV-PsVs, such as HPV16-PsVs, the virus packaging cell line HEK293TT (established from HEK293 embryonal human kidney cells transformed with sheared adenovirus type 5 and simian virus-40) [114] is transfected with an expression plasmid encoding codon-optimised HPV16 L1 and L2 capsid proteins, as well as a reporter plasmid (Figure 1.6) [115]. Thereafter, the L1 and L2 proteins spontaneously self-assemble into icosahedral capsids harbouring the reporter plasmid, resulting in infectious pseudovirions. The reporter plasmid encoding for example firefly luciferase or green fluorescent protein (GFP), replaces the viral genome and can be used to quantify successful infection.

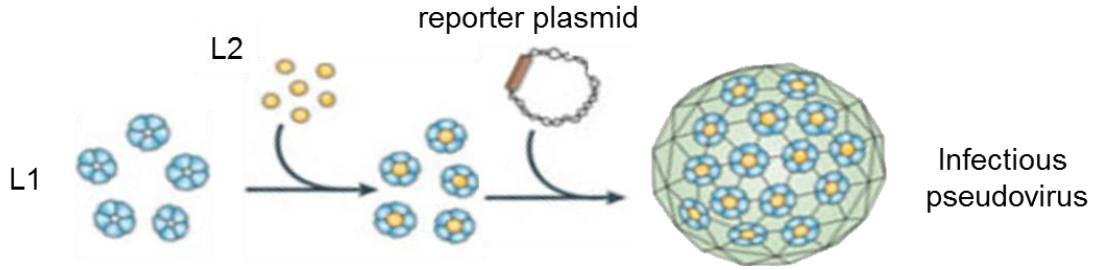

Figure 1.6: Production of infectious HPV-PsVs. HPV-PsVs are produced by transfecting HEK293TT cells with a plasmid encoding type-specific L1 and L2 capsid proteins, as well as a reporter plasmid. This results in the spontaneous self-assembly of non-oncogenic, infectious HPV-PsVs, which can be used to study HPV binding, entry and successful infection.

HPV-PsVs have successfully been used in cell culture experiments as well as *in vivo* experiments. HPV type 16 pseudovirions, being the most common oncogenic HPV type worldwide, are the most widely used in research; however other PsVs types have also been generated and used successfully. Important findings regarding HPV binding and entry have been elucidated using HPV-PsVs; this includes the finding that HSPGs are the initial attachment molecules for HPV, as well as that furin cleavage of the L2 protein is necessary for infection [21,26,116–118].

A major issue with studying HPV using animal models is the highly species-specific modes of infection, i.e. native HPV is unable to cause a productive infection in animals [119]. To overcome this, various animal models using the appropriate animal papillomavirus (eg: bovine papillomavirus in cows) have been used for a variety of applications, such as studying viral transmission and cancer development [119]. The more recent discovery of a murine papillomavirus which is able to infect laboratory mice strains has also provided a valuable and more accessible tool for studying papillomavirus disease and pathology [120,121]. However, the finding that HPV-PsVs successfully recapitulates the initial infection phases in murine genital tissue (following gentle abrasion of the epithelium) has led to the development of a well-established model of HPV infection in mice [122]. This model is advantageous for the study of early entry events, and infection can easily be measured using a variety of read-outs, depending on the reporter plasmid used [122]. For example, live-imaging systems can be used to detect firefly luciferase expression following successful infection [123]. If these systems are unavailable, luciferase assays can be performed on genital tract tissue homogenates. Furthermore, the usage of Gaussia luciferase, which has a signal peptide for secretion, allows luciferase activity to be measured in vaginal lavages which can be performed daily [123]. Therefore, an HPV-PsVs murine cervicovaginal challenge model is a useful tool for studying HPV infection *in vivo*, particularly with regard to modulators of early events in the infection process.

1.4. Hypothesis

It is hypothesised that SP-A and/or SP-D may protect against HPV infection by binding to the virus and functioning as an opsonin, thereby enhancing viral phagocytosis by macrophages and preventing infection of keratinocytes.

1.5. Aim

The aim of this study was to determine whether SP-A and/or SP-D play a role in innate immune recognition of HPV16-PsVs, thereby preventing infection under both *in vitro* and *in vivo* conditions.

1.6. Objectives

- To determine whether HPV16-PsVs bind to purified human SP-A and/or SP-D and whether this affects internalisation by RAW264.7 macrophages *in vitro.*
- To set up the HPV16-PsVs cervicovaginal challenge model [122], using female C57BL/6 mice.
- To observe the effect of surfactant proteins on HPV16-PsVs infection of C57BL/6 mice, using both wildtype and SP-knockout mice.

2. Materials and Methods

2.1. Materials

Unless otherwise stated, chemicals of analytical/reagent grade were used and generally purchased by Merck or Sigma Aldrich. Media, gels and solutions made up in the laboratory are detailed in the Appendix.

2.2. Cell culture

The murine leukemic macrophage cell line RAW264.7 (ATCC®), the human epithelial cervical adenocarcinoma cell line HeLa (ATCC®) and the virus packaging cell line HEK293TT [114,115] were cultured in complete Dulbecco's Modified Eagle Medium (DMEM) (Appendix). All cells were cultured in 75cm^2 cell culture flasks (SPL Life Sciences) and incubated in a humidified atmosphere containing 5% CO_2 at 37°C. Cells were passaged by adding 5mL 0.025% trypsin/0.01% Ethylenediaminetetraacetic acid (EDTA) in phosphate buffered saline (PBS) for 5 minutes at 37°C. 5mL complete medium was then added, and cell suspensions were centrifuged in 15mL Falcon tubes (SPL Life Sciences) at 425 x g for 2 minutes to pellet cells. Media was removed from the tubes and cell pellets resuspended in 10mL complete medium. 2mL of the cell suspension was transferred to a 75cm^2 cell culture flask containing 10mL complete medium. Cells were passaged twice a week.

To count cells for seeding, 10µL cell suspension was added to 90µL trypan blue, which stains dead cells. 10µL of this solution was placed on a Neubauer haemocytometer (Marienfeld) with a coverslip placed on top. Bright unstained live cells were counted using a microscope (Nikon TMS) and cell concentration was determined using the following formula:

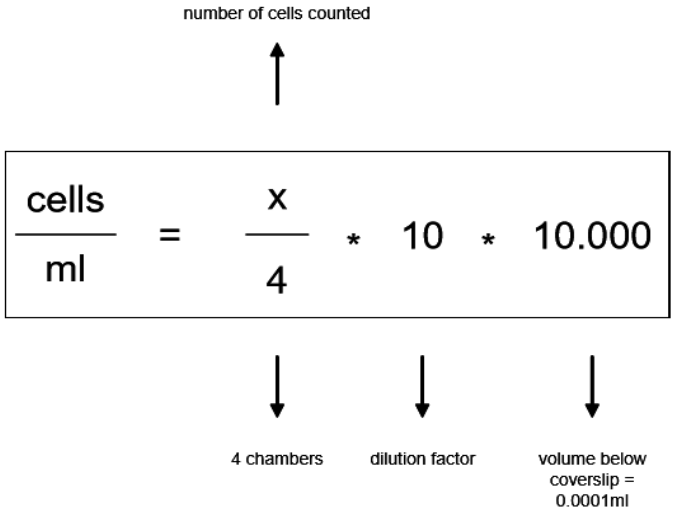

Cells were seeded at the densities described below for individual experiments.

2.3. Studying HPV infection using HPV16-PsVs

To study HPV infection *in vitro* and *in vivo*, non-oncogenic infectious pseudovirions (HPV16-PsVs) were generated according to the protocol by Christopher Buck [115]. These pseudovirions contain a reporter plasmid, which enables quantification of infection once the pseudovirus has successfully infected cells. In the majority of the experiments presented herein, HPV16-PsVs particles containing the firefly luciferase (FLuc) reporter plasmid pGL3 (Promega) were used, which results in the transcription and translation of intracellular luciferase.

In certain *in vivo* experiments, HPV16-PsVs particles containing the Gaussia luciferase (GLuc) reporter plasmid pCMV-GLuc 2 (New England Biolabs) were used. Gaussia luciferase is a protein derived from the marine copepod *Gaussia princeps*, which contains an internal signal peptide for secretion [124]. Since it is secreted, using HPV particles containing Gaussia luciferase can be advantageous in certain experiments (such as time course experiments) as luciferase activity can be measured directly from body fluids (such as vaginal lavages) without sacrificing the animal (see section 2.9.3.2.).

Fluorescently labelled HPV16-PsVs particles can also be used to determine viral internalisation by flow cytometry and microscopy. In these experiments, Alexa Fluor 488 was used to label HPV16-PsVs (see section 2.3.2.).

2.3.1. Production of HPV16-PsVs

To produce HPV16-PsVs, HEK293TT cells were seeded in sixteen 10cm dishes (Greiner Bio-One) in complete DMEM and incubated overnight at 37°C. Per plate, cells were transfected with the following plasmids, using the calcium phosphate method: 5µg pXULL [115] (which encodes codon-optimised HPV16 L1 and L2) together with either 12µg pGL3 (firefly luciferase) or 12µg pCMV-GLuc 2 (Gaussia luciferase). After 48 hours, cells were harvested by trypsinization and centrifuged at 425 x g for 2 minutes in a 50mL Falcon tube to pellet cells. The cell pellet was resuspended in 1mL 1X PBS and transferred to a 1.5mL siliconized Eppendorf tube.

The cell suspension was centrifuged at 956 x g for 5 minutes. The PBS was removed and the cell pellet resuspended in an equal amount of PBS + 9.5mM $MgCl_2$. 1/20 Vol fresh 5% Brij58 was added to lyse the cells, as well as 1µL Benzonase (Sigma Aldrich) and 1µL Exonuclease V (New England Biolabs) for digestion of free (un-encapsidated DNA). The solution was incubated at 37°C for 24 hours with occasional mixing to allow for particle maturation. The lysate was then chilled on ice and 0.17 Vol PBS + 5M NaCl added, followed by three freeze/thawing (-80°C) cycles. The lysate was then centrifuged at 8000 x g for 10 minutes at 4°C to pellet cell debris, followed by Alexa Fluor 488 labelling (section 2.3.2.) and HPV16-PsVs purification (section 2.3.3.).

2.3.2. HPV16-PsVs labelling with Alexa Fluor 488

To assess viral uptake 1 to 24 hours after infection by flow cytometry or fluorescent microscopy, HPV16-PsVs particles were fluorescently labelled with Alexa Fluor 488 succinimidyl ester (AF488, Invitrogen) before CsCl gradient purification (see 2.3.3.). Prior to labelling, the cell lysate's pH was adjusted with addition of 1/10 Vol 1M $NaHCO_3$, pH 8.8. 1/10 Vol AF488 (stock: 10mg/mL in DMSO) was added to the lysate and incubated for 1 hour at room temperature (RT) in the dark, rotating. The pH was then corrected by adding 1/25 Vol 1M $NaPO_4$, pH 6.5.

2.3.3. HPV16-PsVs Purification

Caesium chloride ultracentrifugation was used to separate HPV16-PsVs particles from cell lysates. This was done by loading the lysate onto a discontinuous CsCl gradient, prepared as follows: 4mL light CsCl (1.25 g/mL in 1X HSB, see Appendix) was added to a 13.2mL Ultra-Clear™ centrifuge tube (Beckman Coulter) followed by 4mL heavy CsCl (1.4 g/mL in 1X HSB) which was added gently beneath the light CsCl layer. The interface between the two layers was marked on the tube. The cell lysate was then made up to 3.5mL with 1X HSB buffer and gently added to the top of the CsCl gradient. Tubes were centrifuged for 16-18 hours at 20 000 rpm in a Beckman SW40Ti swinging bucket rotor. Following ultracentrifugation, the tubes were carefully removed from the rotor and clamped to a ring stand in a biosafety cabinet. The viral particles were then extracted from the faint viral band (seen slightly above the CsCl interface) using an 18-gauge needle attached to a 5mL syringe inserted below the CsCl interface. After gently removing the needle from the tube, the remaining liquid was drained into a beaker containing Virkon disinfectant. The sample was then transferred to an Amicon Ultra-4 Centrifugal filter unit (Millipore) and centrifuged at 956 x g for 10 minutes, to concentrate the pseudovirions. This was followed by washing with 3mL HSB buffer and centrifuging at 956 x g for 10 minutes, or until the sample was concentrated to approximately 100µL. The protein concentration of HPV16-PsVs preparations was then quantified using the Pierce™ BCA Protein Assay Kit (Thermo Scientific) (see section 2.7.). HPV16-PsVs preparations were stored at -80°C.

2.3.4. Quality checks of HPV16-PsVs preparations

2.3.4.1. SDS-PAGE and silver staining

SDS-PAGE gels were used to determine the purity of HPV16-PsVs preparations. 3µL of each HPV16-PsVs preparation was loaded and electrophoresed as per section 2.5. AF488-labelled HPV16-PsVs preparations were visualised using a Biospectrum™ 500 Imaging System (Ultra Violet Products, UVP) to detect fluorescent bands at 55kDa, corresponding to AF488 labelled L1 protein which is in excess compared to L2 (10-fold higher than L2) [20]. Gels were then stained to visualise the L1 and L2 proteins (and possible impurities) of the HPV16-PsVs using the Pierce™ Silver Stain Kit (Thermo Scientific), according to the manufacturer's instructions.

Briefly, SDS-PAGE gels were washed in dH_2O and then fixed in a 30% ethanol: 10% acetic acid solution for 15 minutes. This was followed by further washing with 10% ethanol and dH_2O for 5 minutes each. Gels were then sensitized for staining using a sensitizer working solution (provided in kit) for 1 minute, followed by 2 X 1 minute washes with dH_2O. Gels were then stained for 30 minutes using the silver stain solution, followed by 3 minutes of developing using the developing solution (both provided in kit). A predominant L1 band at 55kDa as well as a less predominant L2 band at 75kDa were expected in pure preparations.

2.3.4.2. Luciferase infection assay

Luciferase assays were performed to determine the infectivity of HPV16-PsVs preparations. Briefly, HeLa cells were seeded in 12-well plates (Greiner Bio-One) at a density of 50 000 cells per well and incubated overnight at 37°C. Cells were then infected with HPV16-PsVs in duplicate as follows, for 24 hours:

- HPV16-PsVs only,
- HPV16-PsVs preincubated for 1 hour at 4°C with the HPV16 neutralising antibody H16.V5 (positive control: expected to abolish infection),
- HPV16-PsVs preincubated for 1 hour at 4°C with the HPV18 neutralising antibody H18.J4 (negative control: as HPV18 antibody should not recognise HPV16-PsVs, infection should not be effected),
- HPV16-PsVs treated for 1 hour at 37°C with DNase I endonuclease (Thermo Scientific). This will cleave any un-encapsidated plasmid, so that any measured luciferase is due to infection only.

The H16.V5 and H18.J4 neutralising antibodies were provided by Neil D. Christensen, Pennsylvania State University College of Medicine, USA.

For HPV16-PsVs particles containing FLuc, cells were washed with 500µL 1X PBS and lysed by adding 100µL 1X Cell Culture Lysis Reagent (Promega) followed by scraping with the back of a 100µL-pipette tip. This allowed for any translated luciferase to be released from cells. Cell lysates were then transferred to Eppendorf tubes and centrifuged at 10620 x g for 2 minutes to pellet cell debris. 20µL of each sample's supernatant was added to a white 96-well plate

(Nunc) and measured using a Fluoroskan™ Ascent Microplate Fluorometer and Luminometer (Thermo Scientific) following the Luciferase Assay System (Promega) protocol. 100µL Luciferase Assay Substrate (Promega) was added to each well by the luminometer and luminescence measured with no lag time over 10 seconds integration time.

For HPV16-PsVs particles containing GLuc, 5µL cell supernatant was added to a white 96-well plate (Nunc) and measured using a Fluoroskan™ Ascent Microplate Fluorometer and Luminometer (Thermo Scientific) following the Gaussia Luciferase Assay Kit (New England Biolabs) protocol. Per sample, freshly prepared GLuc Assay Solution consisting of 0.5µL BioLux GLuc Substrate added to 50µL BioLux Assay Buffer (New England Biolabs) was added per well and luminescence measured with 40 seconds lag time over 10 seconds integration time.

Raw luciferase data (arbitrary units) were normalised to protein concentration (mg/mL) of the sample. Protein concentration was determined using the Pierce™ BCA Protein Assay Kit (Thermo Scientific) as per the manufacturer's instructions (section 2.7.).

2.4. Co-Immunoprecipitation

Co-immunoprecipitation (Co-IP) experiments were performed to biochemically determine whether SP-A and/or SP-D interact with HPV16-PsVs, using some reagents of the Pierce™ Co-immunoprecipitation kit (Thermo Scientific). This technique involves using an antibody recognising a protein of interest/bait protein (either HPV16 L1, SP-A or SP-D) and Protein G sepharose beads which bind to the antibody and can be used to "pull down" the protein of interest as well as any interacting/prey proteins. These samples can then be analysed by SDS-PAGE and Western Blotting to detect any prey proteins that have been co-immunoprecipitated with the bait protein.

Prior to Co-IP, 5µg purified human SP-A or recombinant human SP-D (both proteins provided by Howard Clark and Jens Madsen, University of Southampton, UK) were preincubated with 0.2µg HPV16-PsVs (or without HPV16-PsVs as a control) in complete DMEM for 1 hour at 4°C. Lysis/Wash Buffer (Thermo Scientific) was added to bring each solution's total volume to 150µL. 5µL of each of these "input" samples were kept aside for analysis. 2.5µg antibody (either CamVir1 against HPV16-L1, anti-SP-A or anti-SP-D) was then added to the appropriate

samples and incubated overnight at 4°C, rotating. 25µL Protein G Sepharose beads were added to each reaction, and tubes were incubated for 2 hours at 4°C, rotating. Each reaction was added to a separate spin column (Thermo Scientific) to simplify sample collection. Flow through (FT) samples were collected by centrifugation at 1000 x g for 1 minute. The Protein G beads were then washed by adding 200µL Lysis/Wash Buffer and centrifuging at 1000 x g for 1 minute. The wash step was repeated twice. A further wash step was performed with 100µL 1X Conditioning Buffer (Thermo Scientific) followed by centrifugation at 1000 x g for 1 minute to improve elution. 10µL Elution Buffer (Thermo Scientific) was added to each column and centrifuged at 1000 x g for 1 minute. A further 30µL Elution buffer was added to each column and incubated for 5 minutes at RT. Columns were centrifuged at 1000 x g for 1 minute to collect remaining eluate.

Input, FT and eluate samples were analysed by SDS-PAGE followed by Western Blotting (see section 2.5. and 2.6.). 3µL input and FT and 20µL eluate were loaded per gel. After transfer and blocking, CamVir1 primary antibody (Abcam) was added in a 1:2500 dilution in 5% fat free milk powder in PBS-Tween and incubated overnight at 4°C while shaking to detect presence of the HPV16 L1 protein. The membrane was then incubated with a goat-anti-mouse secondary antibody (1:5000 dilution in 5% fat free milk powder in PBS-Tween) and visualised as described in section 2.6.

2.5. Sodium Dodecyl Sulphate Polyacrylamide Gel Electrophoresis (SDS-PAGE)

SDS-PAGE is used to separate proteins based on their molecular weights. SDS-PAGE gels consisting of a 10% separating and 3% stacking gel were prepared (Appendix). Proteins from various experimental samples as indicated were suspended in 5X Lane Marker Sample Buffer (Thermo Scientific) containing dithiothreitol (DTT), then heated at 95°C for 5 minutes prior to loading the desired amount onto the gel. A Colour Prestained Protein Standard, Broad Range protein marker (11–245kDa, New England Biolabs) was used to estimate protein molecular weights. Protein samples were electrophoresed in 1X SDS-PAGE running buffer (Appendix) at 100V for 1 hour.

2.6. Western Blot

Western Blotting was performed to detect specific proteins in cell lysates, homogenates or protein mixtures. Following SDS-PAGE, proteins were transferred to a 0.2µm nitrocellulose membrane (Bio-Rad). The transfer stack was assembled in 1X tris-glycine transfer buffer (Appendix) according to Figure 2.1. Protein transfer was performed in 1X tris-glycine transfer buffer for 1 hour at 100V in the cold to mitigate heat production. Ponceau S (Appendix) was then used to determine successful protein transfer. The membrane was then washed in PBS-Tween (Appendix) to remove residual Ponceau S. Following this, the membrane was incubated in 5% fat free milk powder in PBS-Tween at RT for at least 1 hour shaking, to block non-specific protein binding sites. Primary antibody was added in 5% fat free milk powder in PBS-Tween and incubated overnight at 4°C, shaking. The membrane was then washed with PBS-Tween for 3 X 10 minutes to remove any unbound antibody. Appropriate secondary antibodies conjugated to horseradish peroxidase (HRP) were added in 5% fat free milk powder in PBS-Tween in a 1:5000 dilution and incubated for 1 hour at RT, shaking. The membrane was then washed as abovementioned to remove any unbound secondary antibody. Lumi-Glo chemiluminescent substrate (KPL) was used according to the manufacturer's instructions to visualise the proteins of interest. Chemiluminescence was visualised using a Biospectrum™ 500 Imaging System (Ultra Violet Products, UVP).

To remove any primary and secondary antibody bound to the membrane as a prerequisite for re-probing the membranes, a harsh stripping solution was used (Appendix). Stripping was performed for 5 minutes at RT shaking, and this was repeated 3 times. The membrane was then washed with PBS-Tween 3 X 10 minutes and then blocked with 5% fat free milk powder in PBS-Tween for 1 hour. The membrane was then re-probed with the appropriate primary antibody overnight at 4°C, followed by washing and incubation with the appropriate secondary antibody as described above.

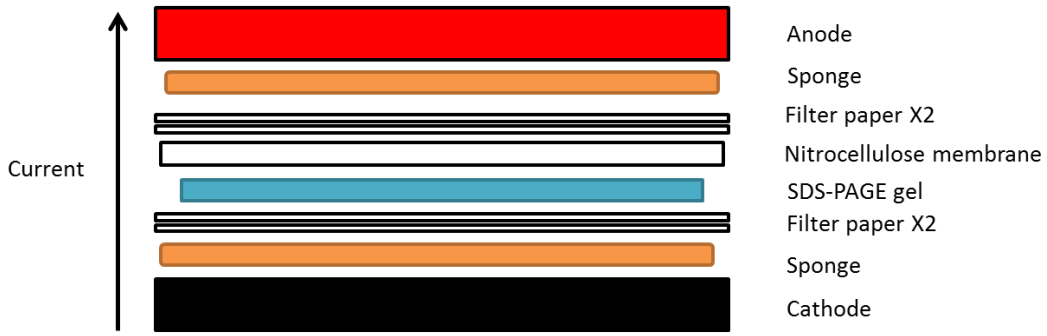

Figure 2.1: Transfer stack assembly for wet transfer Western Blot.

2.7. Protein concentration determination

The protein concentration of various samples was determined using the Pierce™ BCA Protein Assay Kit (Thermo Scientific) as per the manufacturer's instructions. Briefly, 200µL BCA working reagent (solution A and B mixed in a 50:1 ratio) was added to 3µL sample in clear 96-well plates (Greiner Bio-One) and incubated at 37°C for 30 minutes. Absorbance was measured at 562nm using an iMark™ Microplate Reader (Bio-Rad) and Microplate Manager Software (version 6, Bio-Rad). A standard curve of known concentrations (between 0 and 2mg) of bovine serum albumin (BSA) was used to calculate the protein concentration of various samples.

2.8. Flow Cytometry

Various flow cytometry experiments were conducted to quantify viral internalisation by RAW264.7 macrophages. These involved using AF488-labelled HPV16-PsVs, as AF488 emits fluorescence when excited by a 488nm laser, allowing for detection of any internalised virus. All conditions tested were performed in duplicate on RAW264.7 cells, with three independent biological repeats.

2.8.1. Viral internalisation in the presence of SP-A or SP-D

RAW264.7 cells were seeded in 6-well plates (Greiner Bio-One) at a density of $5x10^5$ cells per well and incubated overnight at 37°C. Before addition to cells, per well 0.5µg AF488-labelled HPV16-PsVs were incubated with 5µg purified SP-A, recombinant SP-D or BSA for 1 hour at 4°C. Cells were infected with these preincubated AF488-labelled HPV particles for 1 hour at 37°C. Following infection, medium was removed from each well and cells were washed 3 times with 1X PBS. Cells were harvested by incubating cells with 200µL trypsin/EDTA for 5 minutes at 37°C, which also removed any cell-surface bound virus to allow for quantification of internalisation only [125,126]. 400µL complete DMEM was then added to each well and cells were gently scraped using the back of a 100µL pipette tip to assist with cell harvesting. Cell suspensions were transferred to 1.5mL Eppendorf tubes and centrifuged at 700 x g for 2 minutes at 4°C. The supernatant was removed and each cell pellet resuspended in 500µL FACS wash (Appendix). Cells were centrifuged at 700 x g for 2 minutes at 4°C and the supernatant removed. Cells were fixed by resuspending the cell pellets in 300µL FACS fix (Appendix) and samples were then transferred to 5mL polystyrene round-bottom tubes (Falcon) and kept at 4°C until analysis. Samples were prepared in dark conditions to prevent fading of the AF488 fluorescence.

Data were acquired using a BD FACSCalibur™ together with the BD CellQuest™ Pro software (Version 5.2.1, BD Biosciences). Acquisition parameters were determined using uninfected cells (negative control). The cell population was gated using the dot plot showing forward scatter (FSC) versus side scatter (SSC) of the negative control (Supplementary Figure 1). Gating was done to exclude any contaminants and cell debris. Dot plots of fluorescence in the FL1 channel (AF488 positive cells) versus SSC were generated in BD CellQuest™ Pro and quadrant statistics determined.

Statistical analysis was performed on the percentage of AF488 positive cells (cells observed in the lower right quadrant) for the gated cell population. Data was assessed for normality using the Shapiro-Wilk test in STATA. One-way analysis of variance (ANOVA) and Tukey post-hoc tests were performed using Graph Pad Prism 5 (Graph Pad Software), to determine the differences in viral internalisation between different conditions tested.

2.8.2. SP-A and AF488-HPV16-PsVs interaction

To characterise SP-A-mediated AF488-HPV16-PsVs internalisation by RAW264.7 cells, experiments using mannose, calcium and EDTA were performed. RAW264.7 cells were seeded in 6-well plates at a density of $5x10^5$ cells and incubated overnight at 37°C. 5µg SP-A was preincubated with: 20mM, 100mM and 200mM mannose in PBS; 2mM and 5mM $CaCl_2$; and 2mM and 5mM $CaCl_2$ with 10mM EDTA. This preincubation was done for 1 hour at 37°C. AF488-HPV16-PsVs was added to each tube and incubated for 1 hour at 4°C. Cells were infected, harvested and analysed as described in 2.8.1.

2.9. *In vivo* infection of female C57BL/6 mice with HPV16-PsVs

All *in vivo* experiments were performed on female, 6-10-week-old C57BL/6 mice (University of Cape Town, UCT). Mice were housed in the UCT Research Animal Facility (RAF) Biosafety Level 2 laboratory in individually ventilated cages, with 4-6 mice per cage. Food pellets and water were always available, and cages contained sawdust bedding and shredded tissue paper as well as a red house for enrichment. Animal welfare was monitored daily, which included weighing the mice to detect any weight loss. While any procedures were performed, mice were kept warm using an infrared lamp, and constantly monitored. All experiments were approved by the Faculty of Health Sciences Research Animal Committee at UCT (ethics number: 016/008).

In vivo experiments were based on the protocol by Roberts *et al.* [122] and performed with assistance from Dr Georgia Schäfer or Alisha Chetty. 4 days prior to infection, mice were injected subcutaneously (s.c.) with 100µL 2mg/20g Depo-Provera (Pfizer) to equilibrate hormone levels as well as to help facilitate infection by thinning the vaginal epithelium (Figure 2.2.) [122]. 6 hours before infection, mice were lightly anaesthetised by intra-peritoneal (IP) injection with 125µL 1.5mg/20g ketamine + 0.2mg/20g xylazine. Following this, vaginal lavages were performed with 50µL sterile PBS. 25µL 4% nonoxynol-9 (N-9, US Pharmacopeia) in 3% carboxymethylcellulose (CMC) was then added to the genital tract, as N-9 is known to chemically disrupt the vaginal and cervical epithelium, facilitating HPV infection [127]. After 6 hours, mice were anaesthetized as above and infected intravaginally (i.vag.) with 3µg

HPV16-PsVs (unless otherwise indicated) in 3% CMC. Control mice (uninfected mice) were also anaesthetized and 3% CMC was added i.vag. For time course experiments, vaginal lavages were performed daily with 50µL sterile PBS and stored at -80°C until analysis. Depending on the read-out as indicated, 1 day or 3 days post infection (p.i.), mice were euthanized using halothane and death was confirmed by cervical dislocation. Following confirmation of death, vaginal lavages were performed with 50µL sterile PBS. The peritoneal cavity was opened using dissecting scissors, and the genital tract exposed by moving the cecum and colon. The bladder was then cut away from the vagina, and the genital tract excised. Fat and connective tissue were then removed from the genital tract tissue (Figure 2.3.). The fallopian tubes and ovaries were removed, and the remaining genital tract (uterus, cervix and vagina) was processed as described in section 2.9.1.1, 2.9.3.1 and 2.9.4.

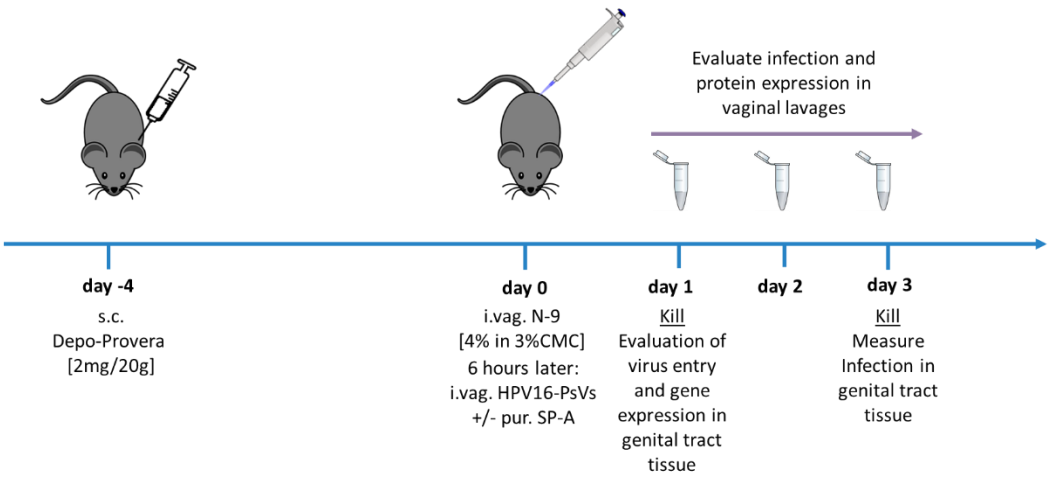

Figure 2.2: Mouse model for HPV16-PsVs infection using C57BL/6 mice, adapted from Roberts *et al.* [122].

To determine the effect of SP-A on HPV16 infection *in vivo*, 3µg HPV16-PsVs was pre-incubated with 1 and 10-fold excess (w/w) of SP-A in 1X PBS (total volume of 25µL per mouse) as indicated, for 1 hour at 4°C prior to infection as mentioned above.

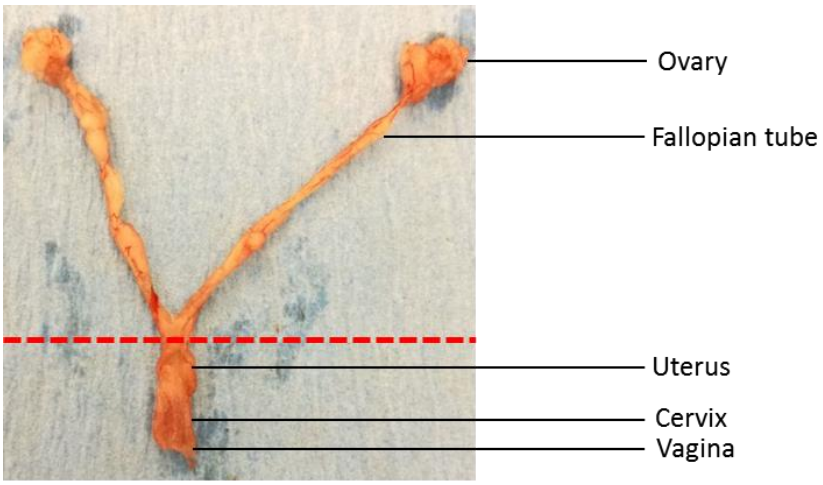

Figure 2.3 Female C57BL/6 mouse genital tract. Red line indicates where tissue was cut, and only tissue below this line was used in experiments.

2.9.1. Processing of samples from *in vivo* HPV16-PsVs infection of female C57BL/6 mice

2.9.1.1. Quantification of infection using firefly luciferase assays

To measure luciferase activity in vaginal lavages, 4µL 5X Cell Culture Lysis Reagent (Promega) was added to 16µL lavage in order to lyse cells shed in the lavage and release any translated luciferase enzyme. This solution was briefly mixed and allowed to incubate for 30 minutes at RT. Following this, samples were centrifuged at 10620 x g for 10 minutes at 4°C. Supernatants were then removed and added to a new Eppendorf tube. 20µL of each sample was added to a white 96-well plate (Nunc) and measured using a Fluoroskan™ Ascent Microplate Fluorometer and Luminometer (Thermo Scientific) following the Luciferase Assay System (Promega) protocol. 100µL Luciferase Assay Substrate (Promega) was added to each well by the luminometer and luminescence measured with no lag time over 10 seconds integration time.

To measure luciferase activity in genital tract tissue, tissue was first snap frozen in liquid nitrogen and stored at -80°C until needed. Tissue was homogenised on ice in 500µL 1X Cell Culture Lysis Reagent (Promega) using a Polytron™ PT1200E handheld homogenizer (Kinematica) for 3 minutes or until the tissue was sufficiently homogenised. Homogenates were then centrifuged at 10620 x g for 10 minutes at 4°C to pellet tissue debris. The

supernatants were then removed and placed into new Eppendorf tubes. Samples were then added to a white 96-well plate and measured as described for the vaginal lavages.

Raw luciferase data (arbitrary units) were normalised to protein concentration (mg/mL) of the sample. Protein concentration was determined using the Pierce™ BCA Protein Assay Kit (Thermo Scientific) (section 2.7.).

2.9.1.2. Quantification of infection using Gaussia luciferase assays

To measure luciferase activity in the vaginal lavages of mice infected with GLuc HPV16-PsVs, 5µL lavage was added directly to a white 96-well plate and measured using a Fluoroskan™ Ascent Microplate Fluorometer and Luminometer (Thermo Scientific) following the Gaussia Luciferase Assay Kit (New England Biolabs) protocol. Per sample, freshly prepared GLuc Assay Solution consisting of 0.5µL BioLux GLuc Substrate added to 50µL BioLux Assay Buffer (New England Biolabs) was added per well and luminescence measured with 40 seconds lag time over 10 seconds integration time.

To measure luciferase activity in the genital tract, tissue was first homogenised and the supernatant removed from the tissue debris as described in section 2.9.1.1. 10µL of the supernatant was added to a white 96-well plate and measured as described for the vaginal lavages above.

Raw luciferase data were normalised as described above.

2.9.2. Protein expression analysis

Western blotting was used to detect expression of SP-A protein in tissue samples from naïve as well as HPV16-PsVs challenged mice at the indicated time points. Briefly, 20µg vaginal lavage or genital tract homogenate was subjected to SDS-PAGE as described in section 2.5. Proteins were then transferred to a 0.2µm nitrocellulose membrane, stained with Ponceau S and blocked as described in section 2.6. Rabbit-anti-mouse SP-A primary antibody was added in 5% fat free milk powder in PBS-Tween at a 1:5000 dilution and incubated overnight at 4°C, shaking. The membrane was then washed 3 X 10 minutes in PBS-Tween. Mouse-anti-rabbit

secondary antibody (Jackson Laboratories) was added in 5% fat free milk powder in PBS-Tween in a 1:5000 dilution and incubated for 1 hour at RT, shaking. The membrane was then washed and visualised as described in section 2.6.

2.9.3. Gene expression analysis

2.9.3.1. RNA extraction

RNA was extracted from uninfected murine tissue (lung and genital tract) and HPV16-PsVs challenged murine tissue (genital tract) using the TRIzol™ Reagent protocol (Invitrogen). Briefly, 50mg tissue was homogenized in 500µL TRIzol (Life Technologies), using a Polytron™ PT1200E handheld homogenizer (Kinematica). Following this, an additional 500µL TRIzol was added to the homogenate and incubated for 5 minutes at RT to allow for complete dissociation of nucleoprotein complexes. 200µL chloroform was then added to the homogenate and the tube inverted 5 times, followed by a 3 minute incubation at RT. Samples were then centrifuged at 12 000 x g for 15 minutes at 4°C to allow for phase separation (lower red phenol-chloroform phase, middle white interphase and upper clear aqueous phase). The upper aqueous phase (containing the RNA) was carefully transferred to a new tube and 500µL isopropanol was added to it. Tubes were then gently inverted and left to incubate at RT for 10 minutes, followed by centrifugation at 12 000 x g for 10 minutes at 4°C. The supernatant was then removed, and the RNA pellet was resuspended in 1mL 75% ethanol. This was then briefly vortexed and centrifuged at 7 500 x g for 5 minutes at 4°C. The supernatant was removed and the pellet allowed to air dry for 10 minutes. RNA pellets were then resuspended in 30µL nuclease free water (Thermo Scientific) and the concentration measured using a NanoDrop 2000 Spectrophotometer (Thermo Scientific). RNA purity was determined by ensuring that sample ratios of absorbance 260/230 and 260/280 were above 2 and 1.8, respectively.

2.9.3.2. DNase I treatment

To remove any genomic DNA from RNA samples, samples were treated with DNase I endonuclease (Thermo Scientific). Briefly, 1µL 10X Reaction Buffer (containing Mg^{2+}) and 1U DNase was added to 1µg extracted RNA. The volume was then made up to 10µL with nuclease free water, and samples were incubated for 30 minutes at 37°C. Samples were then cleaned by ethanol precipitation (section 2.9.3.3.).

2.9.3.3. Ethanol precipitation

Ethanol precipitation was performed to remove any DNase I from RNA samples. Briefly, DNase I treated RNA samples were made up to 400µL with nuclease free water, and 50µL 3M sodium acetate as well as 1.5mL 96% ethanol was added. Samples were vortexed for 10 seconds and stored at -80°C overnight. The following day, samples were centrifuged at 13 000 x g for 20 minutes at 4°C. The supernatant was then removed and 200µL cold 96% ethanol was added to each sample. Following centrifugation at 13 000 x g for 5 minutes, the ethanol was removed and the pellet left to air dry for 20 minutes. The pellet was then resuspended in 10µL nuclease free water and RNA concentration and purity measured as described in section 2.9.3.1.

2.9.3.4. Reverse transcription of RNA

RNA was reverse transcribed using the High Capacity cDNA reverse transcription kit (Applied Biosystems), according to the manufacturer's instructions. Briefly, a 2X Reverse Transcription master mix was prepared containing the following: 0.8µL 100mM deoxynucleotide triphosphate (dNTP) mix, 2µL 10x RT Random Primers, 2µL 10X RT Buffer, 1µL MultiScribe™ Reverse Transcriptase (50U/µL), 1µL RNase Inhibitor and 3.2µL nuclease free water. For each reaction, 1µg RNA was made up to a total volume of 10µL with nuclease free water in PCR tubes. 10µL of the 2X Reverse Transcription master mix was then added to each RNA sample, and mixed by gentle pipetting. PCR tubes were then sealed and briefly centrifuged prior to reverse transcription under the following conditions using the Gene Amp® PCR system 2700 (Applied Biosystems): 25°C for 10 minutes annealing, 37°C for 120 minutes elongation and

85°C for 5 minutes denaturing. The generated cDNA samples were then stored at -20°C until needed.

2.9.3.5. Polymerase chain reaction (PCR)

To determine the expression of selected genes, PCR was performed on the cDNA samples derived from the reverse transcription step (2.9.3.4.) using gene-specific primers (Table 2.1.). The PCR reaction mix containing 2.5µL 10X DreamTaq Buffer (Fermentas), 1µL 10µM forward primer, 1µL 10µM reverse primer, 1µL 10µM dNTP mix, 0.2µL DreamTaq (5U/µL) and 17.5µL nuclease free water was added to 1µL cDNA (or water as negative control) and mixed by gentle pipetting. PCR tubes were then sealed and briefly centrifuged prior to PCR. The parameters in Table 2.2. were used for thermal cycling on the Gene Amp® PCR system 2700 (Applied Biosystems). Following this, PCR products were electrophoresed as described in section 2.9.3.6.

Table 2.1: Primers used for PCR analysis of cDNA

Gene	Forward primer 5'-3'	Length (bp)	Reverse primer 5'-3'	Length (bp)	Amplicon length (bp)
SP-A	ACCTGGATGAGGAGCTTAGACTGC	25	TGCTTGCGATGGCCTCGTTCT	21	225
Gapdh	CCAATGTGTCCGTCGTGGATCT	22	GTTGAAGTCGCAGGAGACAACC	22	148
pGL3	CGGGCGCGGTCGGTAAAGT	19	AACAACGGCGGCGGGAAGT	19	380

Table 2.2: PCR thermal cycling conditions

Step	Temperature (°C)	Time	Cycles
Initial denaturation	95	3 minutes	1
Denaturation	95	30 seconds	35
Annealing	60	30 seconds	
Extension	72	30 seconds	
Final extension	72	5 minutes	1

2.9.3.6. Agarose gel electrophoresis

Agarose gel electrophoresis was used to visualise PCR products. 5µL PCR product was mixed with 1µL 6X DNA loading dye (Appendix) and loaded onto a 100mL 2% agarose gel containing 6µL Sybr Safe (Invitrogen). 5µL O'GeneRuler 100bp DNA ladder (Thermo Scientific) was also loaded onto the gel in order to determine product sizes. Products were electrophoresed for 1 hour at 100V in 1X TAE buffer (Appendix). Gels were visualised using a G:Box Imaging System together with the GeneSnap Imaging software (Syngene).

2.9.4. Immunohistochemistry

To visualise macrophages and viral particles by immunohistochemistry (IHC), the genital tract tissue dissected from uninfected and AF488-HPV16-PsVs (preincubated with BSA or SP-A) infected mice was prepared for cryosectioning following standard procedures. Briefly, the genital tract tissue was first placed in 4% paraformaldehyde for 1 hour to fix the tissue which was then washed 3 X 10 minutes in 1X PBS. Following washing steps, the tissue was suspended in a 30% sucrose solution overnight at 4°C in order to displace any water from cellular spaces and therefore "cryoprotect" the tissue. Excess sucrose solution was then removed from the tissue by gently blotting with paper towel, and tissue was embedded in Optimal Cutting Temperature (OCT, Sakura Finetec USA) compound in a plastic mould (Sakura Finetec USA) and frozen over dry ice. Tissue blocks were stored at -80°C until cryosectioning. Tissue sections of 20µm were cut using a Leica CM1850 cryostat. These sections were placed on microscope slides coated with 3-Aminopropyltriethoxysilane (APES), which allowed the tissue to adhere to the slides. Samples were then air dried overnight, protected from light. Slides were stored at 4°C for up to a week or at -80°C long-term, protected from light.

Before any IHC staining, samples were removed from storage and left at RT for 30 minutes. Sections were then immersed in cold methanol and incubated for 10 minutes at -20°C to fix and permeabilise sections. Sections were then washed 3 times in 1X PBS, 10 minutes each. Following washing, sections were incubated in IHC blocking solution (Appendix) for 1 hour at RT to reduce non-specific staining. To stain for macrophages, sections were incubated with a specific antibody against murine macrophage surface protein F4/80 (rat-anti-mouse F4/80,

Thermo Scientific) at a dilution of 1:1000 in IHC blocking solution overnight at 4°C in a sealed humidified chamber. Non-specific background signal was controlled for by using a rat IgG2B isotype control (Invitrogen) at a dilution of 1:1000 in blocking solution overnight at 4°C in a sealed humidified chamber. Sections were then washed 3 times in 1X PBS, 10 minutes each. Goat-anti-rat AF555 secondary antibody (Invitrogen) was added to the sections at a 1:500 dilution in blocking solution for 90 minutes at RT. This was followed by washing as described above. Sections were then incubated in Hoechst Nuclear Stain (0.5µg/mL in 1X PBS) for 10 minutes at RT, protected from light. After incubation, slides were washed in 1X PBS for 10 minutes. Sections were then mounted with 20mm x 20mm coverslips using Mowiol (Sigma Aldrich), which contained n-propylgallate for its anti-fade properties. Slides were stored at 4°C protected from light until viewing.

Tissue sections were viewed with assistance from Associate Professor Dirk Lang and Mrs. Susan Cooper using a Zeiss LSM880 Airyscan confocal microscope together with Zen 2.3 SP1 software (Zeiss). Ten areas in the epithelium were randomly selected for each condition, using the Hoechst channel only to eliminate bias. Z-stacks were then taken with the Hoechst, AF488 and AF555 channels selected. Z-stack dimensions were then normalised to 18 optical sections per image stack, and maximum intensity projections were done. The area occupied by macrophages (positive for F4/80) in the epithelium was determined by outlining the epithelium in each maximum intensity projection and determining the area of the AF555 stain in these selected regions (see Supplementary Figure 2 for an example). The lower and upper thresholds were set at 18 and 256 greyscale levels, respectively, for each maximum intensity projection. This was done to remove background signal so that the measured signal for AF555 corresponded to the area representing F4/80 macrophage staining.

3. Results

3.1. Determining the biochemical and functional relevance of SP-A and SP-D for HPV16-PsVs infection *in vitro*

In vitro experiments were performed to determine whether SP-A and/or SP-D play a role in immune recognition of HPV16-PsVs. Initially, Co-IP experiments were done to determine whether SP-A and/or SP-D interact with HPV16-PsVs particles. Following this, flow cytometry was used to determine whether any potential interaction between HPV16-PsVs and SP-A or SP-D had a functional consequence on viral internalisation by RAW264.7 macrophages.

3.1.1. Quality control to test the purity and infectivity of HPV16-PsVs preparations

Following the production of HPV16-PsVs, particle purity and functionality was routinely tested. SDS-PAGE followed by silver staining was used to assess purity of the HPV16-PsVs preparations (Figure 3.1.A, left panel). In pure preparations, only 2 bands, i.e. a thick L1 band (55kDa) and thin L2 band (75kDa) were observed as expected. In experiments where AF488 labelled PsVs preparations were generated, the SDS gels were illuminated with a 488nm light source in order to visualise the successfully labelled fluorescent bands prior to silver staining (Figure 3.1.A, right panel).

The infectivity of HPV16-PsVs preparations was assessed by infecting HeLa cells with viral particles that had undergone certain pre-incubations or treatments (Figure 3.1.B.). Pre-incubation of HPV16-PsVs with the appropriate, type-specific neutralising antibody H16.V5 completely abolished infection as expected (Figure 3.1.B.). Conversely, pre-incubation with the HPV18 neutralising antibody H18.J4 (negative control) had no effect on infection, as this antibody fails to bind and neutralise HPV16 (Figure 3.1.B.). Treatment with DNase I endonuclease was performed to assess whether any un-encapsidated plasmid gave rise to the measured luciferase activity. In pure preparations, DNAse treatment showed a similar HPV16-PsVs infectivity compared to untreated control (Figure 3.1.B).

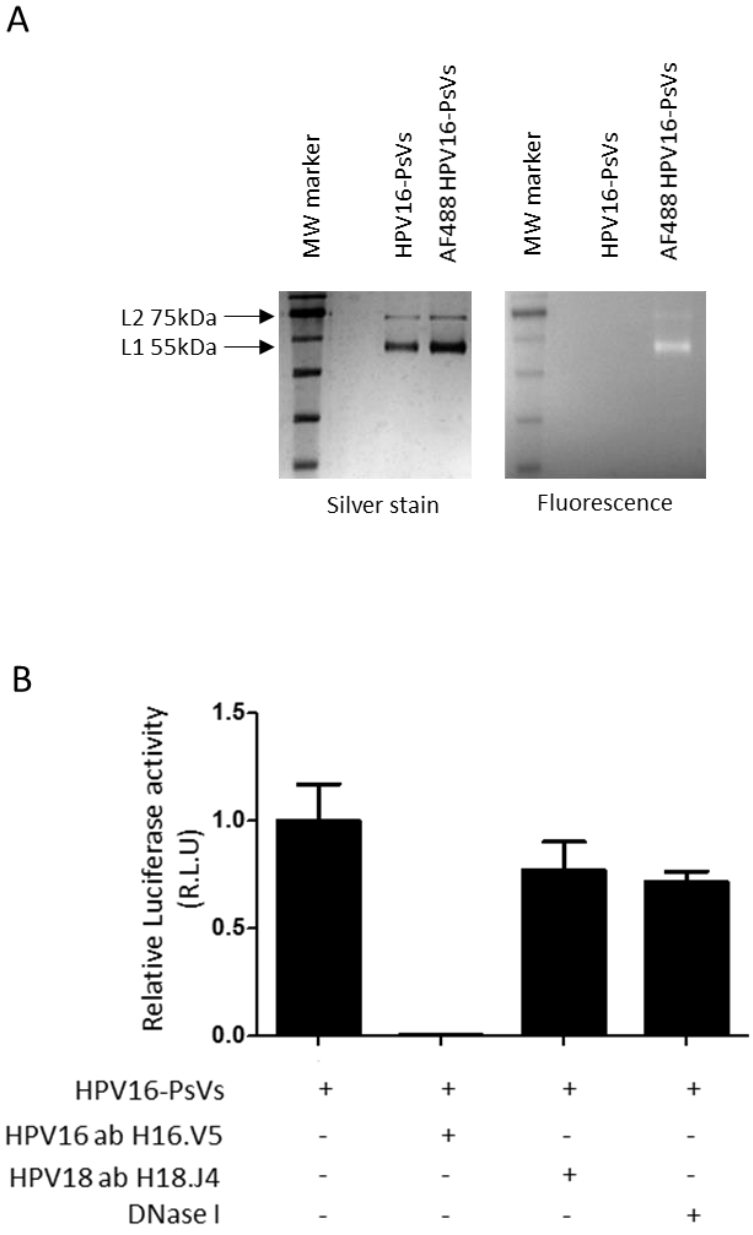

Figure 3.1: Quality control tests to assess purity and infectivity of HPV16-PsVs preparations. A) SDS-PAGE gel showing 2 representative HPV16-PsVs preparations (either unlabelled or labelled with AF488). A thick band corresponding to the L1 protein (55kDa) as well as a thin L2 band (75kDa) were seen in pure preparations. Fluorescent bands were confirmed in AF488 labelled preparations. **B)** HeLa cells were infected with HPV16-PsVs under various conditions for 24 hours before luminescence was measured. Relative luciferase activity (R.L.U) represents luminescence (arbitrary units) normalised to protein concentration (mg/mL), and values are presented as x-fold change relative to HPV16-PsVs only, which was set as 1. Bars depict mean values, with error bars showing standard error of the mean (SEM).

3.1.2. SP-A binds to and enhances HPV16-PsVs uptake by RAW264.7 macrophages

In order to determine whether SP-A and/or SP-D bind to the viral particles, co-immunoprecipitation (Co-IP) was applied. The principle behind Co-IP is that if one immunoprecipitates a protein (using the appropriate IP antibody and protein G Sepharose beads), any interacting proteins will be co-immunoprecipitated. Any unbound proteins can be detected in the flow through (FT) fraction, whereas co-immunoprecipitated proteins are detected in the eluate (see section 2.4.). The pull-down was performed with antibodies against SP-A or SP-D (or HPV16 L1 as a control, as it will recognise HPV16-PsVs) as indicated in Figure 3.2. A-C. Binding of HPV16-PsVs was visualised by Western Blotting using the HPV16 L1 primary antibody CamVir. The control experiment in Figure 3.2.A. demonstrates that the SP-A IP (pull-down) antibody did not cross-react with HPV16-PsVs, while the CamVir IP antibody did not recognise SP-A. In the right panel of Figure 3.2.A. (SP-A as an input), bands were seen in the FT and eluate lanes, but these were due to the CamVir detection antibody recognising a portion of the CamVir IP antibody. This was also found in control experiments with SP-D (not shown). The left panel of Figure 3.2.B. shows that the CamVir IP antibody recognises HPV16-PsVs as expected (as it is eluted), and some HPV16-PsVs was also detected in the FT, most likely due to oversaturation of the IP antibody. Importantly, SP-A binding to HPV16-PsVs can be seen in the right panel of Figure 3.2.B, which shows that HPV16-PsVs could be detected in the eluate when immunoprecipitated with the SP-A antibody. Figure 3.2.C. shows that HPV16-PsVs also bind to SP-D; however, this interaction is much weaker, and only a faint HPV16-PsVs was detected in the eluate with the majority still unbound in the FT.

In order to determine any functional impact of SP-A or SP-D binding for HPV16-PsVs recognition and internalisation by RAW264.7 macrophages, flow cytometry experiments using AF488-HPV16-PsVs were performed. Figure 3.2.D. shows the fluorescence measured in RAW264.7 cells following 1 hour incubation of these cells with AF488-HPV16-PsVs which were pre-incubated with SP-A, SP-D or BSA as a control. It was observed that when the viral particles were pre-incubated with a 10-fold (w/w) excess of SP-A (as determined in pilot experiments, see Supplementary Figure 3), viral internalisation by RAW264.7 macrophages was significantly enhanced ($p<0.001$). Pre-incubation of AF488-HPV16-PsVs with a 10-fold

(w/w) excess of SP-D, however, had no effect on viral internalisation, which was also observed with the BSA control.

Downstream luciferase activity was also determined 48 hours post-infection as a measure of successful infection, i.e. the transcription of the firefly luciferase plasmid encapsidated in the viral particle representing the pseudogenome entry into the nucleus. We noted that the infectivity of RAW264.7 macrophages compared to HeLa cells was extremely low (approximately 15 000-fold less, Figure 3.2.E.). However, when HPV16-PsVs were pre-incubated with a 10-fold (w/w) excess of SP-A, luciferase activity measured in RAW264.7 cells increased by approximately 3-fold, but had no effect on HeLa cell infection (Figure 3.2.E).

From these results, it was decided to concentrate our experiments on viral uptake (rather than infection) using RAW264.7 macrophages and SP-A only, to test our hypothesis that macrophages prevent epithelial HPV infection by effectively engulfing the HPV which is associated with SP-A, culminating in the killing of most of the internalised virus.

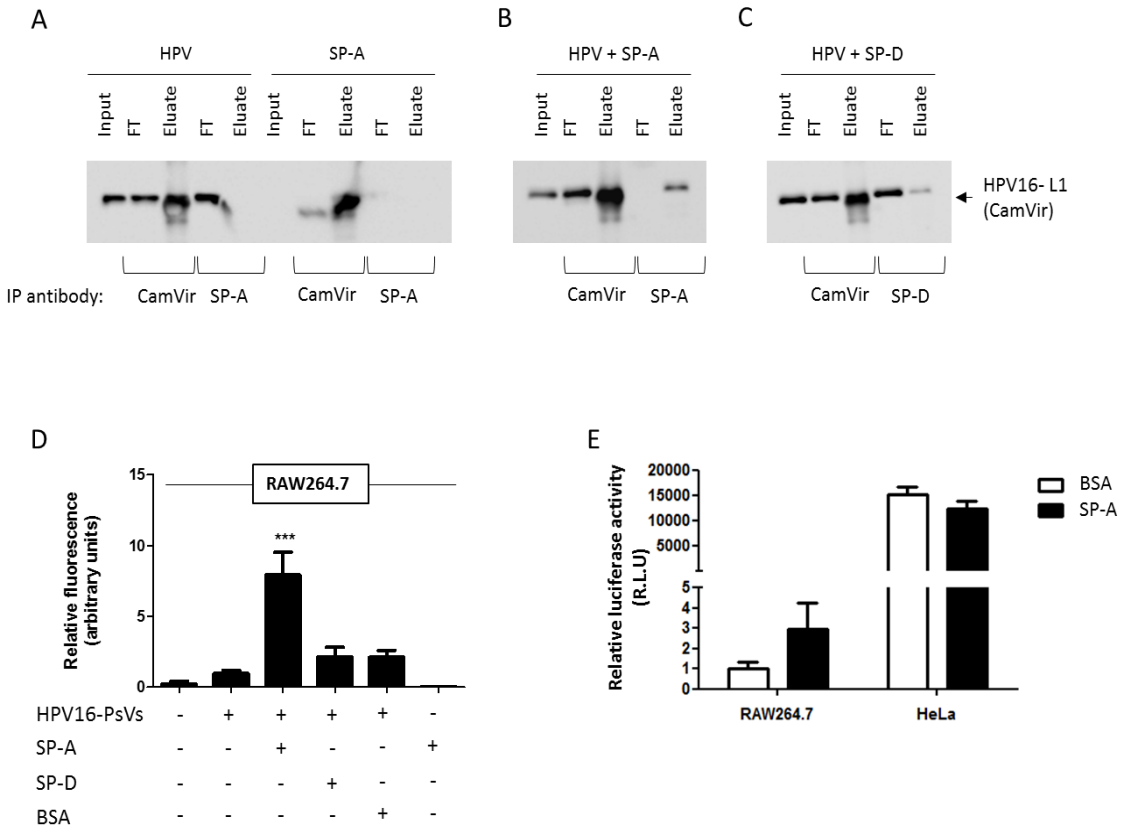

Figure 3.2: SP-A binds to and enhances HPV16-PsVs uptake by RAW264.7 macrophages. A-C) Co-immunoprecipitation experiments displaying the input, flow through (FT) and eluate samples of **(A)** HPV16-PsVs and SP-A alone (controls), **(B)** HPV16-PsVs and SP-A together and **(C)** HPV16-PsVs and SP-D together. Western Blots were performed using the anti-HPV16 L1 antibody (CamVir) to detect the presence of HPV16-L1. **D)** RAW264.7 cells were incubated with AF488 labelled HPV16-PsVs (pre-incubated with purified proteins where indicated) for 1 hour at 37°C. Cells were lifted with trypsin-EDTA to remove surface-bound virions and subjected to flow cytometry to quantify viral internalisation. Experiments were performed in triplicate, quantified by quadrant analysis of the dot blot of three independent experiments (Supplementary Figure 4) and presented as x-fold increase relative to the mean fluorescence intensity of cells infected with untreated HPV16-PsVs which was set as 1. Significances were calculated by means of one-way ANOVA and Tukey post-hoc tests. *** indicates statistical significance between uptake of HPV16-PsVs in the presence of SP-A as compared to the other tested conditions (*** = $p<0.001$). **E)** RAW264.7 and HeLa cells were incubated with HPV16-PsVs for 48 hours. Where indicated, the viral particles were pre-incubated with purified SP-A protein before incubation with the cells. Luciferase activities in the cell lysates as a measure for infection is presented as Relative luciferase activity relative to RAW264.7 cells incubated with untreated HPV16-PsVs which was set as 1. Bars in **D** and **E** depict mean values, with error bars showing SEM.

3.1.3. SP-A-mediated HPV16-PsVs uptake by RAW264.7 macrophages is calcium dependent and CRD independent

To elucidate the mechanisms by which SP-A mediates increased HPV16-PsVs uptake by RAW264.7 macrophages, internalisation experiments in the presence of calcium or mannose were conducted.

Firstly, calcium chloride was used to determine if SP-A-mediated increase in HPV16-PsVs uptake was calcium-dependent as SP-A, being a C-type lectin, typically requires calcium to perform certain functions. EDTA was used to chelate Ca^{2+} ions and further determine if calcium was necessary for this interaction. Figure 3.3. A-C show control experiments displaying viral uptake in the presence of no HPV16-PsVs (Figure 3.3.A.), HPV16-PsVs only (Figure 3.3.B.) and HPV16-PsVs with SP-A (Figure 3.3.C.). Figure 3.3. D-E and I show that addition of 2mM and 5mM calcium chloride significantly increased viral internalisation in the presence of SP-A, with 5mM calcium chloride having the greater effect ($p<0.001$). Addition of 10mM EDTA successfully abolished this effect, as shown in Figure 3.3. F-H and I, thereby confirming that the SP-A-mediated increase in viral uptake by RAW264.7 macrophages was calcium dependent.

Secondly, in order to determine if SP-A interacts with HPV16-PsVs via its CRD, uptake experiments were conducted in the presence or absence of mannose, a competitive inhibitor of the CRD [68,128]. The representative dot plots obtained following flow cytometry (Figure 3.4. A-F) as well as the bar graph in Figure 3.4.G. show that increasing concentrations of mannose had no effect on viral internalisation by RAW264.7 macrophages.

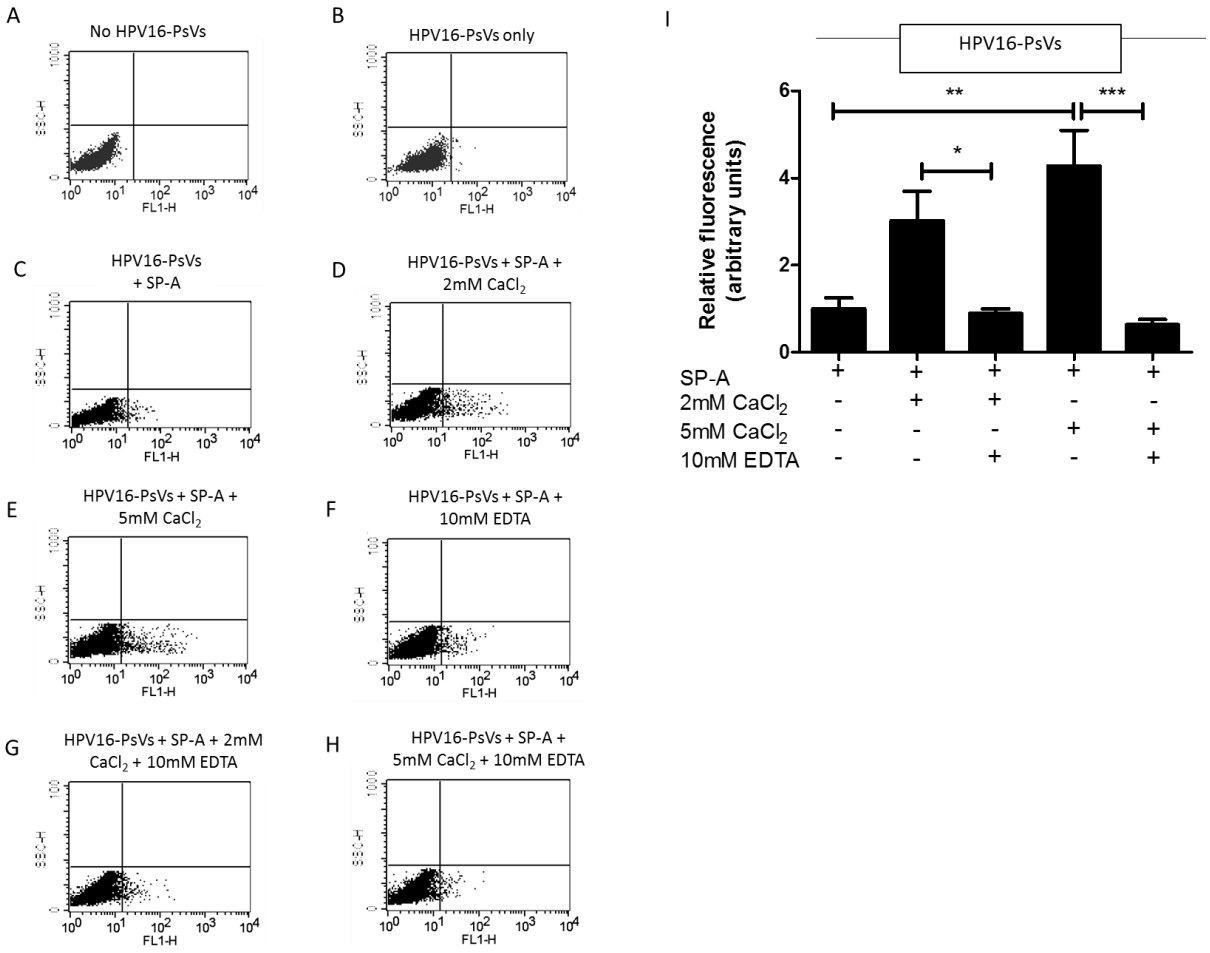

Figure 3.3: SP-A-mediated HPV16-PsVs uptake by RAW264.7 macrophages is calcium-dependent. AF488-HPV16-PsVs were incubated in the presence of 10-fold (w/w) excess SP-A with or without 2mM or 5mM calcium chloride in the presence or absence of 10mM EDTA as indicated. Representative figures **(A-H)** show dot plots of fluorescence in the FL1 channel plotted against side scatter (SSC) for **(A)** No HPV16-PsVs, **(B)** HPV16-PsVs only **(C)** SP-A, **(D)** SP-A + 2mM $CaCl_2$, **(E)** SP-A + 5mM $CaCl_2$, **(F)** SP-A + 10mM EDTA, **(G)** SP-A + 2mM $CaCl_2$ + 10mM EDTA and **(H)** SP-A + 5mM $CaCl_2$ + 10mM EDTA. Figure I shows a summary of the fluorescence measured in the lower right quadrant (AF488 positive) normalised by setting SP-A as 1 for the conditions displayed in Figures C-H. Quantification of three independent experiments performed in duplicate are shown. Statistical significance was determined using one-way ANOVA and Tukey post-hoc tests. *= $p<0.05$, **=$p<0.01$, ***=$p<0.001$. Bars in Figure I depict mean values, with error bars showing SEM.

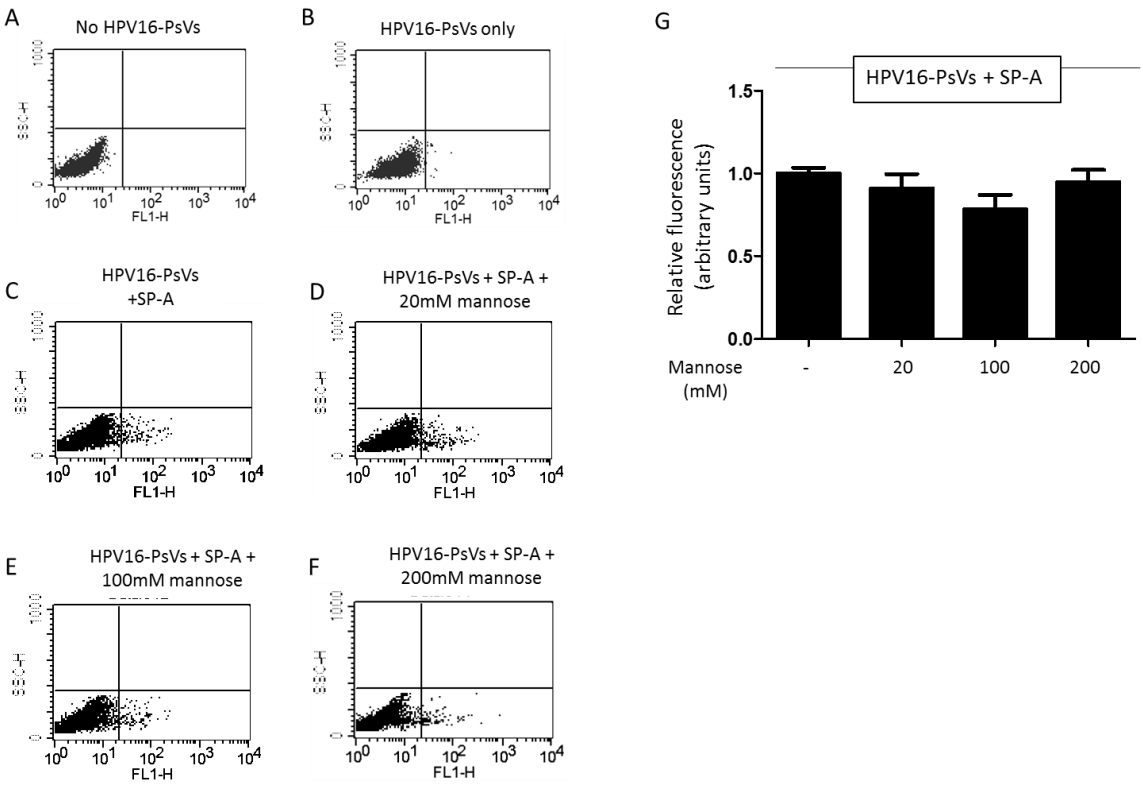

Figure 3.4: The SP-A-mediated increase in HPV16-PsVs uptake by RAW264.7 macrophages is not dependent on the CRD. AF488-HPV16-PsVs were incubated in the presence of a 10-fold (w/w) excess of SP-A and various concentrations of mannose. Representative figures **(A-F)** show dot plots of fluorescence in the FL1 channel plotted against side scatter (SSC) for **(A)** No HPV16-PsVs, **(B)** HPV16-PsVs only, **(C)** SP-A, **(D)** SP-A + 20mM mannose, **(E)** SP-A + 100mM mannose and **(F)** SP-A + 200mM mannose. Figure G shows a summary of the fluorescence measured in the lower right quadrant (AF488 positive) normalised by setting SP-A only as 1 for the conditions displayed in Figures C-F. Quantification of three independent experiments performed in duplicate is presented. Bars in Figure G depict mean values, with error bars showing SEM.

3.2. Set up of a genital HPV16-PsVs infection model at UCT using C57BL/6 mice

While the *in vitro* findings described above suggest a role of SP-A in enhancing immune recognition of incoming HPV16-PsVs, the natural HPV infection environment in the genital tract is very complex as several diverse cell types are potentially involved in immune responses upon challenge with oncogenic HPV, including local epithelial cells and the recruitment of inflammatory cells. To this end, the cervicovaginal challenge model described by Roberts *et al.* [122], which particularly reflects early events in HPV infection, was set up at the UCT RAF as part of this MSc project.

3.2.1. Welfare monitoring of C57BL/6 mice for the duration of HPV16-PsVs challenge

An important aspect of animal work is to ensure that the animals do not undergo distress, which can often be inflicted by certain experimental procedures. Welfare monitoring was performed daily for the entire duration of an experiment to ensure that the mice did not undergo any distress: this included monitoring social behaviour, physical appearance and weight. The experimental procedures performed are described in detail in section 2.9.; they were expected to produce only mild discomfort. Figure 3.5. shows a representative figure of the weights of mice taken daily during an experiment, grouped depending on the HPV16-PsVs dose received. Four days prior to cervicovaginal challenge with HPV16-PsVs, mice were injected with Depo-Provera s.c. (as indicated by the first arrow at day -4) and this had no effect on weight. On the day of cervicovaginal challenge, mice were lightly anaesthetised twice (once before N-9 treatment and again before HPV16-PsVs infection), which caused a slight decrease in weight. Weights then increased again on day 2 and 3, showing that the anaesthetic and cervicovaginal challenge had no adverse effect on welfare. Furthermore, increasing HPV16-PsVs doses (which were also used in section 3.2.2.) had no effect on weight.

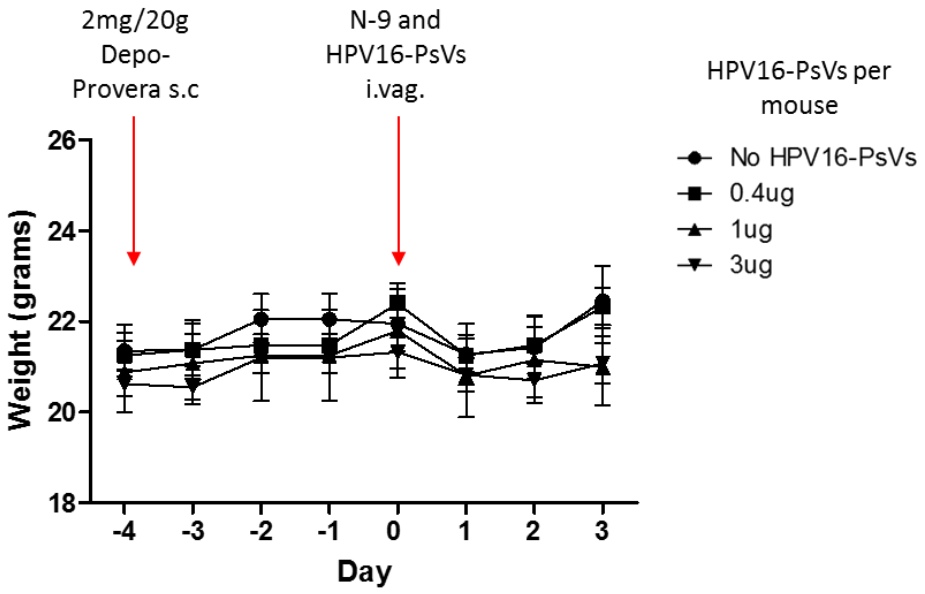

Figure 3.5: Weights of C57BL/6 mice do not fluctuate significantly during an HPV16-PsVs infection experiment. 6-10 weeks old female wildtype C57BL/6 mice were injected with 2mg/20mL Depo-Provera (s.c.), followed 4 days later by pre-treatment with 25µl 4% N-9 in 3% CMC i.vag. for 6 hours prior to HPV16-PsVs infection. Four mice per group were i.vag. infected with increasing doses of the viral particles as indicated. Weights of the mice were measured daily as part of their welfare monitoring. Points depict mean values, with error bars showing SEM.

3.2.2. Establishing optimal infectious doses of HPV16-PsVs for *in vivo* infection of C57BL/6 mice

While the protocol developed by Roberts *et al.* described the conditions for HPV16-PsVs infection of BALB/cAnNCr mice, optimal HPV16-PsVs doses for infection of C57BL/6 mice had to be determined. This was done using three increasing doses of HPV16-PsVs, of which the lowest dose of 0.4µg (approximately 1.2×10^{10} infectious units[1]) closely corresponded to that used by Roberts *et al.* (5×10^{9} infectious units). HPV16-PsVs was delivered in 3% CMC i.vag., and infection was measured by firefly luciferase assays 72 hours later using homogenised genital tract tissue and vaginal lavages (see section 2.9.1.1). Figure 3.6.A. shows a dose-dependent increase in HPV16-PsVs infection in the homogenised genital tract tissue. As firefly luciferase is transcribed and translated as an intracellular protein, one would not expect any luciferase activity in vaginal lavages. However, in our experiments cell lysis buffer was added

[1] 1ng L1 protein = 3×10^{7} infectious units [134]

to harvested lavages in order to lyse any shed cells, and therefore luciferase activity could also be measured in the lavages (Figure 3.6.B.). The pattern of luciferase activity measured in vaginal lavages was comparable to those measured in homogenised genital tract tissue which showed a dose-dependent increase (Figure 3.6.A.); this indicated that both vaginal lavages and genital tract homogenates could be used to quantify infection. The experiments presented in Figure 3.6.A. and B. indicate that infection with 3µg HPV16-PsVs per mouse resulted in the highest luciferase activity which is an index for the highest infection, and therefore this dose was used in all further experiments.

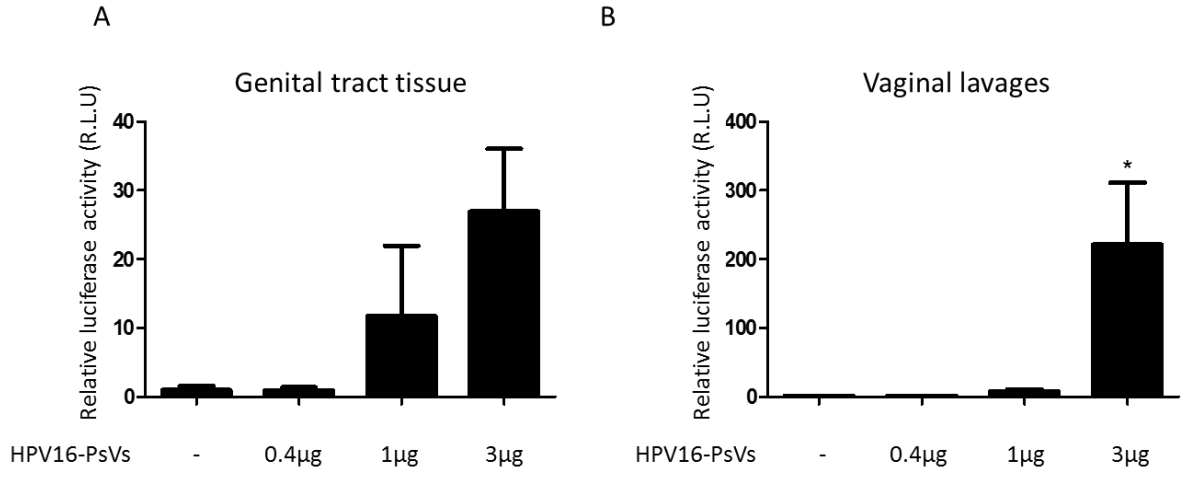

Figure 3.6: C57BL/6 mice exhibit a dose-dependent increase in HPV16-PsVs infectivity. 6-10 weeks old female wildtype C57BL/6 mice were pre-treated and infected as described in Figure 2.2. After 72 hours, vaginal lavages were performed and genital tracts harvested for analysis. Firefly luciferase activity was measured in **(A)** homogenised genital tract tissue and **(B)** vaginal lavage fluid. Data were normalised to total protein concentrations in the samples and are presented as x-fold to average control (no HPV16-PsVs) which was set as 1. Figures show quantification of one experiment, with four mice per viral dose. Statistical significance was determined using one-way ANOVA and Tukey post-hoc tests. *= $p<0.05$. Bars depict mean values, with error bars showing SEM.

3.2.3. Optimising duration of HPV16-PsVs *in vivo* infection and infectious read-out

In order to determine optimal infectious conditions, time course experiments are typically performed. Ideally, infection is tracked by detecting firefly luciferase using *in vivo* imaging systems. If these systems are unavailable, the usage of HPV16-PsVs encapsidating the reporter plasmid for Gaussia luciferase has been reported as a more accessible alternative [123]. As mentioned in section 2.3, Gaussia luciferase has a signal peptide for secretion and thus, luciferase activity can be measured daily from vaginal lavages of the same mouse without needing to euthanise the animal to dissect and homogenise the genital tract. Moreover, Gaussia luciferase can be measured directly from the lavages without the need for lysis of any shed cells as done to determine firefly luciferase (see section 3.2.2.), thereby potentially decreasing variations between time points.

Infection of C57BL/6 mice with GLuc HPV16-PsVs was done in parallel to infection using FLuc HPV16-PsVs, in order to compare which reporter system was most suitable for time course experiments. Figure 3.7.A. and B. show Fluc and GLuc luciferase activity from daily vaginal lavages, respectively. Mice infected with GLuc HPV16-PsVs exhibited at least 10-fold higher luciferase readings as compared to FLuc HPV16-PsVs infected mice. This was particularly notable already 24 hours p.i. Furthermore, a gradual increase in GLuc activity was noted over time, whilst this was not seen when using FLuc.

At the end of the experiment (72 hours p.i.), genital tract tissue from uninfected, FLuc HPV16-PsVs infected and GLuc HPV16-PsVs infected mice was analysed for luciferase activity (Figure 3.7.C.). As expected, mice infected with FLuc HPV16-PsVs had higher luciferase activity measured here compared to Gluc HPV16-PsVs infected mice, as firefly luciferase is an intracellular protein. Therefore, GLuc HPV16-PsVs is ideal for time course experiments, but when analysing genital tract tissue for luciferase activity, FLuc HPV16-PsVs is better suited.

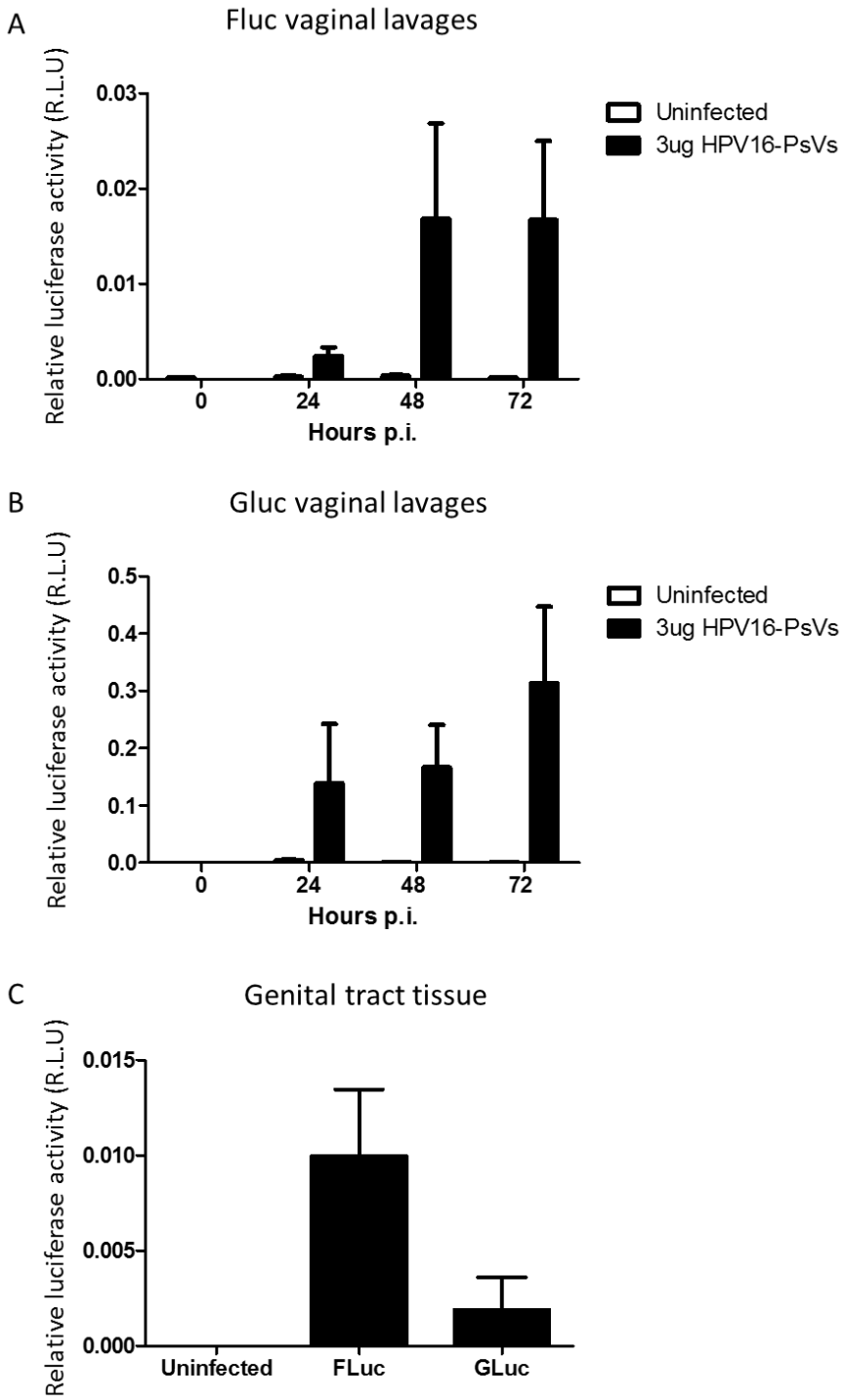

Figure 3.7: Comparison of firefly and Gaussia luciferase as HPV16-PsVs encapsidated reporter genes in time course experiments. 6-10 weeks old C57BL/6 mice were challenged with 3µg HPV16-PsVs (either containing FLuc or GLuc reporter plasmids) as described in Figure 2.2. Mice were lavaged with 50µL sterile PBS daily. **A)** Firefly luciferase activity measured in the vaginal lavages of uninfected versus HPV16-PsVs infected mice. **B)** Gaussia luciferase activity measured in the vaginal lavages of uninfected versus infected mice. **C)** Comparison of luciferase activity measured in genital tract tissue homogenates after infection with FLuc HPV16-PsVs or GLuc HPV16-PsVs after 72 hours. Two independent experiments with four mice per group were performed. Bars depict mean values, with error bars showing SEM.

3.3. Determining the effect of SP-A on HPV16-PsVs infection *in vivo*

After the successful establishment of the *in vivo* HPV16-PsVs challenge model at UCT, various scientific questions can be addressed which will be extremely useful for all current and future studies in the laboratory. Of particularly interest and in the context of this MSc project, the role of SP-A for HPV infection was determined.

3.3.1. SP-A is not expressed in the genital tract or vaginal lavage of naïve C57BL/6 mice

Before determining the effect of SP-A on HPV16-PsVs infection *in vivo*, it was important to first establish whether SP-A was expressed in naïve C57BL/6 mice. As described in section 1.2.3, SP-A is expressed in the female genital tract of humans, but to our knowledge it was unknown whether SP-A is expressed in the female genital tract of C57BL/6 mice. Therefore, Western Blotting was performed (Figure 3.8.), probing for SP-A in the lung and bronchoalveolar lavage (BAL) (representing the positive controls), as well as the genital tract tissue (GT) and vaginal lavage fluid (vag. lavage). Purified human SP-A was also included as a positive control. It was noted that bands corresponding to SP-A protein could be detected in the lung and BAL, but SP-A was not detected in the genital tract or vaginal lavage of naïve C57BL/6 mice.

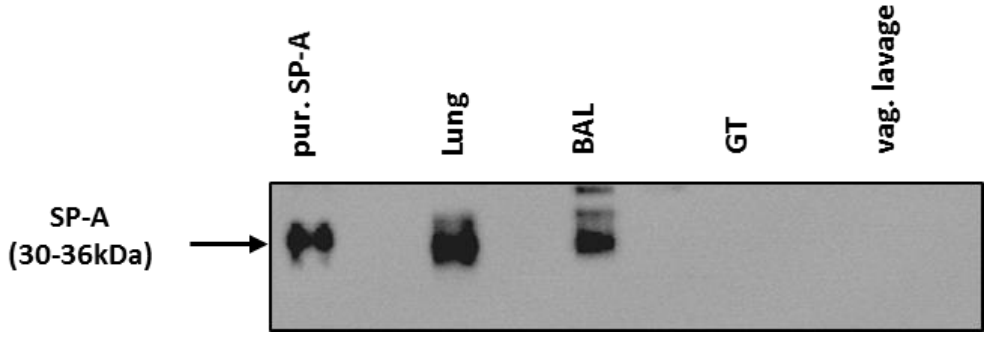

Figure 3.8: SP-A expression in various organs and body fluids of naïve female wildtype C57BL/6 mice. Shown is a Western Blot probed with an antibody for murine SP-A in the lung, bronchoalveolar lavage fluid (BAL), genital tract tissue (GT), and vaginal lavage (vag. lavage) fluid. Tissue and lavages were taken from 6-10 weeks old female C57BL/6 mice that were not exposed to any HPV16-PsVs. 20µg of each sample was loaded per lane, while 0.5µg of purified human SP-A protein was loaded as control. No endogenous SP-A was detected in the female genital tract. Ponceau staining was performed to assure for equal loading (not shown).

3.3.2. HPV16-PsVs infection of C57BL/6 mice does not affect SP-A expression

Although SP-A could not be detected on the protein level in the genital tract of naïve mice (Figure 3.8.), it was possible that exposure to HPV16-PsVs would induce SP-A expression. Therefore, RT-PCR and Western Blot experiments were performed in order to determine whether cervicovaginal challenge with HPV16-PsVs induced SP-A expression in the female genital tract of C57BL/6 mice.

Figure 3.9.A. shows a RT-PCR of four mice per group either uninfected or infected with HPV16-PsVs for 24 hours: amplification of the pGL3 plasmid encapsidated by HPV16-PsVs could be detected in RNA extracted from the genital tract tissue of infected mice. Analysis of SP-A gene expression by RT-PCR showed that SP-A mRNA was not expressed in uninfected genital tract tissue, nor was SP-A mRNA expression induced following infection for 24 hours (Figure 3.9.B.). Lung mRNA was used as a positive control for SP-A expression and Gapdh was used as a reference gene. Furthermore, SP-A protein expression was analysed 24 and 72 hours p.i. in the vaginal lavages and genital tract tissue (Figure 3.10.). Again, no SP-A protein could be detected. Therefore, infection with HPV16-PsVs does not affect SP-A expression in the female genital tract of C57BL/6 mice.

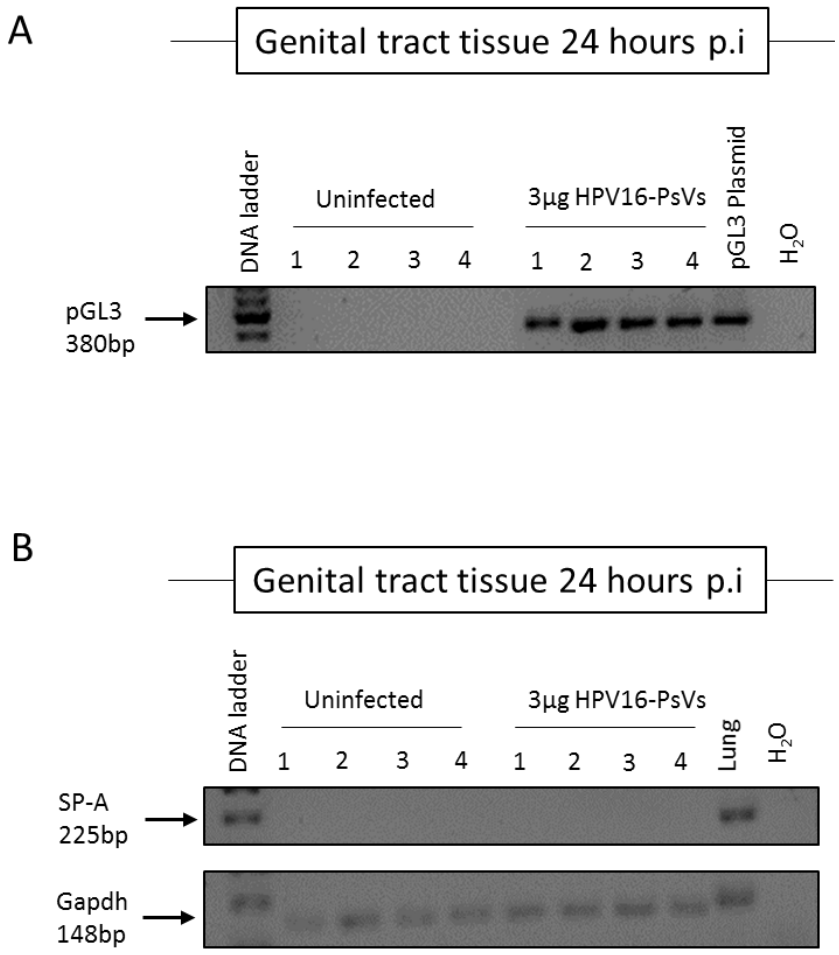

Figure 3.9: Infection of C57BL/6 mice with HPV16-PsVs does not alter SP-A mRNA expression. 6-10 weeks old female wildtype C57BL/6 mice were pre-treated as described in Figure 2.2. Four mice per group were i.vag. infected with 3µg HPV16-PsVs. Genital tract tissue was harvested 24 hours later and RNA extracted for gene expression analysis. **A)** RT-PCR of RNA from genital tract tissue to show successful infection. Amplification of the pGL3 plasmid was used as a positive control and H_2O as a negative control. **B)** RT-PCR of RNA from genital tract tissue showing no change in SP-A expression. Lung RNA was used as a positive control and H_2O as a negative control. Gapdh was used as a reference gene.

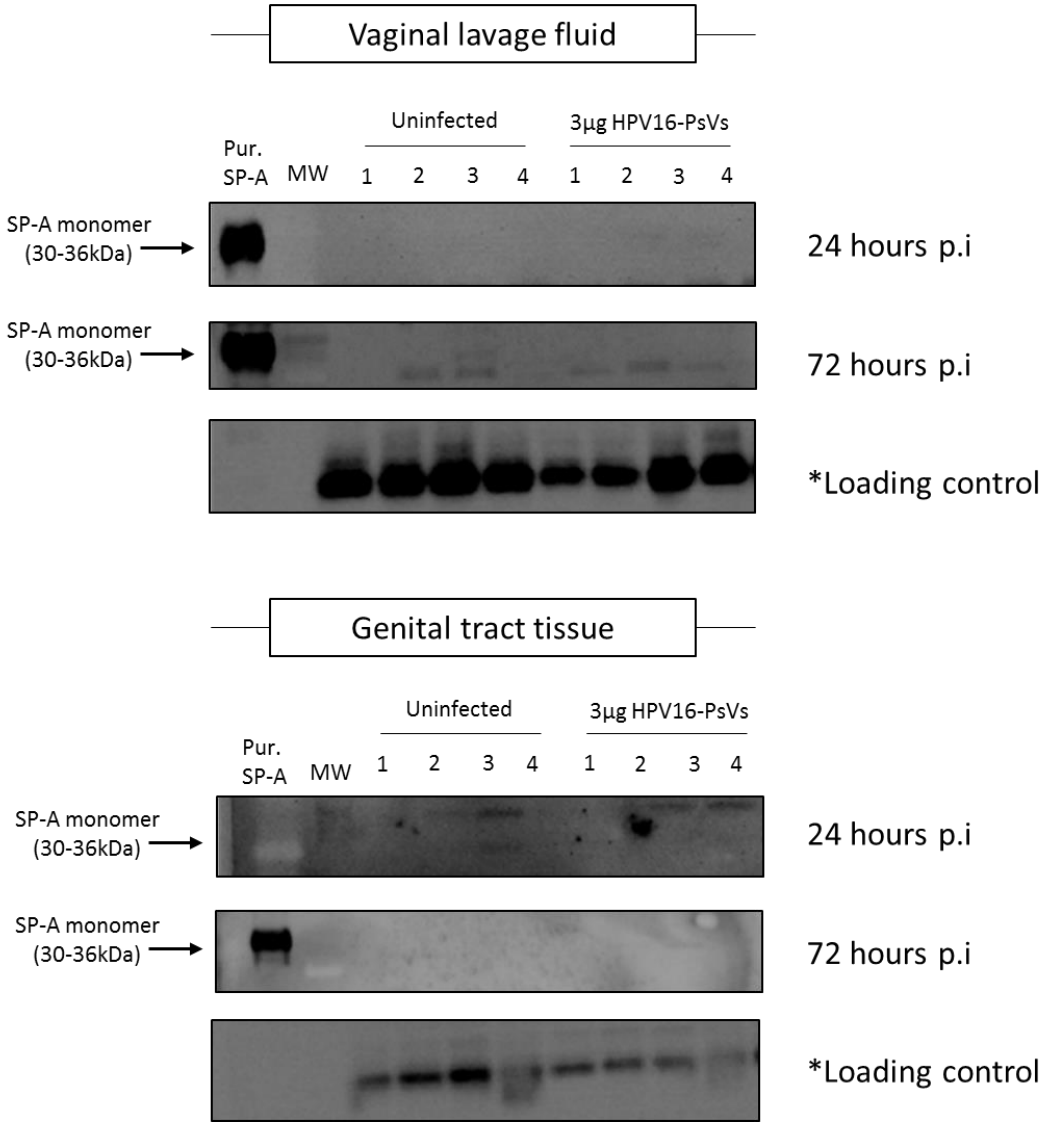

Figure 3.10: Infection of C57BL/6 mice with HPV16-PsVs does not alter expression of SP-A. 6-10 weeks old female wildtype C57BL/6 mice per group were pre-treated as described in Figure 2.2. Four mice per group were i.vag. infected with 3µg HPV16-PsVs. Vaginal lavages were performed 24 and 72 hours p.i. and genital tract tissue was harvested 24 hours or 72 hours p.i. Western Blots of vaginal lavage fluid (top panel) and homogenised genital tract tissue (bottom panel) were probed for the presence of SP-A. 20µg of each sample was loaded per lane, while 0.5µg purified human SP-A protein was loaded as control. *Loading control corresponds to a 45kDa cellular protein that cross-reacts with the CamVir primary antibody [129].

3.3.3. SP-A reduces HPV16-PsVs infection in C57BL/6 mice

In order to assess any effect of SP-A on HPV16-PsVs infection *in vivo*, 1:1 and 1:10 (w/w) HPV16-PsVs to SP-A ratios were tested (shown in Figure 3.11. as 3µg and 30µg SP-A, respectively). Figure 3.11. shows that 30µg SP-A reduced HPV16-PsVs infection, as measured in the vaginal lavage (left panel) and genital tract tissue (right panel). Although this was not deemed to be significant, a clear trend can be seen in luciferase activity measured in the lavages as well as genital tract tissue, with 30µg SP-A reducing HPV16-PsVs approximately 4-fold. From this experiment, a 1:10 HPV16-PsVs to SP-A ratio (30µg SP-A) was chosen as the optimal amount of SP-A to be used in further experiments. This ratio also corresponded to *in vitro* experiments involving RAW264.7 macrophages, where 0.5µg HPV16-PsVs was pre-incubated with 5µg SP-A (Figure 3.2.D.). Pre-incubation of SP-A and HPV16-PsVs was done in the absence of calcium for all *in vivo* experiments, as preliminary experiments showed that addition of calcium here had no effect on infection (Supplementary Figure 5). Calcium would have been present in the genital tract, which may explain why no difference was seen in the presence of additional calcium.

Based on the conditions described in Figure 3.11.A, further experiments determining the effect of SP-A on HPV16-PsVs infection were performed under refined experimental settings. Including BSA as a control protein (see also Figure 3.2.D.), a 10-fold excess (w/w) of SP-A or BSA to HPV16-PsVs was used. When compared to BSA, incubation with SP-A resulted in approximately 4-fold reduction in HPV16-PsVs (Figure 3.11.B), which was measured as firefly luciferase activity in both the vaginal lavage fluid (following addition of lysis buffer to lyse shed cells) and the genital tract tissue.

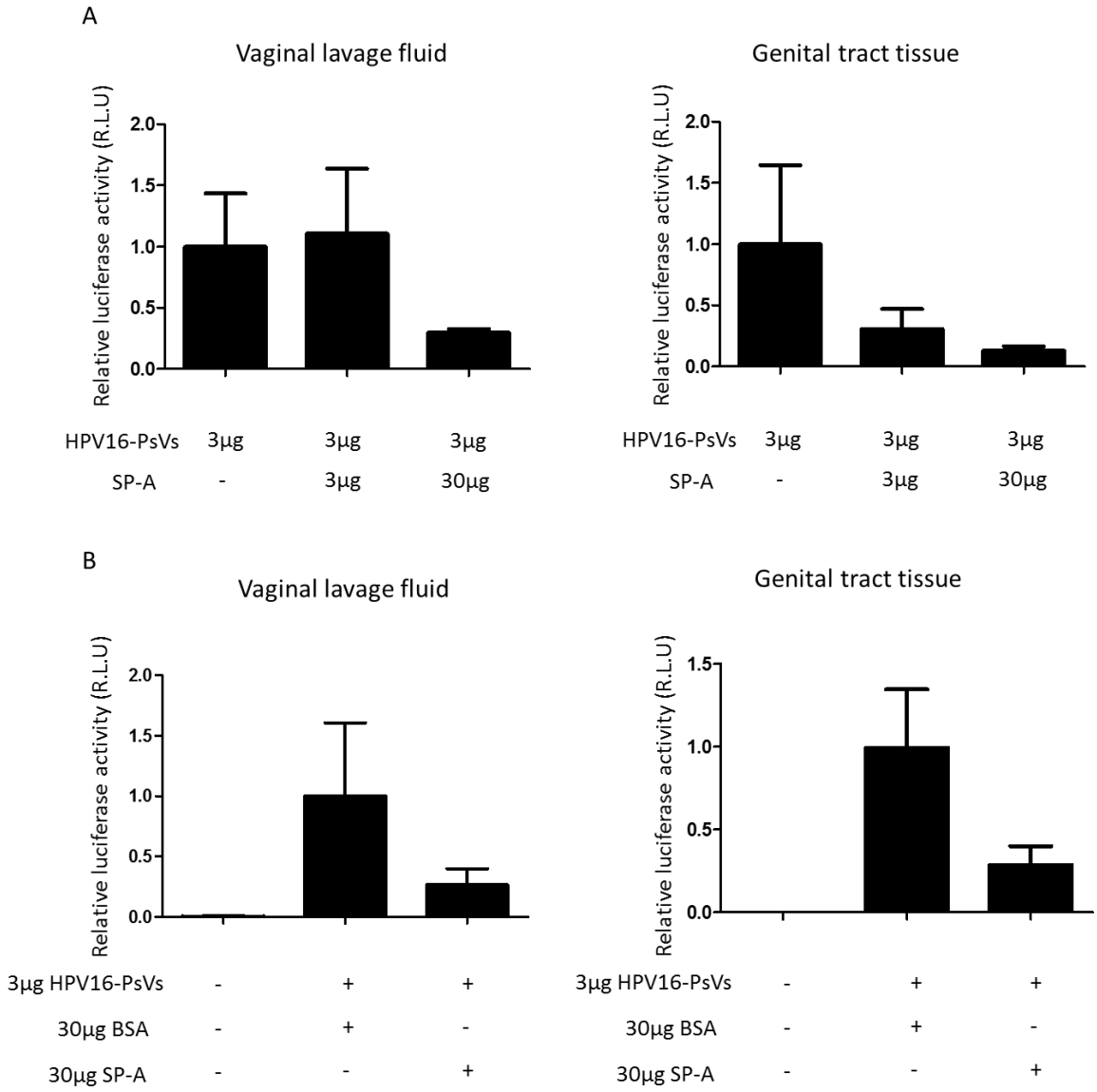

Figure 3.11: SP-A reduces HPV16-PsVs infection in C57BL/6 mice. 6-10 weeks old female wildtype C57BL/6 mice per group were pre-treated as described in Figure 2.2. **A)** HPV16-PsVs encapsidating firefly luciferase were pre-incubated with two increasing amounts of purified SP-A protein for 1 hour on ice. **B)** 3µg HPV16-PsVs were pre-incubated with 30µg purified SP-A protein or 30µg BSA for 1 hour on ice. Mice were euthanised 72 hours p.i., and tissue harvested for analysis. Firefly luciferase activity was measured in vaginal lavage fluid (left panels) and homogenised genital tract tissue (right panels). Data were normalised to total protein in the samples and are presented as x-fold to average control (no SP-A) which was set as 1. Figure A shows the data from one experiment with four mice per condition. Figure B shows pooled data from two independent experiments, with a total of ten mice per condition. Bars depict mean values, with error bars showing SEM.

Time course experiments were performed to further assess the effect of SP-A on HPV16-PsVs infection over 72 hours. This was achieved using GLuc HPV16-PsVs and measuring luciferase activity from vaginal lavages which were performed daily. Figure 3.12. shows luciferase activity measured over 72 hours from mice infected with GLuc HPV16-PsVs pre-incubated with a 10-fold (w/w) excess of either 30µg BSA or 30µg SP-A. It was seen that pre-incubation with SP-A reduced infection as compared to the control, and this effect was most prominent after 24 hours (4-fold decrease in infection). After 48 and 72 hours, SP-A decreased infection by 1.5-fold, showing that SP-A is most protective in the very early stages of infection. Although a trend was clearly observed, these results were not significant.

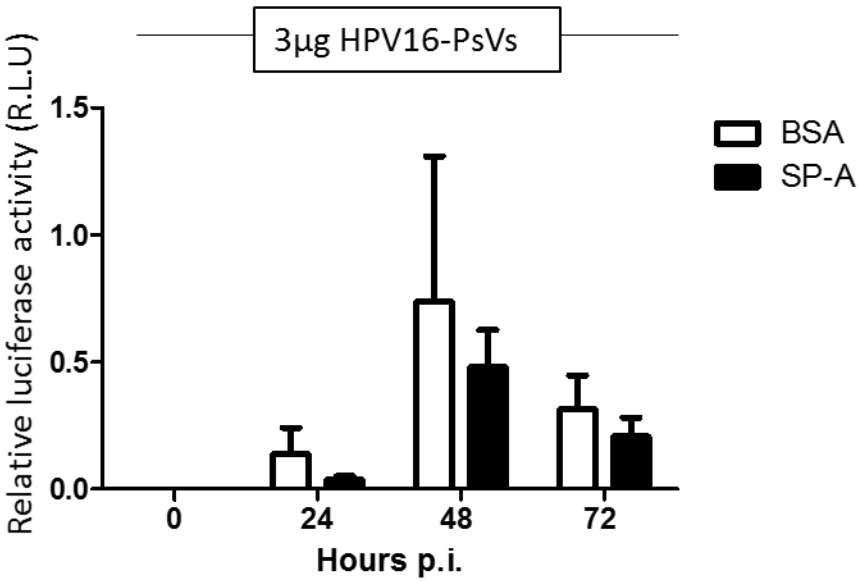

Figure 3.12: SP-A-mediated reduction of HPV16-PsVs infection is maximal at 24 hours p.i. 6-10 weeks old C57BL/6 mice were challenged with 3µg HPV16-PsVs (containing the GLuc reporter plasmid), either pre-incubated with 30µg BSA (control) or 30µg SP-A, following the procedure described in Figure 2.2. Mice were lavaged with 50µL sterile PBS daily over 72 hours, and luciferase activity measured. Relative luciferase activity (R.L.U) represents luminescence (arbitrary units) divided by protein concentration (mg/mL). Shown here is the data from one experiment, with 6 mice per group. Bars depict mean values, with error bars showing SEM.

3.3.4. The presence of SP-A does not affect macrophage recruitment in the genital tract of C57BL/6 mice

To determine whether pre-incubation of AF488-HPV16-PsVs with SP-A influenced macrophage recruitment in the genital tract, IHC followed by confocal microscopy was used. Genital tract tissue was excised 24 hours p.i., as the SP-A-mediated reduction in infection was most pronounced after 24 hours (Figure 3.12.). The left panel of Figure 3.13.A. shows that there was no clear difference in macrophage recruitment in the epithelium after 24 hours for each condition tested. This was supported by quantification of the area of F4/80 macrophage staining (Figure 3.13.B.), which showed no significant difference in the area occupied by macrophages for each condition. Furthermore, under the chosen conditions AF488-HPV16-PsVs could not be detected in the genital tract tissue, but successful infection was validated using vaginal lavages (Figure 3.12.).

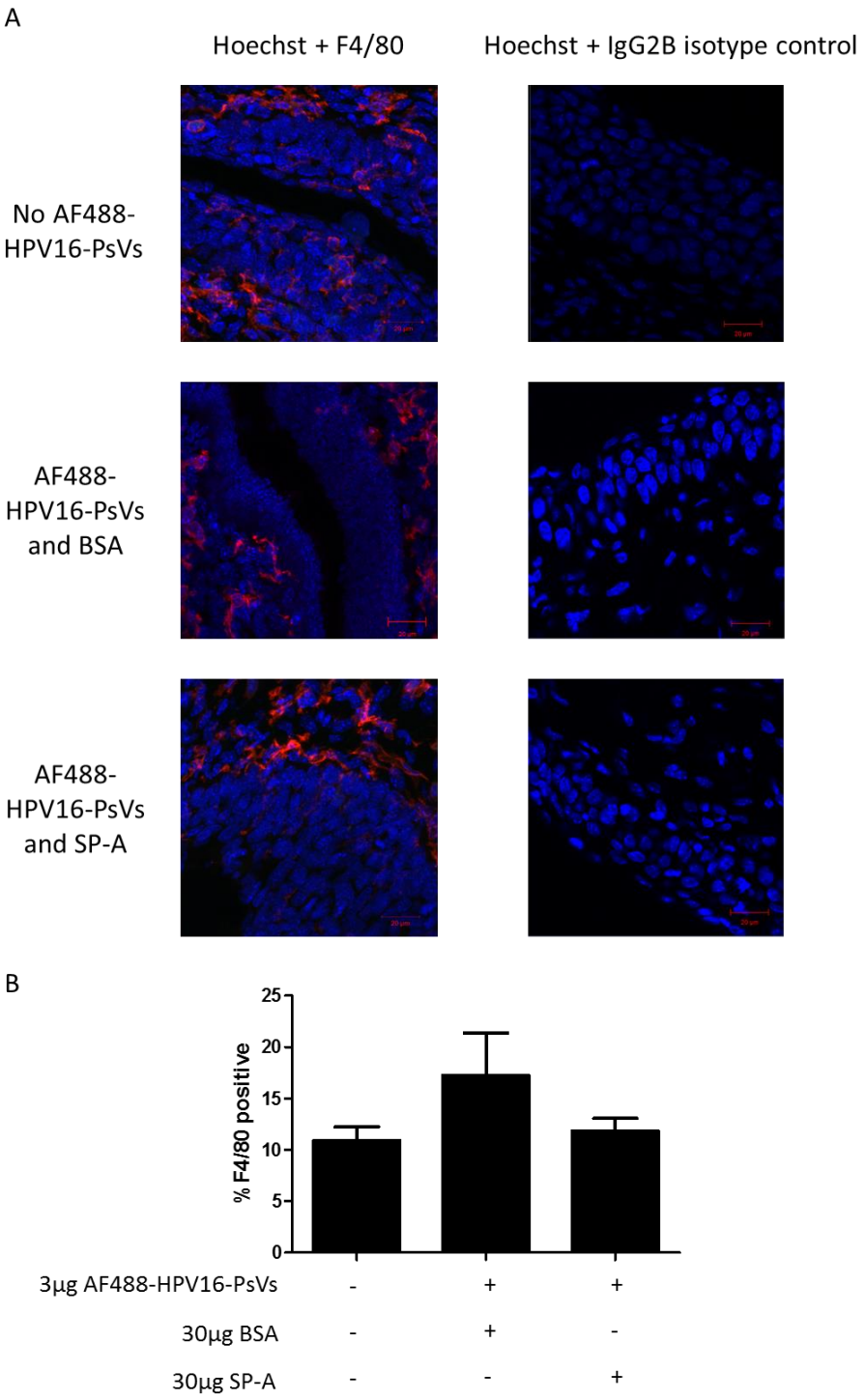

Figure 3.13: The presence of SP-A does not alter macrophage recruitment during HPV16-PsVs infection. 6-10 weeks old C57BL/6 mice were challenged with 3µg AF488-HPV16-PsVs either pre-incubated with 30µg BSA (control) or 30µg SP-A, following the procedure described in Figure 2.2. Genital tract tissue was excised, embedded in OCT and cryosectioned, followed by staining with F4/80 antibody and Hoechst nuclear stain. **A)** Representative maximum intensity projections of F4/80 (left panel) and IgG2B isotype control (right panel) for no HPV16-PsVs, HPV16-PsVs and BSA and HPV16-PsVs and SP-A. **B)** Bar graph showing the average percentage area of F4/80 positive staining in the epithelium for each condition, using 10 maximum intensity projections per condition for quantification. Bars in Figure B depict mean values, with error bars showing SEM.

4. Discussion

HPV successfully manages to evade the host immune response which can result in persistent infections and ultimately cancer development, with cervical cancer being the predominant HPV-associated malignancy. The majority of cervical cancer cases occur in the developing world, where the high incidence of HIV/AIDS is known to exacerbate these cases [130]. Although highly efficient prophylactic vaccines exist to prevent HPV16 and HPV18 infection, these are largely unavailable in low-resource settings due to the high costs involved and the requirement for one or two repeat vaccinations (depending on the age of first vaccination). Moreover, they do not cover all the oncogenic HPV types, and the extent of cross-protection against other oncogenic HPV types is largely unknown. This is specifically relevant in sub-Saharan Africa, where oncogenic HPV35 and 45 are highly prevalent due to their association with changes in immunodeficiency levels [131]. Fortunately, there are some pilot state-funded school-based vaccination projects underway to immunise adolescent girls in South Africa [45]. Nevertheless, it is expected that high-risk HPV will remain responsible for substantial disease burden for decades.

Studying means to enhance the innate immune recognition of the virus may, in the long term, lead to the development of alternative cost-effective, broad-spectrum approaches to preventing HPV infection. To this end, this research focused on the innate immune proteins SP-A and SP-D as potential candidates to impact HPV infection, as these molecules are known to enhance clearance of various viral and bacterial pathogens in the lung as well as other sites of the body [58]. As proof of concept, this study was limited to pseudovirions of HPV type 16, representing the most common oncogenic HPV type globally. Initially, *in vitro* experiments on the impact of surfactant proteins on HPV16-PsVs infection were performed, which were then studied in an *in vivo* mouse model.

4.1. The interaction of SP-A with HPV16-PsVs and the functional consequences *in vitro*

In order to determine whether SP-A and/or SP-D bind to HPV16-PsVs, Co-IP experiments were performed. It was observed that SP-A, but not SP-D, could bind to HPV16-PsVs (Figure 3.2. B-C). Since SP-A and SP-D often act as opsonins by binding to certain pathogens, these experiments gave the first indication that SP-A, but not SP-D, may have a potential role in recognising HPV16-PsVs. This was further supported when the functional consequences of this binding were analysed by examining viral internalisation by RAW264.7 macrophages in the presence of either SP-A or SP-D: indeed, it was observed that SP-A enhanced viral internalisation, while SP-D had no effect (Figure 3.2.D.). This further supported the hypothesis that SP-A may opsonise HPV16-PsVs, thereby increasing immune cell recognition of the virus and viral clearance. It is important to note that HPV16-PsVs infection, i.e. the arrival in the nucleus and successful transcription of the reporter gene luciferase (encapsidated in the viral particle representing the pseudogenome), was extremely low in RAW264.7 macrophages compared to the luciferase activity measured in the epithelial cell line HeLa, whose infectivity was not affected by SP-A (Figure 3.2.E). This is supported by the general assumption that HPV has a very strict tissue tropism *in vivo* and exclusively infects basal epithelial cells, as its life cycle is dependent on the differentiation of basal cells into keratinocytes. While macrophages are not known to be infected by HPV, the data presented herein indicate that they can internalise (and probably "kill") the virus reducing its potential to infect epithelial cells, which was enhanced in the presence of SP-A. This molecule therefore presented an interesting candidate for further study in terms of enhancing immune recognition of HPV, thereby preventing infection.

When the mode of SP-A-mediated increase in viral internalisation by RAW264.7 macrophages was further studied, it was observed that this interaction was calcium- but not mannose-dependent. Previous crystallographic and solution binding studies have elucidated the calcium binding sites of SP-A: one site is located in the CRD, whilst another site is located in an anionic portion of the neck region [67]. It is likely that the calcium binding site in the neck region is important in the context of HPV16-PsVs, as the CRD seems to not be involved in binding and increased viral internalisation as revealed by the competition studies using mannose (Figure 3.4.). The non-involvement of SP-A's CRD in binding to HPV16-PsVs is not

surprising as HPV is not known to display glycosylated surface/capsid proteins. SP-A may instead recognise HPV16-PsVs in an alternate manner, such as via the neck domain. Further studies are needed to confirm this hypothesis, for example by using recombinant fragments of SP-A and determining which portion of the protein interacts with the virus.

4.2. Establishment of the HPV16-PsVs murine challenge model at UCT

The *in vitro* results described above supported the hypothesis that SP-A may opsonise HPV16-PsVs, thereby increasing viral recognition by immune cells such as macrophages, leading to viral clearance and decreased infection. While cell culture experiments were valuable in initially studying the interaction between SP-A and HPV16-PsVs, they cannot sufficiently recapitulate the early events of sexual HPV transmission. The site of natural infection, i.e. the female genital tract, is very complex as several diverse cell types are potentially involved in infection as well as immune responses upon challenge with oncogenic HPV, including local epithelial cells and recruitment of inflammatory cells.

To study the described *in vitro* findings further, *in vivo* studies are not only appropriate to confirm these observations but also to identify underlying mechanisms which contribute to the SP-A and HPV16-PsVs relationship. To this end, an HPV16-PsVs murine cervicovaginal challenge model, which is being widely used in the field, was set up at UCT as part of this MSc project. This model was developed by Roberts *et al.* [122] in 2007 as the first animal model to recapitulate the early events of human sexual transmission of HPV infecting the cervicovaginal epithelium. While productive papillomavirus infection with authentic virions is difficult and highly species- and tissue-restricted, HPV pseudovirions can transduce murine genital epithelium under the specific conditions developed by Roberts *et al.* [122]. These conditions include progesterone treatment for four days, abrasion of the genital tract immediately before exposure to the pseudovirus, and tissue analysis for reporter gene expression 72 hours after inoculation. Very recently, a murine papillomavirus mouse model has been developed [121] which allows the study of anogenital disease and cancers associated with papillomaviruses, rather than early (non-productive) events as described in this thesis. However, since all *in vitro* experiments were performed using HPV16-PsVs, it was

ideal to continue using these same particles together with the *in vivo* model described by Roberts *et al.* [122].

With the aim to study the effect of SP-A on HPV16-PsVs infection *in vivo*, various experimental parameters had to be optimised. For this study, C57BL/6 mice instead of BALB/cAnNCr mice (as per the protocol by Roberts *et al.*[122]) were used for HPV16-PsVs challenge experiments, because SP-A knockout mice were available in this strain to be used in future studies. Firstly, the optimal HPV16-PsVs dose was determined as 3µg HPV16-PsVs (9 x 10^{10} infectious units) per mouse (Figure 3.6.), which was a higher dose than that described by Roberts *et al.* (5 x 10^{9} infectious units). This could be explained by the different mouse strain used as well as different technical approaches to assess infection: since no live imaging system was available to measure luminescence, readings were obtained using homogenised genital tract tissue as well as vaginal lavages. Both firefly and Gaussia luciferase resulted in comparable patterns of infection. While Gaussia luciferase (being a secreted enzyme) was highly detectable in the vaginal lavages, some firefly luciferase (although being primarily an intracellular enzyme) was also detected in the lavages, probably due to the release of the enzyme from shed cells following the addition of a cell lysis buffer. Overall, it was found that depending on the experimental read-out, either firefly or Gaussia luciferase could be reliably used. For example, for time course experiments, GLuc-containing HPV16-PsVs was deemed to be more suitable than FLuc HPV16-PsVs. Using GLuc-HPV16-PsVs allowed for luciferase activity to be measured daily, as Gaussia luciferase was secreted and no cell lysis buffer was needed (Figure 3.7.). While firefly luciferase activity could also be measured in lavages from FLuc-HPV16-PsVs, these values were at least 10-fold lower than when using GLuc-HPV16-PsVs, and they did not increase over the 72-hour time-course (Figure 3.7.). Therefore, GLuc-HPV16-PsVs was better suited for time course experiments.

It is important to note that the HPV16-PsVs murine challenge model used here did not cause distress, as procedures were mild and did not negatively affect the well-being of the mice. Mice did not develop any pathologies because the model used pseudovirions only carrying a reporter gene, and the model was designed to study early stages of infection running over a very short period of seven days. Now that this HPV16-PsVs murine challenge model has been established at UCT, it will prove to be an invaluable tool in our laboratory to study other

modulators of HPV16 infection *in vivo* such as the recently identified HPV-restriction molecule vimentin [126].

4.3. SP-A expression in the murine genital tract and its impact on HPV16-PsVs infection *in vivo*

Before the effect of SP-A on HPV16-PsVs infection could be studied *in vivo*, it was necessary to determine endogenous SP-A expression in naïve and HPV-infected animals. While SP-A expression in the human female genital tract has been described previously [101], to our knowledge it was unknown whether SP-A was expressed in the murine female genital tract. Therefore, SP-A protein expression was initially analysed in naïve C57BL/6 mice prior to HPV16-PsVs challenge experiments. No endogenous SP-A could be detected in the vaginal lavages or the genital tract tissue of naïve C57BL/6 mice while it was abundantly present in the lung and alveolar lavage fluid as expected (Figure 3.8.). Next, the effect of HPV16-PsVs challenge on induction of endogenous SP-A expression was to be determined. Various studies have described the upregulation of SP-A following infection with certain pathogens (such as *Klebsiella pneumoniae* [132]), with the increase in expression suggested to have a protective effect against infection. In the Swiss Black murine female genital tract, SP-D has been shown to be upregulated following infection with *C.muridarum* [108]. However, no SP-A expression was observed following HPV16-PsVs infection, neither on mRNA level nor on protein level (Figure 3.9. and Figure 3.10.).

The absence of SP-A in the genital tract of C57BL/6 mice made the use of SP-A knockout mice become obsolete. Instead of studying a loss-of-function approach to determine whether mice deficient in SP-A were more susceptible to incoming HPV virions as initially planned, the focus of this project was shifted to the question whether artificial supplementation with exogenous SP-A had an effect on HPV challenge.

To this end, HPV16-PsVs were pre-incubated with purified SP-A protein before inoculation into the female C57BL/6 murine genital tract. As seen already in cell culture, the 1:10 HPV16-PsVs to SP-A (w/w) ratio, which caused the largest increase in HPV16-PsVs internalisation by RAW264.7 macrophages, also caused the most substantial decrease in HPV16-PsVs infection *in vivo* (Figure 3.11). This observation supported the hypothesis that SP-A may facilitate HPV

recognition by immune cells leading to an overall decrease in infection of epithelial cells. While these results were not significant, a definite trend was seen for each individual experiment performed. When studied over 72 hours, it was noted that the most substantial decrease in infection was 24 hours p.i. (Figure 3.12). This could be explained by SP-A being an innate immune protein, thereby typically exerting its protective effects early during an infection.

Since it was hypothesised that macrophages were likely to be involved in the SP-A-mediated reduction of HPV16-PsVs infection, macrophage recruitment was studied using IHC and confocal microscopy. Our results indicated that SP-A had no effect on macrophage recruitment during infection with HPV16-PsVs after 24 hours (Figure 3.13.). Furthermore, although successful infection was confirmed using vaginal lavages, the AF488 labelled HPV16-PsVs particles could not be detected in infected genital tract tissue after this period. These results may not be an accurate reflection of what may be occurring in the genital tract after HPV16-PsVs infection, for a number of reasons. Firstly, the time point chosen for genital tract extraction (24 hours p.i.) may have been unsuitable for visualising HPV16-PsVs infection. This time point was chosen as SP-A had the most substantial effect on HPV16-PsVs by reducing infection by 4-fold 24 hours p.i. (Figure 3.12.); however, Roberts *et al.* examined tissue 2 hours p.i. and AF488-HPV16-PsVs was detectable [122]. After 24 hours, it was likely that capsid degradation had already occurred, or the fluorescent AF488 signal may have been bleached. Secondly, the usage of N-9 to chemically disrupt the genital epithelium may have been unsuitable for macrophage recruitment experiments. Although disruption of the genital epithelium is absolutely required for successful HPV infection, both in this mouse model as well as in the natural setting, N-9 is transiently proinflammatory [133]. It is therefore plausible that any effect on macrophage recruitment due to SP-A and/or HPV16-PsVs infection would have been masked. In future experiments, it may be more suitable to use a cytobrush to mechanically disrupt the genital epithelium, which may more appropriately mimic the natural process. This might also explain why the effect of SP-A on HPV infection compared to controls did not reach statistical significance; N-9 mediated inflammation and macrophage recruitment might have concealed underlying effects. Thirdly, the technique used to analyse macrophage recruitment also has its limitations: because the area was measured from a 2-dimensional maximum intensity projection, it did not account for any macrophages which

may have overlapped those found in different layers of the tissue section. While cell counting was an alternative option, this method is more biased than measuring the area occupied and it does not account for changes in macrophage complexity or size due to activation. In the future, it may be beneficial to study different immune cells, such as Langerhans cells. Additionally, the inflammatory response following inflammation can be measured by analysing cytokine responses.

Therefore, although the HPV16-PsVs murine challenge model described here is widely used in the field to address various HPV-related research questions, it may be unsuitable for studying innate immune responses in the murine female genital tract, and some optimisation is required in future studies, such as alternative epithelial cell disruption techniques, alternative time points for read-outs and alternative immune markers to study. This would allow for more insight on the mechanism by which SP-A reduces HPV16-PsVs infection.

5. Conclusion

In this study, it was aimed to determine whether surfactant proteins A and D enhanced the immune recognition of HPV16-PsVs in the female genital tract, thereby preventing new infection. *In vitro*, it was observed that SP-A interacted with HPV16-PsVs and enhanced uptake of the pseudovirus by RAW264.7 macrophages in a calcium-dependent and CRD independent manner. In the context of an *in vivo* HPV16-PsVs murine cervicovaginal challenge model, it was determined that SP-A reduced HPV16-PsVs infection in female C57BL/6 mice. Although some optimisation is still required, the set-up of the HPV16-PsVs challenge model at UCT will open new doors to address several HPV-related research questions *in vivo*. As exemplified by this study, the impact of HPV-binding molecules potentially inhibiting infection can be studied. In the long term, once the correct region of SP-A which binds to HPV16-PsVs has been identified, analogues or recombinant fragments of SP-A could be incorporated into topical microbicides as an alternative measure to reduce overall HPV infection.

References

1 Schäfer, G., Blumenthal, M. J. and Katz, A. A. (2015) Interaction of human tumor viruses with host cell surface receptors and cell entry. Viruses **7**, 2592–2617.

2 Trottier, H. and Franco, E. L. (2006) The epidemiology of genital human papillomavirus infection. Vaccine **1**, 4–15.

3 zur Hausen, H. (2002) Papillomaviruses and cancer: from basic studies to clinical application. Nat. Rev. Cancer **2**, 342–350.

4 Bernard, H. U., Burk, R. D., Chen, Z., van Doorslaer, K., Hausen, H. zur and de Villiers, E. M. (2010) Classification of papillomaviruses (PVs) based on 189 PV types and proposal of taxonomic amendments. Virology 70–79.

5 Stanley, M. A. (2012) Epithelial cell responses to infection with human papillomavirus. Clin. Microbiol. Rev. **25**, 215–222.

6 Muñoz, N., Xavier Bosch, F., Castellsagué, X., Díaz, M., De Sanjose, S., Hammouda, D., Shah, K. V. and Meijer, C. J. L. M. (2004) Against which human papillomavirus types shall we vaccinate and screen? The international perspective. Int. J. Cancer **111**, 278–285.

7 Mesri, E. A., Feitelson, M. A. and Munger, K. (2014) Human viral oncogenesis: A cancer hallmarks analysis. Cell Host Microbe, Elsevier Inc. **15**, 266–282.

8 Ferlay J, Soerjomataram I, Ervik M, Dikshit R, Eser S, Mathers C, Rebelo M, Parkin DM, Forman D, Bray, F. (2014) Cancer incidence and mortality worldwide: sources, methods and major patterns in GLOBOCAN 2012. Int. J. Cancer E359–E386.

9 ICO Information Centre on HPV and Cancer. (2017) Human Papillomavirus and Related Diseases Report 1–78.

10 Harro, C. D., Pang, Y. Y., Roden, R. B., Hildesheim, a, Wang, Z., Reynolds, M. J., Mast, T. C., Robinson, R., Murphy, B. R., Karron, R. a, et al. (2001) Safety and immunogenicity trial in adult volunteers of a human papillomavirus 16 L1 virus-like particle vaccine. J. Natl. Cancer Inst. **93**, 284–292.

11 Strickler, H. D., Burk, R. D., Fazzari, M., Anastos, K., Minkoff, H., Massad, L. S., Hall, C., Bacon, M., Levine, A. M., Watts, D. H., et al. (2005) Natural history and possible reactivation of human papillomavirus in human immunodeficiency virus-positive women. J. Natl. Cancer Inst. **97**, 577–586.

12 Grulich, A. E., van Leeuwen, M. T., Falster, M. O. and Vajdic, C. M. (2007) Incidence of cancers in people with HIV / AIDS compared with immunosuppressed transplant recipients: a meta-analysis. Lancet **370**, 59–67.

13 Abraham, A. G., Strickler, H. D., Jing, Y., Gange, S. J., Timothy, R., Moore, R. D., Klein, M., Kitahata, M., Kirk, G. and Hogg, R. (2014) Invasive cervical cancer risk among HIV-infected women: North American multi-cohort collaboration prospective study. J Acqui Immune Defic Syndr **62**, 405–413.

14 Doorbar, J. (2005) The papillomavirus life cycle. J. Clin. Virol. 7-15.

15 Pim, D. and Banks, L. (2010) Interaction of viral oncoproteins with cellular target molecules: Infection with high-risk vs low-risk human papillomaviruses. Apmis **118**, 471–493.

16 Oh, S. T., Longworth, M. S. and Laimins, L. a. (2004) Roles of the E6 and E7 proteins in the life cycle of low-risk human papillomavirus type 11. J. Virol. **78**, 2620–2626.

17 Moody, C. A. and Laimins, L. A. (2010) Human papillomavirus oncoproteins : pathways to transformation. Nat. Rev. Cancer, Nature Publishing Group **10**, 550–560.

18 Chow, L. T., Broker, T. R. and Steinberg, B. M. (2010) The natural history of human papillomavirus infections of the mucosal epithelia. Apmis **118**, 422–449.

19 Baker, T. S., Newcomb, W. W., Olson, N. H., Cowsert, L. M., Olson, C. and Brown, J. C. (1991) Structures of bovine and human papillomaviruses. Analysis by cryoelectron microscopy and three-dimensional image reconstruction. Biophys. J. **60**, 1445–1456.

20 Buck, C. B., Cheng, N., Thompson, C. D., Lowy, D. R., Steven, A. C., Schiller, J. T. and Trus, B. L. (2008) Arrangement of L2 within the papillomavirus capsid. J. Virol. **82**, 5190–5197.

21 Kines, R. C., Thompson, C. D., Lowy, D. R., Schiller, J. T. and Day, P. M. (2009) The initial steps leading to papillomavirus infection occur on the basement membrane prior to cell surface binding. Proc. Natl. Acad. Sci. U. S. A. **106**, 20458–20463.

22 Schiller, J. T., Day, P. M. and Kines, R. C. (2010) Current understanding of the mechanism of HPV infection. Gynecol. Oncol., Elsevier B.V. **118**, S12–S17.

23 Culp, T. D., Budgeon, L. R., Marinkovich, M. P., Meneguzzi, G. and Christensen, N. D. (2006) Keratinocyte-secreted laminin 5 can function as a transient receptor for human papillomaviruses by binding virions and transferring them to adjacent cells. J. Virol. **80**, 8940–8950.

24 Cerqueira, C., Samperio Ventayol, P., Vogeley, C. and Schelhaas, M. (2015) Kallikrein-8 proteolytically processes Human papillomaviruses in the extracellular space to facilitate entry into host cells. J. Virol. **89**, JVI.00234-15.

25 Bienkowska-Haba, M., Patel, H. D. and Sapp, M. (2009) Target cell cyclophilins facilitate human papillomavirus type 16 infection. PLoS Pathog. **5**, 1–11.

26 Richards, R. M., Lowy, D. R., Schiller, J. T. and Day, P. M. (2006) Cleavage of the papillomavirus minor capsid protein, L2, at a furin consensus site is necessary for infection. Proc. Natl. Acad. Sci. U. S. A. **103**, 1522–1527.

27 Day, P. M., Lowy, D. R. and Schiller, J. T. (2008) Heparan sulfate-independent cell binding and infection with furin-precleaved papillomavirus capsids. J. Virol. **82**, 12565–12568.

28 Day, P. M. and Schelhaas, M. (2014) Concepts of papillomavirus entry into host cells. Curr. Opin. Virol., Elsevier B.V. **4**, 24–31.

29 Bergant Marusic, M., Ozbun, M. A., Campos, S. K., Myers, M. P. and Banks, L. (2012) Human Papillomavirus L2 Facilitates Viral Escape from Late Endosomes via Sorting Nexin 17. Traffic **13**, 455–467.

30 Zhang, W., Kazakov, T., Popa, A. and DiMaio, D. (2014) Vesicular Trafficking of Incoming Human Papillomavirus 16 to the Golgi Apparatus and Endoplasmic Reticulum Requires Gamma -Secretase Activity. MBio **5**, 1–11.

31 Schneider, M. A., Spoden, G. A., Florin, L. and Lambert, C. (2011) Identification of the dynein light chains required for human papillomavirus infection. Cell. Microbiol. **13**, 32–46.

32 Kanodia, S., Fahey, L. and Kast, W. M. (2007) Mechanisms Used by Human Papillomaviruses to Escape the Host Immune Response. Curr. Cancer Drug Targets **7**, 79–89.

33 Ciesielska, U., Nowińska, K., Podhorska-Okołów, M. and Dzięgiel, P. (2012) The role of human papillomavirus in the malignant transformation of cervix epithelial cells and the importance of vaccination against this virus. Adv. Clin. Exp. Med. **21**, 235–244.

34 Tindle, R. W. (2002) Immune evasion in human papillomavirus-associated cervical cancer. Nat. Rev. Cancer **2**, 1–9.

35 Barnard, P., Payne, E. and Mcmillan, N. A. J. (2000) The Human Papillomavirus E7 Protein Is Able to Inhibit the Antiviral and Anti-growth Functions of Interferon- alpha. Virology **419**, 411–419.

36 Cho, Y., Kang, J., Cho, M., Cho, C., Lee, S., Choe, Y., Kim, Y., Choi, I., Park, S., Kim, S., et al. (2001) Down modulation of IL-18 expression by human papillomavirus type 16 E6 oncogene via binding to IL-18. FEBS Lett. **501**, 139–145.

37 Hasan, U. A., Bates, E., Takeshita, F., Biliato, A., Accardi, R., Bouvard, V., Mansour, M., Vincent, I., Gissmann, L., Sideri, M., et al. (2007) TLR9 Expression and Function Is Abolished by the Cervical Cancer-Associated Human Papillomavirus Type 16. J. Immunol. 3186–3197.

38 Beutler, B. (2004) Inferences , questions and possibilities in Toll -like receptor signalling. Nature 257–263.

39 Stanley, M. (2006) Immune responses to human papillomavirus. Vaccine **1**, 16–22.

40 Palefsky, J. M. and Holly, E. A. (2003) Immunosuppression and Co -infection with HIV. J. Natl. Cancer Inst. **94143**, 5–10.

41 Harper, D. M., Franco, E. L., Wheeler, C., Ferris, D. G., Jenkins, D., Schuind, A., Zahaf, T., Innis, B., Naud, P., De Carvalho, N. S., et al. (2004) Efficacy of a bivalent L1 virus -like particle vaccine in prevention of infection with human papillomavirus types 16 and 18 in young women: A randomised controlled trial. Lancet **364**, 1757–1765.

42 Villa, L. L., Costa, R. L. R., Petta, C. a., Andrade, R. P., Ault, K. a., Giuliano, A. R., Wheeler, C. M., Koutsky, L. a., Malm, C., Lehtinen, M., et al. (2005) Prophylactic quadrivalent human papillomavirus (types 6, 11, 16, and 18) L1 virus -like particle vaccine in young women: A randomised double-blind placebo-controlled multicentre phase II efficacy trial. Lancet Oncol. **6**, 271–278.

43 Joura, E. a., Giuliano, A. R., Iversen, O.-E., Bouchard, C., Mao, C., Mehlsen, J., Moreira, E. D., Ngan, Y., Petersen, L. K., Lazcano-Ponce, E., et al. (2015) A 9-Valent HPV Vaccine against Infection and Intraepithelial Neoplasia in Women. N. Engl. J. Med. **372**, 711–723.

44 Schiller, J. T. and Lowy, D. R. (2012) Understanding and learning from the success of prophylactic human papillomavirus vaccines. Nat. Rev. Microbiol. **10**, 681–692.

45 National Department of Health. (2014) Human Papilloma Virus (HPV) programme.

46 (2009) HPV vaccine for prevention of cervical cancer: key issues and challenges for developing countries. JNMA. J. Nepal Med. Assoc. **48**, I–II.

47 Agosti, J. M. and Goldie, S. J. (2007) Introducing HPV vaccine in developing countries --key challenges and issues. N. Engl. J. Med. **356**, 1908–1910.

48 Hildesheim, A., Herrero, R., Wacholder, S., Rodriguez, A. C., Solomon, D., Bratti, M. C., Schiller, J. T., Gonzalez, P., Dubin, G., Porras, C., et al. (2007) Effect of human papillomavirus 16/18 L1 viruslike particle vaccine among young women with preexisting infection: a randomized trial. JAMA **298**, 743–753.

49 Cutts, F. and S Franceschi, S Goldie, X Castellsague, S de Sanjose, G Garnett, WJ Edmunds, P Claeys, KL Goldenthal, D. H. & L. M. (2007) Human papillomavirus and HPV vaccines: a review. Bull. World Heal. Organ. **85**, 812–819.

50 Herrero, R. (2009) Human papillomavirus (HPV) vaccines: limited cross-protection against additional HPV types. J. Infect. Dis. **199**, 919–922.

51 de Vuyst, H., Alemany, L., Lacey, C., Chibwesha, C. J., Sahasrabuddhe, V., Banura, C., Denny, L. and Parham, G. P. (2013) The Burden of Human Papillomavirus Infections and Re lated Diseases in Sub-Saharan Africa. Vaccine **31**, 1781–1791.

52 Huang, H. S., Pyeon, D., Pearce, S. M., Lank, S. M., Griffin, L. M., Ahlquist, P. and Lambert, P. F. (2012) Novel antivirals inhibit early steps in HPV infection. Antiviral Res., Elsevier B.V . **93**, 280–287.

53 Buck, C. B., Thompson, C. D., Roberts, J. N., Müller, M., Lowy, D. R. and Schiller, J. T. (2006) Carrageenan is a potent inhibitor of papillomavirus infection. PLoS Pathog. **2**, 0671–0680.

54 Marais, D., Gawarecki, D., Allan, B., Ahmed, K., Altini, L., Cassim, N., Gopolang, F., Hoffman, M., Ramjee, G. and Williamson, A. L. (2011) The effectiveness of Carraguard, a vaginal microbicide, in protecting women against high-risk human papillomavirus infection. Antivir. Ther. **16**, 1219–1226.

55 Pattle, R. E. (1955) Properties, function and origin of the alveolar lining layer. Nature **175**, 1125–1126.

56 Kishore, U., Bernal, A. L., Kamran, M. F., Saxena, S., Singh, M., Sarma, P. U., Madan, T. and Chakraborty, T. (2005) Surfactant proteins SP-A and SP-D in human health and disease. Arch. Immunol. Ther. Exp. (Warsz). **53**, 399–417.

57 Wright, J. R. (2005) Immunoregulatory functions of surfactant proteins. Nat. Rev. Immunol. **5**, 58–68.

58 Ujma, S., Horsnell, W. G. C., Katz, A. A., Clark, H. W. and Schafer, G. (2016) Non-Pulmonary Immune Functions of Surfactant Proteins A and D. J. Innate Immun. **9**, 3–11.

59 Haczku, A. (2008) Protective role of the lung collectins surfactant protein A and surfactant protein D in airway inflammation. J. Allergy Clin. Immunol., Elsevier Ltd **122**, 861–879.

60 Bruns, G., Stroh, H., Veldman, G. M., Latt, S. A. and Floros, J. (1987) The 35 kd pulmonary surfactant-associated protein is encoded on chromosome 10. Hum. Genet. **27**, 58–62.

61 Crouch, E., Rust, K., Veilell, R., Donis-kellerll, H. and Grossos, L. (1993) Genomic Organization of Human Surfactant Protein D (SP-D). J. Biol. Chem. **268**, 2976–2983.

62 Håkansson, K., Lim, N. K., Hoppe, H. J. and Reid, K. B. (1999) Crystal structure of the trimeric alpha-helical coiled-coil and the three lectin domains of human lung surfactant protein D. Structure **7**, 255–264.

63 Kishore, U., Greenhough, T. J., Waters, P., Shrive, A. K., Ghai, R., Kamran, M. F., Bernal, A. L., Reid, K. B. M., Madan, T. and Chakraborty, T. (2006) Surfactant proteins SP-A and SP-D: Structure, function and receptors. Mol. Immunol. **43**, 1293–1315.

64 Crouch, E., Persson, a, Chang, D. and Heuser, J. (1994) Molecular structure of pulmonary surfactant protein D (SP-D). J. Biol. Chem. **269**, 17311–17319.

65 Drickamer, K. (1988) Two distinct classes of carbohydrate recognition domains in animal lectins. J. Biol. Chem. **263**, 9557–9560.

66 Jakel, A., Qasseem, A. S., Kishore, U. and Sim, R. B. (2013) Ligands and receptors of lung surfactant proteins SP-A and SP-D. Front. Biosci. 1129–1140.

67 Head, J. F., Mealy, T. R., McCormack, F. X. and Seaton, B. A. (2003) Crystal Structure of Trimeric Carbohydrate Recognition and Neck Domains of Surfactant Protein A. J. Biol. Chem. **278**, 43254–43260.

68 Jäkel, A., Clark, H., Reid, K. B. M. and Sim, R. B. (2010) The human lung surfactant proteins A (SP-A) and D (SP-D) interact with apoptotic target cells by different binding mechanisms. Immunobiology **215**, 551–558.

69 LeVine, a M., Whitsett, J. a, Gwozdz, J. a, Richardson, T. R., Fisher, J. H., Burhans, M. S. and Korfhagen, T. R. (2000) Distinct effects of surfactant protein A or D deficiency during bacterial infection on the lung. J. Immunol. **165**, 3934–3940.

70 LeVine, A. M., Kurak, K. E., Bruno, M. D., Stark, J. M., Whitsett, J. a. and Korfhagen, T. R. (1998) Surfactant protein-A-deficient mice are susceptible to Pseudomonas aeruginosa infection. Am. J. Respir. Cell Mol. Biol. **19**, 700–708.

71 Caynor, C. D., Mccormack, F. X., Voelker, D. R., Mcgowan, S. E. and Schlesinger, L. S. (1995) Pulmonary surfactant protein A mediates enhanced phagocytosis of mycobacterium tuberculosis by a direct interaction with human macrophages. J. Immunol. **155**, 5343–5351.

72 J. Scott Ferguson, Dennis R. Voelker, F. X. M. and L. S. S. (1999) Surfactant Protein D Binds to Mycobacterium tuberculosis Bacilli and Lipoarabinomannan via Carbohydrate-Lectin Interactions Resulting in Reduced Phagocytosis of the Bacteria by Macrophages 1 **163**, 312–321.

73 Ferguson, J. S., Martin, J. L., Azad, A. K., McCarthy, T. R., Kang, P. B., Voelker, D. R., Crouch, E. C. and Schlesinger, L. S. (2006) Surfactant protein D increases fusion of Mycobacterium tuberculosis-containing phagosomes with lysosomes in human macrophages. Infect. Immun. **74**, 7005–7009.

74 Hartshorn, K. L., White, M. R., Shepherd, V., Reid, K., Jensenius, J. C. and Crouch, E. C. (1997) Mechanisms of anti-influenza activity of surfactant proteins A and D: comparison with serum collectins. Am. J. Physiol. **273**, L1156–L1166.

75 LeVine, a M., Whitsett, J. a, Hartshorn, K. L., Crouch, E. C. and Korfhagen, T. R. (2001) Surfactant protein D enhances clearance of influenza A virus from the lung in vivo. J. Immunol. **167**, 5868–5873.

76 Reading, P. C., Morey, L. S. and Crouch, E. C. (1997) Collectin-mediated antiviral host defense of the lung : evidence from influenza virus infection of mice . Collectin-Mediated Antiviral Host Defense of the Lung : Evidence from Influenza Virus Infection of Mice. J. Virol. **71**, 8204–8212.

77 LeVine, A. M., Elliott, J., Whitsett, J. a., Srikiatkhachorn, A., Crouch, E., DeSilva, N. and Korfhagen, T. (2004) Surfactant protein-D enhances phagocytosis and pulmonary clearance of respiratory syncytial virus. Am. J. Respir. Cell Mol. Biol. **31**, 193–199.

78 Ghildyal, R., Hartley, C., Varrasso, a, Meanger, J., Voelker, D. R., Anders, E. M. and Mills, J. (1999) Surfactant protein A binds to the fusion glycoprotein of respiratory syncytial virus and neutralizes virion infectivity. J. Infect. Dis. **180**, 2009–2013.

79 Lahti, M., Löfgren, J., Marttila, R., Renko, M. and Klaavuniemi, T. (2002) Surfactant Protein D Gene Polymorphism Associated with Severe Respiratory Syncytial Virus Infection. Pediatr Res **51**, 696–699.

80 Lüfgren, J., Rämet, M., Renko, M., Marttila, R. and Hallman, M. (2002) Association between Surfactant Protein A Gene Locus and Severe Respiratory Syncytial Virus Infection in Infants. J Infect Dis. **185**, 283–289.

81 Simoons-Smit, A. M., Kraan, E. M., Beishuizen, A., Strack van Schijndel, R. J. and Vandenbroucke-Grauls, C. M. (2006) Herpes simplex virus type 1 and respiratory disease in critically-ill patients: Real pathogen or innocent bystander? Clin. Microbiol. Infect., European Society of Clinical Infectious Diseases **12**, 1050–1059.

82 van Iwaarden, J. F., van Strijp, J. a, Visser, H., Haagsman, H. P., Verhoef, J. and van Golde, L. M. (1992) Binding of surfactant protein A (SP-A) to herpes simplex virus type 1-infected cells is mediated by the carbohydrate moiety of SP-A. J. Biol. Chem. **267**, 25039–25043.

83 Thawer, S., Auret, J., Schnoeller, C., Chetty, A., Smith, K., Darby, M., Roberts, L., Mackay, R.-M., Whitwell, H. J., Timms, J. F., et al. (2016) Surfactant Protein-D Is Essential for Immunity to Helminth Infection. PLOS Pathog. **12**, 1–18.

84 Schagat, T. L., Wofford, J. a and Wright, J. R. (2001) Surfactant protein A enhances alveolar macrophage phagocytosis of apoptotic neutrophils. J. Immunol. **166**, 2727–2733.

85 Savill, J. (1997) Apoptosis in resolution of inflammation. J. Leukoc. Biol. **61**, 375–380.

86 Gardai, S. J., Xiao, Y. Q., Dickinson, M., Nick, J. a., Voelker, D. R., Greene, K. E. and Henson, P. M. (2003) By binding SIRP-a or calreticulin/CD91, lung collectins act as dual function surveillance molecules to suppress or enhance inflammation. Cell **115**, 13–23.

87 Li, G., Siddiqui, J., Hendry, M., Akiyama, J., Edmondson, J., Brown, C., Allen, L., Levitt, S., Poulain, F. and Hawgood, S. (2002) Surfactant protein-A-deficient mice display an exaggerated early inflammatory response to a beta-resistant strain of influenza A virus. Am. J. Respir. Cell Mol. Biol. **26**, 277–82.

88 Hawgood, S., Ochs, M., Jung, A., Akiyama, J., Allen, L., Brown, C., Edmondson, J., Levitt, S., Carlson, E., Gillespie, A. M., et al. (2002) Sequential targeted deficiency of SP-A and -D leads to progressive alveolar lipoproteinosis and emphysema. Am. J. Physiol. Lung Cell. Mol. Physiol. **283**, L1002-10.

89 Wert, S. E., Yoshida, M., LeVine, a M., Ikegami, M., Jones, T., Ross, G. F., Fisher, J. H., Korfhagen, T. R. and Whitsett, J. a. (2000) Increased metalloproteinase activity, oxidant production, and emphysema in surfactant protein D gene-inactivated mice. Proc. Natl. Acad. Sci. U. S. A. **97**, 5972–5977.

90 Mackay, R.-M. A., Grainge, C. L., Lau, L. C., Barber, C., Clark, H. W. and Howarth, P. H. (2016) Airway surfactant protein D (SP-D) deficiency in adults with severe asthma. Chest 1165–1172.

91 Honda, Y., Takahashi, H., Kuroki, Y., Akino, T. and Abe, S. (1996) Decreased Contents of Surfactant Proteins A and D in BAL Fluids of Healthy Smokers. Chest 1006–1009.

92 Lin, Z., deMello, D., Phelps, D. S., Koltun, W. A., Page, M. and Floros, J. (2001) Both human SP-A1 and Sp-A2 genes are expressed in small and large intestine. Pediatr. Pathol. Mol. Med. **20**, 367–86.

93 Madsen, J., Kliem, a, Tornoe, I., Skjodt, K., Koch, C. and Holmskov, U. (2000) Localization of lung surfactant protein D on mucosal surfaces in human tissues. J. Immunol. **164**, 5866–5870.

94 Hogenkamp, A., Herías, M. V., Tooten, P. C. J., Veldhuizen, E. J. A. and Haagsman, H. P. (2007) Effects of surfactant protein D on growth, adhesion and epithelial invasion of intestinal Gram-negative bacteria. Mol. Immunol. **44**, 3517–3527.

95 Saka, R., Wakimoto, T., Nishiumi, F., Sasaki, T., Nose, S., Fukuzawa, M., Oue, T., Yanagihara, I. and Okuyama, H. (2016) Surfactant protein-D attenuates the lipopolysaccharide-induced inflammation in human intestinal cells overexpressing toll-like receptor 4. Pediatr. Surg. Int., Springer Berlin Heidelberg **32**, 59–63.

96 Quintanilla, H. D., Liu, Y., Fatheree, N. Y., Atkins, C. L., Hashmi, S. S., Floros, J., McCormack, F. X., Rhoads, J. M. and Alcorn, J. L. (2015) Oral Administration of Surfactant Protein-A Reduces Pathology in an Experimental Model of Necrotizing Enterocolitis. J. Pediatr. Gastroenterol. Nutr. **60**, 613–620.

97 Hu, F., Ding, G., Zhang, Z., Gatto, L. A., Hawgood, S., Poulain, F. R., Cooney, R. N. and Wang, G. (2016) Innate immunity of surfactant proteins A and D in urinary tract infection with uropathogenic Escherichia coli. Innate Immun. **22**, 9–20.

98 Kurimura, Y., Nishitani, C., Ariki, S., Saito, A., Hasegawa, Y., Takahashi, M., Hashimoto, J., Takahashi, S., Tsukamoto, T. and Kuroki, Y. (2012) Surfactant protein D inhibits adherence of uropathogenic Escherichia coli to the bladder epithelial cells and the bacterium-induced cytotoxicity: a possible function in urinary tract. J. Biol. Chem. **287**, 39578–39588.

99 Liu, J., Hu, F., Liang, W., Wang, G., Singhal, P. C. and Ding, G. (2010) Polymorphisms in the surfactant protein a gene are associated with the susceptibility to recurrent urinary tract infection in chinese women. Tohoku J. Exp. Med. **221**, 35–42.

100 Garcia-Verdugo, I., Tanfin, Z. and Breuiller-Fouche, M. (2010) Surfactant protein A: An immunoregulatory molecule involved in female reproductive biology. Int. J. Biochem. Cell Biol., Elsevier Ltd **42**, 1779–1783.

101 MacNeill, C., Umstead, T. M., Phelps, D. S., Lin, Z., Floros, J., Shearer, D. a. and Weisz, J. (2004) Surfactant protein A, an innate immune factor, is expressed in the vaginal mucosa and is present in vaginal lavage fluid. Immunology **111**, 91–99.

102 Leth-Larsen, R., Floridon, C., Nielsen, O. and Holmskov, U. (2004) Surfactant protein D in the female genital tract. Mol. Hum. Reprod. **10**, 149–154.

103 Miyamura, K., Malhotra, R., Hoppe, H. J., Reid, K. B. M., Phizackerley, P. J. R., Macpherson, P. and Bernal, A. L. (1994) Surfactant proteins A (SP-A) and D (SP-D): Levels in human amniotic fluid and localization in the fetal membranes. Biochim. Biophys. Acta (BBA)/Lipids Lipid Metab. **1210**, 303–307.

104 Madhukaran, S. P., Kishore, U., Jamil, K., Choolani, M. and Lu, J. (2015) Decidual expression and localization of human surfactant protein SP-A and SP-D, and complement protein C1q. Mol. Immunol., Elsevier Ltd **66**, 197–207.

105 Madhukaran, S. P., Koippallil Gopalakrishnan, A. R., Pandit, H., Marri, E. D.-, Kouser, L., Jamil, K., Alhamlan, F. S., Kishore, U. and Madan, T. (2015) Expression of surfactant proteins SP-A and SP-D in murine decidua and immunomodulatory effects on decidual macrophages. Immunobiology, Elsevier GmbH. **221**, 377–386.

106 Lee, D.-C., Romero, R., Kim, C. J., Chaiworapongsa, T., Tarca, A. L., Lee, J., Suh, Y.-L., Mazaki-Tovi, S., Vaisbuch, E., Mittal, P., et al. (2011) Surfactant Protein-A as an Anti-Inflammatory Component in the Amnion: Implications for Human Pregnancy. J. Immunol. **4**, 6479–6491.

107 Oberley, R. E., Goss, K. L., Ault, K. A., Crouch, E. C. and Snyder, J. M. (2004) Surfactant protein D is present in the human female reproductive tract and inhibits Chlamydia trachomatis infection. Mol.Hum.Reprod. **10**, 861–870.

108 Oberley, R. E., Goss, K. L., Hoffmann, D. S., Ault, K. A., Neff, T. L., Ramsey, K. H. and Snyder, J.

M. (2007) Regulation of surfactant protein D in the mouse female reproductive tract in vivo. Mol. Hum. Reprod. **13**, 863–868.

109 Gaiha, G. D., Dong, T., Palaniyar, N., Mitchell, D. a, Reid, K. B. M. and Clark, H. W. (2008) Surfactant protein A binds to HIV and inhibits direct infection of CD4+ cells, but enhances dendritic cell-mediated viral transfer. J. Immunol. **181**, 601–609.

110 Madsen, J., Gaiha, G. D., Palaniyar, N., Dong, T., Mitchell, D. a. and Clark, H. W. (2013) Surfactant Protein D Modulates HIV Infection of Both T-Cells and Dendritic Cells. PLoS One **8**, 1–13.

111 Aksoy, P., Gottschalk, E. Y. and Meneses, P. I. (2016) HPV entry into cells. Mutat. Res. Mutat. Res., Elsevier B.V. 1–10.

112 Sexton, C. J., Williams, A. T., Topley, P., Shaw, R. J., Lovegrove, C., Leigh, I. and Stables, J. N. (1995) Development and characterization of a novel xenograft model permissive for human papillomavirus DNA amplification and late gene expression. J Gen Virol **76 (Pt 12**, 3107–3112.

113 Dollard, S. C., Wilson, J. L., Demeter, L. M., Bonnez, W., Reichman, R. C., Broker, T. R. and Chow, L. T. (1992) Production of human papillomavirus and modulation of the infectious program in epithelial raft cultures. Genes Dev. **6**, 1131–1142.

114 Buck, C. B., Pastrana, D. V, Lowy, D. R. and Schiller, J. T. (2004) Efficient intracellular assembly of papillomaviral vectors. J. Virol. **78**, 751–7.

115 Buck, C. B., Pastrana, D. V, Lowy, D. R. and Schiller, J. T. (2005) Generation of HPV pseudovirions using transfection and their use in neutralization assays. Methods Mol. Med. **119**, 445–462.

116 Joyce, J. G., Tung, J., Craig, T., Cook, J. C., Lehman, E. D., Sands, J. a, Jansen, K. U., Keller, M., Przysiecki, C. T. and Keller, P. M. (1999) The L1 Major Capsid Protein of Human Papillomavirus Type 11 Recombinant Virus-like Particles Interacts with Heparin and Cell-surface Glycosaminoglycans on The L1 Major Capsid Protein of Human Papillomavirus Type 11 Recomb. J. Biol. Chem. **274**, 5810–5822.

117 Giroglou, T., Florin, L., Schäfer, F., Streeck, R. E. and Sapp, M. (2001) Human papillomavirus infection requires cell surface heparan sulfate. J. Virol. 1565–1570.

118 Johnson, K. M., Kines, R. C., Roberts, J. N., Lowy, D. R., Schiller, J. T. and Day, P. M. (2009) Role of Heparan Sulfate in Attachment to and Infection of the Murine Female Genital Tract by Human Papillomavirus. J. Virol. **83**, 2067–2074.

119 Campo, M. S. (2002) Animal models of papillomavirus pathogenesis. Virus Res. **89**, 249–261.

120 Ingle, A., Ghim, S., Joh, J., Chepkoech, I., Bennett Jenson, A. and Sundberg, J. P. (2011) Novel laboratory mouse papillomavirus (MusPV) infection. Vet. Pathol. **48**, 500–5.

121 Hu, J., Cladel, N. M., Budgeon, L. R., Balogh, K. K. and Christensen, N. D. (2017) The mouse papillomavirus infection model. Viruses **9**, 1–13.

122 Roberts, J. N., Buck, C. B., Thompson, C. D., Kines, R., Bernardo, M., Choyke, P. L., Lowy, D. R. and Schiller, J. T. (2007) Genital transmission of HPV in a mouse model is potentiated by nonoxynol-9 and inhibited by carrageenan. Nat. Med. **13**, 857–861.

123 Cuburu, N., Cerio, R., Thompson, C. D. and Day, P. M. (2015) Mouse Model of Cervicovaginal Papillomavirus Infection. Cerv. Cancer Methods Protoc. **1249**, 2–5.

124 Verhaegent, M. and Christopoulos, T. K. (2002) Recombinant Gaussia luciferase: Overexpression, purification, and analytical application of a bioluminescent reporter for DNA hybridization. Anal. Chem. **74**, 4378–4385.

125 Drobni, P., Mistry, N., McMillan, N. and Evander, M. (2003) Carboxy-fluorescein diacetate, succinimidyl ester labeled papillomavirus virus-like particles fluoresce after internalization and interact with heparan sulfate for binding and entry. Virology **310**, 163–172.

126 Schafer, G., Graham, L. M., Lang, D., Blumenthal, M. J., Bergant Marusic, M. and Katz, A. A. (2017) Vimentin modulates infectious internalisation of HPV16 pseudovirions. J. Virol. 1–40.

127 Niruthisard, S., Roddy, R. E. and Chutivongse, S. (1991) The Effects of Frequent Nonoxynol-9 Use on the Vaginal and Cervical Mucose. Sex Transm Dis 176–179.

128 Sano, H., Chiba, H., Iwaki, D., Sohma, H., Voelker, D. R. and Kuroki, Y. (2000) Surfactant proteins A and D bind CD14 by different mechanisms. J. Biol. Chem. **275**, 22442–22451.

129 Shafti-Keramat, S., Handisurya, A., Kriehuber, E., Meneguzzi, G., Slupetzky, K. and Kirnbauer, R. (2003) Different heparan sulfate proteoglycans serve as cellular receptors for human papillomaviruses. J. Virol. **77**, 13125–35.

130 Blumenthal, M. J., Ujma, S., Katz, A. A. and Schäfer, G. (2017) The Role of Type 2 Diabetes for the Development of Pathogen-Associated Cancers in the Face of the HIV / AIDS Epidemic. Front. Microbiol. **8**, 1–10.

131 Clifford, G. M., de Vuyst, H., Tenet, V., Plummer, M., Tully, S. and Franceschi, S. (2016) Effect of HIV infection on human papillomavirus types causing invasive cervical cancer in Africa. J. Acquir. Immune Defic. Syndr. **73**, 332–339.

132 Li, L., Guo, X., Olszewski, E., Fan, Z., Ai, Y., Han, Y., Xu, L., Li, J. and Wang, H. (2015) Expression of Surfactant Protein-A during LPS-Induced Otitis Media with Effusion in Mice. Otolaryngol. -- Head Neck Surg. **153**, 433–439.

133 Milligan, G. N., Dudley, K. L., Bourne, N., Reece, A. and Stanberry, L. R. (2002) Entry of Inflammatory Cells Into the Mouse Vagina Following Application of Candidate Microbicides. Sex. Transm. Dis. **29**, 597–605.

134 Wiens, M. E. and Smith, J. G. (2015) Alpha-Defensin HD5 Inhibits Furin Cleavage of Human Papillomavirus 16 L2 To Block Infection. J. Virol. **89**, 2866–2874.

Appendix

Composition of solutions used

Complete medium: Dulbecco's Modified Eagle Medium (DMEM), 10% foetal calf serum (FCS) (Biochrom), Penicillin (100 U/mL) and Streptomycin (100 mg/mL).

SDS-PAGE Separating gel 10%: 1.5M Tris-HCl, pH 8.8; 10% (w/v) SDS; 40% acrylamide; 10% (w/v) ammonium persulphate; 0.01% tetramethylethylenediamine (TEMED).

SDS-PAGE Stacking gel 3%: 1M Tris-HCl, pH 6.8; 10% (w/v) SDS; 40% Acrylamide; 10% (w/v) ammonium persulphate; 0.01% TEMED.

10X SDS-PAGE running buffer: 30g solid Tris; 144g solid glycine; 10g SDS powder; add dH_2O to 1L. This stock solution was diluted 10-fold before use.

5X reducing protein loading buffer: 10µL 1M DTT in 90µL 5X Non-Reducing Lane Marker (Thermo Scientific).

10X Tris-Glycine transfer buffer: 30.3g Tris base; 144g glycine; add dH_2O to 1L.

1 X Tris-Glycine transfer buffer: 100mL 10X Tris-Glycine transfer buffer; 200mL methanol; add dH_2O to 1L.

Ponceau S stain: 0.2% Ponceau S, 5% acetic acid.

PBS-Tween: 100mL 10 X PBS; 1mL Tween, make up to 1L with dH_2O.

Harsh stripping solution: 8.75mL 8M guanidinium chloride; 200µL Tris-HCl pH 7.4; 50µL 2M DTT; 1mL dH_2O.

TE buffer: 10mM Tris-HCl; 1mM EDTA, pH 8.0.

2X HBS buffer: 50mM HEPES; 280mM NaCl; 1.5mM Na_2HPO_4, pH 7.1. Filter sterilised.

5X HSB buffer: 125mM HEPES; 2.5M NaCl; 0.1% Brij58; 5mM $MgCl_2$; 500µM EDTA; 2.5% ethanol; filter sterilised.

Light CsCl: 54g CsCl in 200mL 1xHSB buffer, filter sterilised.

Heavy CsCl: 77.6g CsCl in 200mL 1xHSB buffer, filter sterilised.

FACS wash: 0.5% BSA in PBS, opt. 5mM EDTA, 2mM NaN_3.

FACS fix: 1% (v/v) formaldehyde in FACS wash.

50X TAE buffer: 242 g Tris, 57.1 mL glacial acetic acid, 100 mL 0.5 M EDTA (pH 8.0), made up to 1L with dH_2O.

6X DNA loading dye: 3.75mL 30% glycerol, 25mg bromophenol blue 0.25%, dH_2O to 10mL.

Blocking solution (for IHC): 1% BSA in 1X PBS.

Supplementary Figures

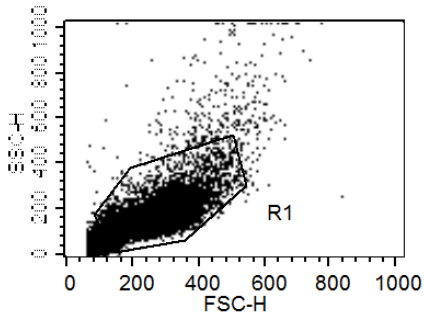

Supplementary Figure 1: Flow cytometry analysis of RAW264.7 cell population using a dot plot of FSC versus SSC. The population was gated (R1) to exclude any cell debris or contaminants in flow cytometry experiments.

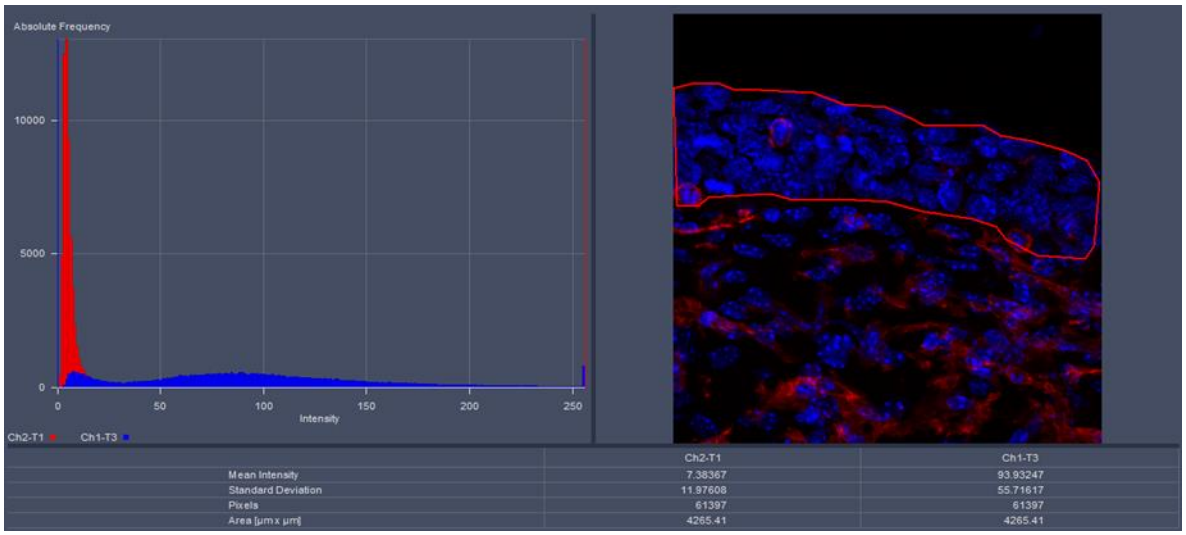

Supplementary Figure 2: Example of selecting epithelium for macrophage area calculations. Epithelial tissue was selected manually using the transmitted light and Hoechst channels to determine epithelial structure. The area of F4/80 staining in the epithelium was then quantified by setting the lower and upper thresholds at 18 and 256, respectively, to remove any background signal.

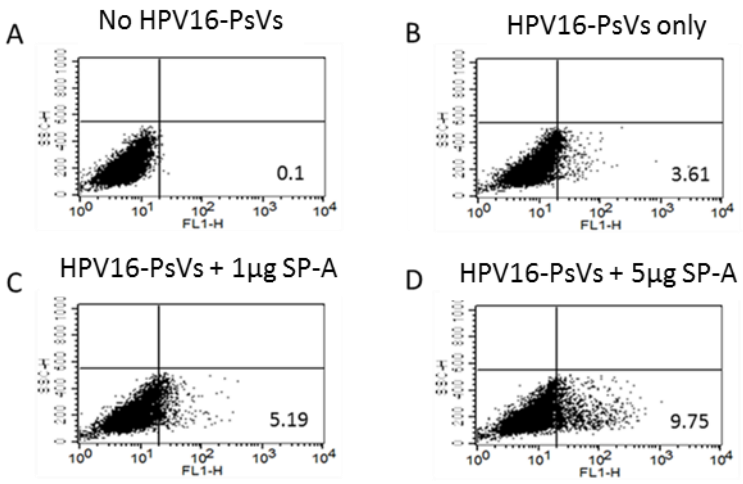

Supplementary Figure 3: Pilot experiments determined that 5µg SP-A (10-fold excess w/w) enhances viral uptake by RAW264.7 macrophages. RAW264.7 cells were infected with **(A)** No AF488-HPV16-PsVs and **(B)** AF488-HPV16-PsVs only (0.5µg) as experimental controls. 0.5µg AF488-HPV16-PsVs were also pre-incubated with either **(C)** 1µg or **(D)** 5µg SP-A for 1 hour prior to incubation with RAW264.7 cells. Fluorescence in the FL1 channel was plotted against side scatter (SSC). Values in the lower right (LR) quadrant indicate the percentage AF488 positive cells in the cell population.

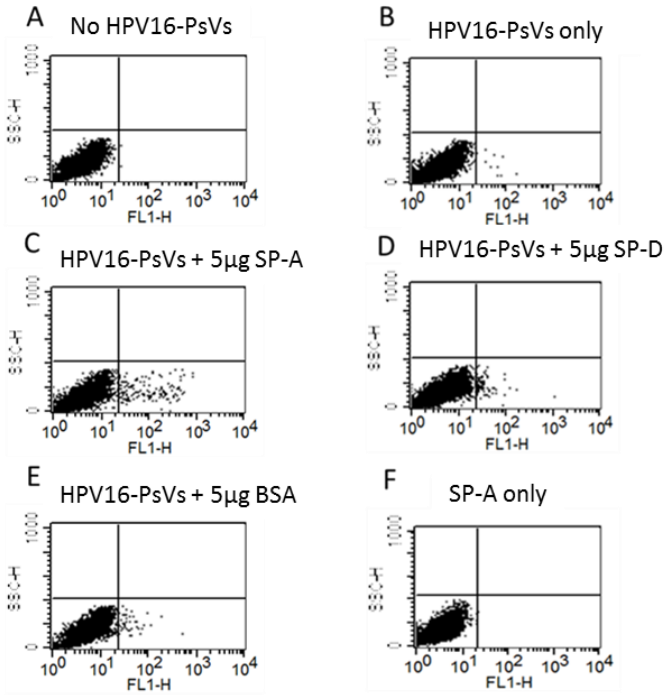

Supplementary Figure 4: Representative dot plots showing AF488-HPV16-PsVs internalisation by RAW264.7 macrophages. Fluorescence was measured in the FL1 channel and plotted against side scatter for (A) no AF488-HPV16-PsVs, (B) AF488-HPV16-PsVs only, (C) AF488-HPV16-PsVs and 5µg SP-A, (D) AF488-HPV16-PsVs and 5µg SP-D, (E) AF488-HPV16-PsVs and 5µg BSA, (F) SP-A only. Values in the lower right (LR) quadrant indicate the percentage of AF488 positive cells in the cell population.

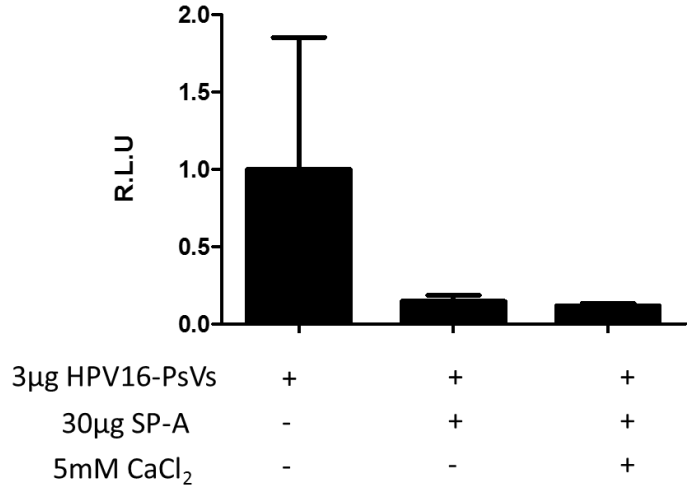

Supplementary Figure 5: Addition of calcium has no effect on SP-A-mediated reduction of HPV16-PsVs infection *in vivo*. 3µg HPV16-PsVs were pre-incubated with 30µg purified SP-A protein or 30µg SP-A and 5mM $CaCl_2$ for 1 hour on ice. Mice were then infected with these pre-incubated HPV16-PsVs particles. Mice were euthanised 24 hours p.i., and tissue harvested for analysis. Firefly luciferase activity was measured in vaginal lavage fluid (left panels) and homogenised genital tract tissue (right panels). Data were normalised to total protein in the samples and are presented as x-fold to average control (no SP-A) which was set as 1.